LEVEL II

AD A109558

COMPUTER SCIENCE TECHNICAL REPORT SERIES

DTIC
ELECTE
JAN 12 1982
S E D

UNIVERSITY OF MARYLAND
COLLEGE PARK, MARYLAND
20742

FILE COPY

82 01 12 061

LEVEL II

TR-913
DAAG-53-76C-0138

July, 1980

TOWARD THE RECOGNITION OF BUILDINGS AND ROADS ON AERIAL PHOTOGRAPHS

Mohamad Tavakoli*
Azriel Rosenfeld
Computer Vision Laboratory
Computer Science Center
University of Maryland
College Park, MD 20742

Technical rept.

ABSTRACT

This paper describes steps toward the recognition of cultural features such as buildings and roads on aerial photographs. The approach involves several successive stages of grouping of edge segments. Straight line segments are fitted to sets of edge pixels; compatibilities between pairs of these segments, based on gray level and geometric information, are computed; and the segments are then grouped into building-like and road-like groupings based on these compatibilities. Examples of the results obtained using this approach are given, and some variations on the initial stages of the process are also investigated.

The support of the Defense Advanced Research Projects Agency and the U.S. Army Night Vision Laboratory under Contract DAAG-53-76C-0138 (DARPA Order 3206) is gratefully acknowledged, as is the help of Kathryn Riley in preparing this paper.

*Permanent address: College of Engineering, Shiraz University, Shiraz, Iran.

411074

1. Introduction

This paper describes an approach to the extraction of cultural features such as roads and buildings from aerial photographs. The approach involves three stages, at which successively more global knowledge about the features is used to guide the extraction process.

The approach taken in this paper was motivated by the following considerations:

a) It is necessary to develop methods that can deal with cases where map information, giving the approximate locations of the features to be extracted, is unavailable.

b) An effort has been made to use methods that can be implemented by parallel processing techniques, particularly at the lower levels. If inherently sequential methods, such as road tracking, are used too extensively, it will be difficult to implement the feature extraction process in real time.

c) In order to reduce computational costs, the approach has been broken up into stages, at which increasingly global and more specialized knowledge about the features to be extracted is used. The first stage involves local operations on pixels, using general information about the local properties (gray level, color, contrast, etc.) that pixels belonging to the features are likely to have. Since at this stage we are examining every pixel, it is important that only simple computations be performed. The principal output of this stage is a set of line segments representing fragments of feature edges, and labelled with various property values computed for these fragments. The second stage groups these edge segments into pieces of features ("feature segments"), based on "semi-local" properties of the features (curvature, parallel-sidedness, etc.); the third stage groups the feature segments into global features, using global information about their shapes and spatial relationships. Thus at each stage, the computations are more complex, but they are applied to a smaller set of data.

d) Since the approach involves several successive stages of segmentation or grouping, if errors are made at an early stage, they may be difficult to correct at later stages. It is important to preserve the correspondences between entities at successive levels--i.e., between edge segments and the pixels that comprise them, and between feature segments and the edges of which they are composed; this will make it easier to locate the sources of any errors. It is also highly desirable to avoid firm decisions at any stage, and to avoid the use of processes that involve thresholds, but rather to make fuzzy or "probabilistic" decisions whenever possible, thus deferring commitments until they are confirmed by corroborating evidence. Note that when firm decisions are made, inputs that differ by arbitrarily small amounts may give rise to drastically different outputs. If such decisions must be made, they should be based on as much information as possible.

The successive stages in our approach are described in the following sections of this paper, and specific motivations are given for the types of knowledge used at each stage.

2. Edge segments and groups: general concepts

2.1 Edge pixels

Cultural features often contrast with their surrounds, and are usually bounded by sharp, locally straight edges. These characteristics can be used as guidelines in classifying pixels as possibly belonging to such features. On the other hand, information about feature shapes and spatial relationships would normally not be very useful in making decisions about pixels, unless the information is very specific, i.e., template-like. Knowing that houses are rectangular, for example, does not help us in classifying a pixel as being possibly part of a house, so that we can say very little about how it should be related to other pixels if it is indeed part of a house.

If the features have characteristic gray levels or colors, we should certainly use these properties in making decisions at the pixel level; but in nonmultispectral imagery, it will usually not be possible to characterize features in this way. Moreover, if we do classify the pixels based on their gray levels, we will often obtain large connected components of constant gray level; thus using a very local classification criterion (the pixel's gray level) may give rise to relatively global segments, and this will often be unwarranted.

These considerations have led us to propose the use of an edge-based approach at the pixel level. We first use local operators to estimate the magnitude and direction of the gradient at each point. We then use an iterative process at the pixel level to adjust the magnitudes and directions in the following way:

a) The magnitude is increased in the presence of high magnitudes at neighboring points in the tangential direction, provided their directions are smooth continuations of that direction; and it is decreased in the absence of such neighbors. This strengthens the edge responses at points that lie on straight or smoothly curved edges, and weakens them elsewhere.

b) At the same time, the direction is adjusted to make it agree more closely with these neighboring directions; the amount of adjustment depends on the magnitude at these neighbors. This tends to smooth out irregularities in the edge responses caused by noise.

c) An iterative scheme could also be used [1] for edge thinning: The magnitude is reduced in the presence of higher magnitudes at neighboring points in the gradient direction, and increased in the presence of lower magnitudes. If this is done iteratively, the magnitudes at the tops of the "ridges" of responses increase, while those at other points decrease, so that the edge responses are thinned.

Thus this process should produce sets of high-magnitude responses that lie on (thin) straight (or smoothly curved) edge segments, and such that the associated directions are locally very consistent. Note that the process involves no thresholds or decisions, and that it is readily implementable in parallel.

Figure 1 illustrates the results of applying such processes to the edge responses in a small portion of an aerial photograph of the Occoquan, VA, area. The desired enhancement effects are all quite apparent. No thinning was done, so that the magnitude reinforcement process tends to thicken the edges; but this is not considered harmful, since in any case line segments will be fitted to the edges at the next step, and these will be much the same whether or not the edges are thin--in fact, they may be more reliable if the edges are thick. The specific algorithms used were described in an earlier technical report [2]. Many variations on these algorithms could have been used, and would have yielded similar results; e.g., see [3]. An edge enhancement relaxation scheme could also have been used [4].

2.2 Edge segments

We now want to construct a data representation based on entities more global than pixels; this will allow us to use more global knowledge about cultural features, e.g., simple types of shape information, to classify these entities. Straight or smoothly curved edge segments are obvious choices for these entities, since the pixel-level processes tend to produce sets of edge responses that lie along such segments.

Extracting edge segments inherently involves some sort of threshold criterion, since one must decide whether or not to construct a segment corresponding to a given collection of edge responses. Such decisions should be easier for enhanced responses, but they are still nontrivial, and should be made on the basis of as much information as possible. If we simply threshold the (enhanced) edge magnitudes, we are making the decisions on a pixel by pixel basis, using only the information concerning that pixel, which is undesirable. (Note, however, that when we do this for enhanced responses, the information associated with a pixel also reflects the nature of its neighbors.)

A somewhat safer idea is to make decisions about pixels in the context of their neighborhoods. For example, one might "accept" a pixel if its own magnitude, and the magnitudes of two of its neighbors in the tangential directions, are sufficiently high. (Note that this idea is very compatible with the enhancement process; it essentially accepts just those pixels that would be strongly enhanced.) At the same time, one can establish links between each accepted pixel and its neighbors; these links can then be used to define connected components of accepted pixels, which then constitute the desired edge segments. Such a linking approach is used by Navatia and Babu [5]. Alternatively, one can use a global straightness criterion in defining the connected components by requiring each pixel's direction to lie close to the average direction of the already accepted pixels [2]; this breaks up smooth curves into segments having relatively low net changes in slope from one end to the other. Figure 2 illustrates the types of edge segments obtained using this criterion.

It would be even more desirable to make decisions about entire groups of linkable dge pixels; but the number of such groups is enormous, and it is utterly impractical to consider all of them. However, suppose that we are only interested in groups of edge pixels that lie on a curve of a given shape, e.g., on a straight line. In this case we can use a Hough transform approach to map collinear sets of edge responses into compact peaks in the Hough space. We must then use a threshold criterion to detect the peaks, but this criterion is now being applied to an entire group of collinear edge pixels, rather than on a pixel by pixel basis. It should be mentioned that we obtain a cleaner Hough space when we use enhanced edge responses, since the slope estimates are much more consistent than in the raw responses, and this in turn makes the estimates of the distances of lines from the origin much more consistent. Of course, we should not merely use slope and distance (and response magnitude) to define clusters in Hough space; other properties associated with the edge responses, e.g. the gray levels on the two sides of the edge, should also be used if appropriate, to differentiate between responses that (probably) belong to different edges. It may even be desirable to use position along the line as a feature, in order to avoid clustering responses that are far apart in the image and have no responses between them. Such global approaches to edge segment construction deserve further investigation.

2.3 Groups of segments

We now have a set of edge segments, with each of which we can associate various properties, including its length, average slope, average strength, etc., as well as properties of the gray levels on the two sides of the segment's constituent edge pixels, e.g., the means and standard deviations of these gray levels. If desired, we can now use this information to search for missing parts of edges in the original image, so as to fill gaps in the edge segments and create longer ones. We can also now group the edge segments into cultural feature segments, based on our knowledge about the expected geometrical properties of these segments. In this section we discuss some possible approaches to edge segment grouping. For simplicity, we consider two simple types of grouping, based, respectively, on good continuation and on parallelism.

Straight segments that are collinear, or curved segments that "point toward" one another, can be linked using criteria based on strength, length, distance, and good continuation, as well as similarity of properties [6]. (This assumes, of course, that such linking is consistent with what we know about the features that we are trying to extract.) Linking across large gaps can be done much more reliably at the segment level than at the pixel level, since the information that we have about the segments (slope, property similarity, etc.) is more reliable than the corresponding information about pixels. At the same time, exploration of large gaps at the pixel level would involve an excessive amount of computation per pixel.

This type of linking involves pairwise decisions; as pointed out in Section 2.2., it would be preferable to make decisions about entire groups of segments as to whether or not they constitute good groupings, rather than making decisions about two segments at a time. In general, it is not practical to consider all possible combinations of segments; but if we restrict ourselves to sets of collinear segments (or more generally, segments that lie on a curve of known shape), it is computationally feasible to evaluate all possible sets of consecutive segments as possible groupings. Various criteria for evaluating sets of collinear segments have been formulated that yield perceptually reasonable results [7]; Figure 3 illustrates one simple possibility.

In addition to segment linking based on collinearity or good continuation, one usually also wants to link pairs of "anti-parallel" segments, representing pairs of parallel edges whose dark sides or light sides face one another, since cultural features often have parallel sides. In the work of Nevatia and Babu [5] and of Brooks [8], links are formed only for pairs having no segments between them; but in general, we should be allowed to link two segments even if there are other segments between them, since these other segments may be due to noise, or may represent features internal to the given one (e.g., a penthouse on a building, a divider strip on a highway). Thus in general we must compute link merits for many pairs of segments, and then choose "best" pairs for actual linking. The merit function may depend on the strengths, slopes, lengths, and property value similarity of the segments, as well as on their degree of overlap and on the distance between them, and on any special knowledge that we may have about the properties of the desired features. Note that the merit may be asymmetrical; for example, if a short segment and a long segment face one another, the merit of linking the short one to the long one may be much higher than that of linking the long one to the short one. Given the merits for all pairs of segments, we can link all pairs having (mutually) highest merit; once we have done this, the linked segments are no longer candidates for linking, so that some of the remaining pairs may now have mutually highest merit and can now be linked. This process can be repeated until no further linking is possible. Figure 4 shows the results of applying this process using a very simple merit function, namely the fraction by which one segment overlaps the other divided by the distance between them, provided the segments have approximately equal slopes. Several variations of this approach have also been tried, with essentially identical results [9]. An additional example is shown in Figures 1'-4', which are analogous to Figures 1-4.

The antiparallel linking schemes just described are all based on pairwise decisions. As before, it would be preferable to evaluate groupings of segments that form antiparallel strips, rather than linking such segments two at a time. This would allow us to combine the collinear and antiparallel linking processes into a single strip clustering process. Here again, a Hough-like approach might be used to detect clusters arising from strips.

3. Edge segments: buildings and roads

Up to now we have discussed general approaches to the problem of edge segment construction and grouping. In this section we develop a more specialized approach, aimed at extracting groupings that represent buildings and roads on an aerial photograph. Edge segments are constructed as described in Section 2.2. We associate various properties with each segment, including its length, average edge strength, average gray level on each side of it, etc. These properties are used to derive initial probabilities that the segment is part of a road, part of a building, or neither (we refer to this last alternative as "other"). Groups of segments are then formed, and the segment probabilities are updated based on properties of the groups.

3.1 Average gray level calculation

In order to calculate the initial probability assignments, we have to find the average gray level on both sides of a line. The algorithm for calculation of average gray level on both sides of an edge segment is as follows:

1) Generate a strip of width "d" on each side of the segment. Find the co-ordinates of the points inside the two strips as well as the number of points on each side.
2) Calculate the average gray level on each side by dividing the sum of the gray levels by the number of points on each side.

The algorithm starts by reading in the coordinates of the end points of each line. Then the slope of the line is calculated. At this point it is determined whether the angle (θ) of the line with respect to the x-axis is between 0 and 90 degrees or is between 90 and 180 degrees. This differentiation is necessary in order to define a sense for each side of the line segment.

Referring to Figure 5, the end points are designated as end point 1 and end point 2. The sides are denoted similarly. Using the conventions in Figure 5, the following equations can be written for each edge segment and for the boundaries of the strips on both sides of each segment. When θ is not equal to 90 degrees we have:

$y_0(x) = mx + mx_1 + y_1$

$y_{13}(x) = -x/m + x_1/m + y_1$

$y_{14}(x) = -x/m + x_2/m + y_2$

$y_{11}(x) = mx - m(x_1 + \Delta x) + y_1 - \Delta y$

$y_{12}(x) = mx - m(x_1 - \Delta x) + y_1 + \Delta y$

where $\Delta x = d \sin\theta$, $m = (y_1 - y_2)/(x_1 - x_2)$

$\Delta y = d \cos\theta$ when $0 \leq \theta < 90$

and $\Delta y = -d \cos\theta$ when $90 < \theta < 180$

When θ is equal to 90 degrees we have the following equations for the boundary lines of the strip. This case is shown in Figure 4 and the equations are:

$x_0 = x_1 = x_2$, $x_{11} = x_0 + d$

$x_{12} = x_0 - d$, $y_{13} = y_1$

$y_{14} = y_2$

The digitized image is given in the form of a rectangular matrix of elements $g(i,j)$ in which (i,j) are the Cartesian coordinates of a point and $g(i,j)$ is the value of the brightness at the point (i,j).

In order to calculate the gray level averages inside the strips, we sum up the gray levels of those points which satisfy the conditions below and divide by the number of points in the strip:

$$\text{Average gray level} = \sum_{i,j} g(i,j)/n$$

The points inside each strip should satisfy the following conditions:

1) When $0° \le \theta < 90°$

a) For side "1"

$x_2 \le i \le x_1 + \Delta x$ $\quad$ $y_2 - \Delta y \le j \le y_1$

$y_{11}(i) < j < y_0(i)$ $\quad$ $y_{14}(i) < j < y_{13}(i)$

b) For side "2"

$x_2 - \Delta_x \le i \le x_1$ $\quad$ $y_2(i) \le j < y_1 + \Delta y$

$y_0(i) < j < y_{12}(i)$ $\quad$ $y_{14}(i) < j < y_{13}(i)$

2) When $90° < \theta < 180°$

a) For side "1"

$x_1 \le i \le x_2 + \Delta x$ $\quad$ $y_2 \le j \le y_1 + \Delta y$

$y_0(i) < j < y_{11}(i)$ $\quad$ $y_{14}(i) < j < y_{13}(i)$

b) For side "2"

$x_1 - \Delta x \le i \le x_2$ $\quad$ $y_2 - \Delta y \le j \le y_1$

$y_{12}(i) < j < y_0(i)$ $\quad$ $y_{14}(i) < j < y_{13}(i)$

3) When $\theta = 90$

a) For side "1"

$x_1 - d \le i < x_1$ $\quad$ $y_1 \le j \le y_2$

b) For side "2"

$x_1 < i < x_1 + d$ $\quad$ $y_1 \le j \le y_2$

3.2 Initial probability assignment

One of the most useful properties that can be used for calculation of the initial probability assignment vector is the average gray level in a strip on each side of the segment. These averages can then be compared with typical gray levels of cultural features such as roads or buildings. The minimum difference of these side average gray levels from the typical gray levels of roads and buildings is used as a figure of merit in the calculation of initial probabilities.

Roads and buildings are the brightest objects on the photographs that we used. They also have similar gray levels (similar reflectances) in the scene. Using these facts, in what follows an automatic method for estimating the gray level is described.

1) Calculate the average gray level in a strip on each side of each line segment.
2) Sort the line segments in decreasing order of length.
3) Select the longest p% of the lines (usually 5%).
4) Calculate the average gray levels of the brightest sides of the lines selected in step (3).

The average gray level calculated in this way can be accepted as a good estimate for the typical gray level of the objects.

To define the process of calculating the figures of merit more precisely, each line segment in the scene has two sides. The average gray levels of the strips along the two sides of the segment are denoted by g1 and g2 (see Figure 7).

Suppose that the typical average gray levels of roads and buildings are gr and gh respectively. Then the differences

$$f1 = |gr - g1| \quad \text{and} \quad f2 = |gr - g2|$$

measure the dissimilarity between the two sides of the line segment and the gray level of a typical road. Therefore, the function sr = min(f1,f2) is a measure of the gray level similarity between the given line segment and a typical road. Similarly the differences

$$h1 = |gh - g1| \quad \text{and} \quad h2 = |gh - g2|$$

measure the dissimilarity between the two sides of the line segment and the gray level of a typical building, and the function sh = min(h1,h2) is a measure of the gray level similarity between the given line segment and a typical building.

Finally,

$$s = \min(sr, sh)$$

will be small if the gray level average on one of the sides of the line segment is close to the gray level of a typical building or road. Therefore, if s is small the line segment is more probable to be an edge of a road or a building than to be an "other" type of edge, whereas if s has a large value, the probability that the line segment is in the "other" class is high.

In order to express the value of s as a figure of merit, linear functions are used. Let di (i = 1,2,3) represent the figures of merit. To define them as linear functions of s, the following linear expression is used for calculation of a road figure of merit. This linear function is shown in Figure 8 by thin solid lines.

$$d1 = \begin{cases} (1/dgr-1/gr)(g-gr) + 1 \\ \quad \text{when } (g^2r-2gr\cdot dgr)/(gr-dgr) \le g \le gr \\ 0 \quad \text{when } g^2r/(gr-dgr) < g < (g^2r-2gr\cdot dgr)/(gr-dgr) \\ (1/gr-1/dgr)(g-gr) + 1 \\ \quad \text{when } gr \le g \le g^2r/(gr-dgr) \end{cases}$$

Here dgr is the deviation allowed for road gray level; beyond it, the figure of merit of "other" will become greater than the figure of merit of road. The value of g is

$$g = g1 \quad \text{if } f1 < f2$$

and

$$g = g2 \quad \text{if } f1 > f2$$

Similarly the figure of merit for a line segment being a piece of building is shown by the thick solid lines in Figure 8 and its expression is as follows:

$$d2 = \begin{cases} (1/dgh-1/gh)(g-gh) + 1 \\ \quad \text{when } (g^2h-2gh\cdot dgh)/(gh-dgh) \le g \le gh \\ 0 \quad \text{when } g^2h/(gh-dgh) < g < (g^2h-2gh\cdot dgh)/(gh-dgh) \\ (1/gh-1/dgh)(g-gh) + 1 \\ \quad \text{when } gh \le g \le g^2h/(gh-dgh) \end{cases}$$

Here dgh is the deviation allowed for building gray level; beyond it, the figure of merit of "other" becomes greater than the figure of merit of buildings. The value of g is

$$g = g1 \quad \text{if } h1 < h2$$

and

$$g = g2 \quad \text{if } h1 > h2$$

When sr < sh road is more probable; therefore we use the dashed line for calculation of the figure of merit for "other". Similarly when sr > sh buildings are more probable and the dotted line is used for calculation of the figure of merit for "other". In summary, the figure of merit for the "other" class is calculated using the following formula:

When sr < sh

$$d3 = \begin{cases} |gr - g|/gr & \text{when } 0 < g < 2gr \\ 1 & \text{when } g \geq 2gr \end{cases}$$

Similarly when sr > sh

$$d3 = \begin{cases} |gh - g|/gh & \text{when } 0 < g < 2gh \\ 1 & \text{when } g \geq 2gh \end{cases}$$

The initial probability for each label is obtained by dividing the figure of merit of each label by the sum of the figures of merit of the three labels. Defining the initial probability in this manner, we have

$$p_{\lambda}^{(0)}(i) = di / \sum_{i=1}^{3} di \qquad i = 1,2,3$$

where di (i = 1,2,3) is the figure of merit of each label using the previous linear formulation and λ is the edge segment label.

When we use the functions in Figure 8, many segments will have probability 1 of belonging to the "other" class. These segments can be discarded as noise.

4. Pairs of segments: buildings and roads

The next step after noise cleaning is to group the line segments in a meaningful manner. In order to do this, models of the edges constituting objects should be used. The models of roads and buildings used in the program will now be described.

a) The model of edges belonging to a piece of a road

From the function of a road, it follows that certain physical and geometrical requirements must be satisfied. The properties used in this model are as follows:

1) The spectral properties of a road correspond to materials such as concrete and asphalt and it is usually homogeneous.
2) A piece of an edge of a road should have an anti-parallel edge.
3) A piece of an edge of a road is usually connected to other neighboring pieces with low angle deviation.

b) The model of edges belonging to a building

Similarly, the physical and geometrical properties of a building are:

1) The spectral properties of the roof of the building.
2) The similarity of gray level inside the edges constituting a building.
3) A piece of an edge of a building is connected to other pieces.
4) The edges of a building form a closed figure (usually with right angles).

In order to use the above models the geometric relationships between each pair of lines within a neighborhood in the scene should be studied. In general, using the conventions of Figure 5, every pair of lines in the scene belongs to one of sixteen cases. These cases are listed in Table 1. The entry "side" in Table 1 refers to the object side of the given segment.

In order to find the object side of a line segment, first the two values sr and sh are calculated. Then, using the following decision rules the object side is found:

```
when sr < sh
  if f1 < f2    side = 1
else            side = 2
```

and

```
when sr > sh
  if h1 < h2    side = 1
else            side = 2
```

Assume that the pair of lines under study are labeled as line A and line B. The angles of the two lines with respect to the x-axis are θ_A and θ_B respectively. Depending on the orientation of the pair of lines, different angles between the two lines are possible. Figure 9 shows examples of the angle θ between two lines. The plus sign indicates the side of the road or building. According to this convention the angle between two collinear lines is 180°.

4.1 Compatible pairs

We now give the details of the algorithm for finding compatible pairs of segments, i.e., pairs that might be consecutive edge segments of a building or road. Referring to the model of edges constituting the objects, each of these pairs of lines should satisfy certain conditions in order to be accepted as a candidate compatible pair. In general, these conditions are:

a) Similarity of gray level of a strip along a line connecting their ends with respect to the object side of the pairs.

b) Conditions on the geometrical configuration of the pair of lines.

To check the similarity condition, the average gray level on the object side of the pair of lines is calculated by

$$g = (gA + gB)/2$$

where gA and gB are the average gray levels of the strips along the object sides of lines A and B. Then, the corresponding average gray level of a strip along a line connecting the ends of the lines is calculated. The difference between this value and g is a measure of the gray level similarity of the line connecting the two ends with the pair of lines. If this difference is within the limits used in calculation of the figures of merit, then the similarity condition is satisfied.

In a case where the distance between the ends is very small, that is, comparable with the width of the strip used in calculation of the gray level, the similarity measure is not reliable. This is because the number of points used in calculation of the gray level is limited. In cases where the distance between the ends of pair under study is less than the width of the strip used in calculation of the average gray level, the similarity condition will not be checked. In this case the pair is considered as a compatible candidate if the appropriate geometrical conditions are satisfied.

Geometrical conditions are important in making two lines compatible. Figure 10 and Figure 11 show examples of geometrically compatible and incompatible pairs, respectively. To differentiate between geometrically compatible and incompatible pairs, certain constraints on the geometrical locations of the end points are necessary. The ratio of the distances between end points can be used to reject the geometrically incompatible pairs.

In what follows, the first four cases in Table 1 will be analyzed and their compatibility conditions derived. The other cases have similar conditions.

Case (1)

Referring to Figure 12, there are five different configurations. In this case the compatibility of line A with respect to line B at end (2) or the compatibility of line B with respect to line A at end (1) is considered. Table 2 summarizes the conditions imposed in these cases. The parameter m in the table is taken to be 1.5. This allows some overlap between the pairs of compatible line segments. The angle between the two lines is

$$\theta = \pi + |\theta_A - \theta_B| \qquad \text{if } \theta_B \leq \theta_A$$

and

$$\theta = \pi - |\theta_A - \theta_B| \qquad \text{if } \theta_B \geq \theta_A$$

Case (2)

In this case seven different configurations are considered. These are shown in Figure 13. The compatibility of end (1) of line A or line B is considered. Table 3 summarizes the required conditions. The angle between the two lines in this case is

$$\theta = 2\pi - |\theta_A - \theta_B| \qquad \text{when } ya2 < y0$$

and

$$\theta = |\theta_A - \theta_B| \qquad \text{when } ya2 > y0$$

where

$$y_0 = mb \cdot xa2 - mb \cdot xb1 + yb1$$

and mb is the slope of line B. The conditions at end (2) of the lines are similar to the end (1) conditions. To find these conditions a1 and b1 should be changed to a2 and b2 except that in this case

$$y_0 = mb \cdot xa1 - mb \cdot xb1 + yb1$$

The side similarity for some configurations is different in this case.

Case (3)

When the compatibility of end (1) of line A with end (2) of line B is considered, there are five different configurations. Figure 14 shows these configurations. The conditions are summarized in Table 4. The angle between the lines is

$$\theta = \pi + |\theta_A - \theta_B|.$$

The other possibility is to study the compatibility of end (2) of line A with end (1) of line B. Here again there are five different configurations. Figure 15 shows these configurations. The conditions are summarized in Table 5. The angle between the lines is

$$\theta = \pi - |\theta_A - \theta_B|.$$

Case (4)

The conditions for this case are summarized in Table 6 and Table 7. The different configurations are shown in Figure 16 and Figure 17. The angle between the lines is

$$\theta = |\theta_A - \theta_B|$$

when the compatibility of end (1) of line A is considered. Similarly the angle is

$$\theta = 2\pi - |\theta_A - \theta_B|$$

when the compatibility of end (2) of line A is in question.

So far the geometrical and similarity conditions for the pairs of compatible segments have been found. In what follows the algorithm for finding compatible pairs will be explained.

Algorithm for Finding Compatible Pairs

1) Choose those line segments whose "other" property is not equal to 1.
2) For end "1" of each line, find the shortest distances from other end points of line segments.
3) Find the object side of the given line and the other lines found in (2).
4) Check the geometrical and similarity conditions for the given line and the other lines found in (2). Reject those lines for which the required conditions are not satisfied.
5) If all the lines are rejected go to (8).
6) Find the angle of the line with respect to the remaining lines in (4). Choose the line which has the smallest angle (e.g. greater than 25°) with respect to the line under study.
7) Choose the other end of the line found in (6) and go on to (2).
8) Choose the other end of the given line and go to (2). If the other end has already been tested go to (9).
9) Continue the above process for the other line segments.

4.2 Antiparallel pairs

The edges of cultural features usually occur in pairs, as in the sides of roads and of buildings. To identify these features the edges should be clustered into antiparallel pairs (i.e. pairs of facing edges that are parallel but have opposite senses). Clustering must take into account information from the picture in the regions around the edges. For example, a road usually has a uniform gray level and thus it is reasonable to expect the facing sides of an antiparallel pair of edges to have similar gray levels.

The present method finds the pairs of lines that are anti-parallel up to a certain angle difference (usually 25°) when similarity of gray level between the pairs is satisfied.

The basic procedure is as follows. A strip is moved along the object side of each side segment. The movement is continued until the similarity is lost or the distance moved is greater than the largest expected object size in the scene. While the strip moves, it hits other line segments. Among these line segments the following segments are rejected:

a) If they are not anti-parallel

b) If the difference in the angle is greater than a threshold.

The similarity is defined as the difference between the average gray level of the moving strip and the average gray level of the object side of the edge segment:

$|g-gmove| <$ level of similarity

where g = average gray level of the line segment

and gmove = average gray level of the moving strip.

The level of similarity used in the program is taken as 7, which is a rather tolerant condition. When the strip hits a candidate line the level of similarity is automatically changed to the value of the contrast of the candidate line. Note that this change of the level may stop the movement of the strip.

Among the remaining lines the one which has the smallest distance is selected as anti-parallel. To find the shortest distance between two anti-parallel line segments, at each end of the two segments perpendicular lines are drawn to the other line. If the intersection of the perpendicualr with the facing line is located outside of the line, the distance is neglected. Among the remaining distances, the minimum is selected as the distance between the two lines. Figure 18 shows an example of calculating the distance between two lines. As shown in this figure, among the four distances

$$di \quad (i = 1,2,3,4)$$

d3 and d4 are rejected and

$$d = \min(d1,d2)$$

is selected as the distance between the two lines.

To check whether the intersection of the perpendicular line is between the end points of a line the following decision rules are used:

if θ is not equal to 90 degrees

and $x1 \leq xint \leq x2$ the intersect point is between the end points

else if θ is equal to 90 degrees

and $y1 \leq xint \leq y2$ the intersect point is between the end points.

Here (xint,yint) are the coordinates of the intersection point.

This method of finding anti-parallel pairs of lines has the following advantages:

a) Each line is not compared with all other lines.

b) When several lines are facing a line, the method allows all of these lines to choose the same line as anti-parallel.

c) The method uses the context of the lines on the picture, namely, the similarity of the gray levels inside the object.

In what follows the algorithm for finding anti-parallel pairs is explained.

<u>Algorithm for finding anti-parallel pairs</u>

1) Choose a line segment and find its object side.

2) Generate the strip (a width of 4 points is used), and find the average gray level inside the strip.

3) Move this strip parallel to the segment. While the similarity and the total movement distance are less than the specified levels, note the lines hit by the strip. If no lines are found go to (5). Otherwise, reject those lines where the angle difference is greater than the specified threshold and the facing side is not opposite to the original line. Set the similarity level equal to

the contrast of the line found and continue the process.

4) For the candidate lines found in (3) choose the one which has the minimum distance. Mark the line found in order not to process it again.

5) Continue the process for the remaining lines.

The maximum moving distance in the above algorithm is quite relaxed; it is set to be equal to be 1/4 of the size of the picture. For scenes containing small objects this distance can be reduced in order to reduce computation time. The angle difference can be set arbitrarily. The program is not sensitive to this threshold since the strip moves along the object side of the edge and so it is expected that we get another side of the object as the best candidate.

5. Groups of segments: buildings and roads

After application of the programs described up to now, we have groups of compatible and antiparallel pairs of segments. Using the model of roads and buildings, we want to update the probabilities that were initially obtained using gray level information. Based on these probabilities we can recognize objects with good confidence or fair confidence.

We begin by dividing the groups of compatible pairs into the following categories:

A) Closed groups

B) Semiclosed groups

C) Other lines and groups

In what follows each of the above categories will be explained in more detail.

A) Closed groups

By a closed group, we mean that the start and the end segment labels are the same. Figure 19 shows an example of this type of group. In this figure A,B,C.... are the labels in a compatible group.

It is obvious that this kind of closed group is a good candidate for being the group of edges of a building. To check whether this closed group is a building, we test for solidness inside the object sides, and also check that each line segment in the group is antiparallel to a line in the group. To check solidness we use the same operator that was used in finding the antiparallel pairs. This test also guarantees the similarity of gray level inside the object.

The above check can differentiate between the cases (b) and (c) in Figure 19. Thus a closed group with the above conditions can be considered a building with good confidence.

B) Semiclosed groups

A semiclosed group is defined as a group with a gap less than the longest line connecting the ends of compatible pairs in the group. Figure 20 demonstrates an example of this type. As in the case of a closed group, if the following tests are valid, then the group is accepted as a building with good confidence.

1) Solidness

2) Each line should be antiparallel to a line in the group.

Operators similar to those used for checking closed groups are used here.

C) Other lines and groups

Here again the model of the edges constituting a building or road will be used for the recognition of the remaining lines or groups. The important features are the angles between the compatible pairs and information on anti-parallel pairs. Figure 21 shows examples of possible cases that may occur in the scene. In this figure θmin is around 200°. Special care should be taken in cases where the anti-parallel pairs or compatible pairs are not available, due to cutoff at an edge of the frame.

We now describe in detail the algorithm for updating the probabilities of "other" lines or groups. A reinforcement algorithm is employed to update the probabilities of the remaining line segments by rewarding and punishing (increasing or decreasing a component of the probability vector). Here again the model of the edges constituting the objects will be used for the updating process. The most important features are the angles between compatible pairs and information on antiparallel pairs. For example, two anti-parallel lines should reinforce each other for both buildings and roads.

We begin by dividing the "other" lines and groups into the following categories.

1) Groups consisting of two compatible lines

2) Groups consisting of more than two compatible lines

3) Single lines

In what follows the criteria for classification of each of the above categories will be explained in more detail.

1) Groups consisting of two compatible lines

The two compatible lines are called A and B. There are four cases.

Case a

Both A and B have no anti-parallel lines due to cutoff at the edges of the frame. Figure 22 shows examples of this case.

If the angle θ between the lines is close to 90°, there is a high probability that the lines are a part of a building. If the angle θ is greater than 90° the probability that the edge is a part of a road is higher. Similarly, if the angle is less than 90° the probability of being "other" is higher. In order to express this situation the following figures of merit are defined:

$$d1 = f1(\theta)\ [P_A^{(0)}(1) + P_B^{(0)}(1)]$$

$$d2 = f2(\theta)\ [P_A^{(0)}(2) + P_B^{(0)}(2)]$$

$$d3 = f3(\theta)\ [P_A^{(0)}(3) + P_B^{(0)}(3)]$$

where d1, d2, and d3 are the figures of merit for road, building, and other, respectively. The functions $fi(\theta)$ $(i = 1,2,3)$ are defined as follows:

if $0 \leq \theta \leq \pi/4$

$$f1(\theta) = 0,\ f2(\theta) = 0,\ f3(\theta) = 1$$

if $\pi/4 < \theta \leq \pi/2$

$$f1(\theta) = 0,\ f2(\theta) = 1-|\cos\theta|,\ f3(\theta) = 0.25$$

if $\pi/2 < \theta \leq \pi$

$$f1(\theta) = |\cos\theta|,\ f2(\theta) = 1-|\cos\theta|,\ f3(\theta) = 0.25$$

if $\pi < \theta < 2\pi$

$$f1(\theta) = 0.5,\ f2(\theta) = 0,\ f3(\theta) = 0.5$$

Case b

One of the lines has no anti-parallel due to cutoff at an edge of the frame, and the other line has an anti-parallel line. Figure 23 shows examples of this case.

In this case again the figures of merit are defined as

$$d1 = f1(\theta)\ [P_{A'}^{(0)}(1) + 2P_B^{(0)}(1) + P_A^{(0)}(1)]$$

$$d2 = f2(\theta)\ [P_{A'}^{(0)}(2) + 2P_B^{(0)}(2) + P_A^{(0)}(2)]$$

$$d3 = f3(\theta)\ [P_{A'}^{(0)}(3) + 2P_B^{(0)}(3) + P_A^{(0)}(3)]$$

where label A' is the label of the anti-parallel line of A. The functions $fi(\theta)$ $(i = 1,2,3)$ are the same as before. In this definition the probability components of line B are counted twice. This is because line B reinforces both lines A' and A.

For these two cases the update probability is defined as

$$P_\lambda^{(1)}(i) = di / \sum_{i=1}^{3} di \qquad (i = 1,2,3)$$

where λ is the label of the line under study.

Case c

Both A and B have anti-parallel lines. Figure 24 shows possible examples of this case. In order to recognize this case lines are drawn between the midpoint of each line and the corresponding anti-parallel line. If the intersection of these two lines is located between the lines, we have a building with good confidence and therefore:

$$P_\lambda^{(1)}(1) = 0, \qquad P_\lambda^{(1)}(2) = 1, \qquad P_\lambda^{(1)}(3) = 0$$

for λ = A,B,A',B'.

If the intersection is outside the lines we have a road with good confidence:

$$P_\lambda^{(1)}(1) = 1, \qquad P_\lambda^{(1)}(2) = 0, \qquad P_\lambda^{(1)}(3) = 0$$

for λ = A,B,A',B'.

Case d

This case includes all situations not covered by cases (a-c)--e.g., both A and B have no anti-parallel lines and this is not due to cutoff. In these cases no change is made to the probabilities.

In the above four cases if the anti-parallel line of A or B was previously recognized as a part of a road or as a part of a building, A or B is considered as a line with no anti-parallel. The reason for this is that the anti-parallel line was previously recognized as a part of an object and therefore it should not reinforce these lines.

2) Groups consisting of more than two compatible lines

In this case a line may have two compatible lines at its ends. Examples of possible roads in this case are shown in Figure 25 and an example of a possible building is shown in Figure 26. Notice that the example of a possible building shows the situation after the recognition of closed and semi-closed groups.

A piece of an edge segment A is classified as road with good confidence if the following conditions are satisfied:

a) If it possesses an antiparallel line A'

b) If $\theta_1 > \theta\text{min}$ and $\theta_2 > \theta\text{min}$

c) If $\theta_1' > \theta\text{min}$ and $\theta_2' > \theta\text{min}$

or if the line has no antiparallel because of cutoff but the neighboring compatible line satisfies the above conditions.

Since we do not allow sharp turns for roads θmin is set to be 110°.

Special care should be taken with the start and end lines of a group where the condition for one angle, θ_1 or θ_2 is satisfied. The other special case is when one or both of the compatible lines have no antiparallel because of cutoff. In this case the condition on θ_1' or θ_2' will not be checked.

There are other cases where a line does not have an antiparallel line but not because of cutoff. An example of this is shown in Figure 27. In this case if both compatible neighbors at the ends are classified as road with good confidence, then this piece will also be classified as road with good confidence. For all the above cases

$$P_\lambda^{(1)}(1) = 1, \quad P_\lambda^{(1)}(2) = 0, \quad P_\lambda^{(1)}(3) = 0$$

for $\lambda = A, A'$.

An edge segment is classified as a road with low confidence if it satisfies the following conditions:

a) It has no anti-parallel, not due to cutoff

b) Only one compatible neighbor is a road with good confidence.

In this case the probability is updated as follows:

$$P_A^{(1)}(1) = 0.5, \quad P_A^{(1)}(2) = 0, \quad P_A^{(1)}(3) = 0.5$$

To classify cases where θ_1 or θ_2 is less than θmin, the following procedure is applied:

a) Within the group, we start from the line with angle less than θmin; then other neighboring lines are found that satisfy the same angle condition. Now we have a semi-closed group candidate. If the tests stated for semi-closed groups are valid, then we classify these line segments as buildings with good confidence.

b) If the semi-closed tests are not valid, the classification is done according to the category of groups consisting of two compatible lines. Here the lines are considered two by two and the classification is done as before.

The recognition for other cases (e.g., none of the lines have antiparallels) is done according to the category of groups consisting of two lines as before.

3) Single lines

These are single lines with no compatible lines at the ends. The following rules are applied for classification of single lines.

a) Classify a single line as road if it has an anti-parallel line.

b) Classify it as "other" if it has no anti-parallel.

A simple verification step for isolated road lines is added in order to reject noisy lines that have prematurely been recognized as road with good confidence. The isolated road lines are verified if they have a minimum acceptable length for roads.

6. Examples

The algorithms described in Sections 3-5 were applied to three images showing portions of a suburban area near Occoquan, VA (compare Figs. 1'-4').

Figure 28 shows one of the images, and Figure 29 shows the lines extracted from it. The average gray levels were calculated using strips of width 4, based on knowledge about the resolution of the image. The typical gray levels of roads and buildings were taken to be equal in calculating the probability vectors. The histogram of "other" probabilities is shown in Figure 30. From this histogram it is clear that we can completely differentiate between two classes of object boundaries, namely objects and noise. Figure 31 shows the line segments whose probabilities of being a piece of road or building are not equal to zero. This figure shows quite an improvement in rejecting the noise edges. Figure 32 shows the results of finding compatible segments, and Figure 33 shows the results of finding anti-parallel segments: the midpoints of the anti-parallel pairs are connected together. Figures 34 and 35 show the high confidence buildings and roads; Figures 36 and 37 show the buildings and roads with probabilities ≥ 0.75, and Figures 38 and 39 show those with probabilities ≥ 0.5.

Two other examples are shown in Figures 40 - 50 and 51- 61; these are analogous to Figures 28 - 39, except that the histograms of "other" probabilities are not shown. Two further examples taken from the same aerial photograph, but involving non-residential buildings, are shown in Figures 62-69 and 70-77.

7. Variations

7.1 Edge segment adjustment

The bottom-up nature of the approach described in Sections 3-5 makes the results dependent on good choices of the initial edge segments. In this section several experiments are described aimed at improving the positions, orientations, or lengths of these segments.

a) Changing the segment's position

In this experiment the line segments were moved a few steps in each direction so that they remained parallel with the given line. Two different figures of merit, namely the maximum gradient and minimum standard deviation of the gray level on both sides of each line, were used to evaluate the position of a line segment. Referring to Figure 7a, at each step the new end coordinates are

$$x11 = x1+\Delta x \qquad x21 = x2+\Delta x$$

$$y11 = y1-\Delta y \qquad y21 = y2-\Delta y$$

for side 1 and

$$x12 = x1-\Delta x \qquad x22 = x2-\Delta x$$

$$y12 = y1+\Delta y \qquad y22 = y2+\Delta y$$

for side 2 where $\Delta x = di \sin\theta$

$$\Delta y = di \cos\theta \quad \text{when} \quad 0 \le \theta < 90$$

and $$\Delta y = -di \cos\theta \quad \text{when} \quad 90 \le \theta < 180$$

where di is the distance moved at step i and θ is the angle of the line with respect to the x-axis.

At each step the average gray levels on side 1 and side 2 are calculated. The gradient at step i is

$$gi = g2-g1$$

where g1 and g2 are the average gray levels on side 1 and side 2. The maximum gradient is calculated as

$$gmax = max|gi|$$

The end coordinates of the line associated with the position of the maximum gradient are selected as the new coordinates of the line segment.

Figure 79 shows the effects of this method on the line segments of Figure 29 for four steps of movement in each direction and di = 1,2,3,4. The result of this experiment is that no major change of position was made for long line segments, but there were some bad effects on the short line segments. The reason is that short line segments are moved towards the neighboring long segments where the gradient is maximum.

Another figure of merit, the minimum standard deviation of the gray levels along the line segments, was also used to relocate the lines. The standard deviation at step i is

$$\sigma_i^2 = \sum_{k,j} (g(k,j)-g)$$

where g(k,j) is the gray level of point (k,j) and g is the average gray level inside each strip. The minimum standard deviation is calculated as

$$\sigma_i min = min|\sigma_i|$$

Figure 80 shows the effects of this experiment. As shown in this figure the line segments have the tendency to relocate themselves where the gray levels are more uniform. The result is that they usually move towards the center of the objects and therefore more confusion will occur.

b) <u>Changing the segment's angle</u>

In this experiment each line segment is rotated around its center point in both directions, a few degrees at each step. As before, two different figures of merit were used to relocate the line segments. Referring to Figure 81, at each step the new coordinates are

$$x_1' = x_1 - \Delta x \qquad x_2' = x_2 + \Delta x$$

$$y_1' = y_1 + \Delta y \qquad y_2' = y_2 - \Delta y$$

where $\Delta x = \ell \sin \varphi_i/2 \sin(\theta+\varphi i/2)$

$\Delta y = \ell \sin \varphi_i/2 \cos(\theta+\varphi i/2)$

where φ_i is the angle of rotation at each step and ℓ is the length of the line. In this formulation if the line is rotated anti-clockwise φ_i is taken to be a positive number; otherwise φ_i is taken to be a negative number.

Figure 82 shows the results of changing the angles after relocating the lines in the position of maximum gradient. In general no improvement has been made regarding the positions of the line segments in the scene. Similarly, Figure 83 shows the result of changing the angles and relocating the lines in the position of minimum standard deviation. Here again no improvement has been made.

In the above experiments φ_i is taken to be ix5° and four steps of rotation are allowed. The width of the strip along the line segment is taken to be 4. Other experiments such as first rotation and then translation or vice versa have been performed and similar results have been found. The results are shown in Figures 84 to 87.

c) Changing the segment's length

When lines are fitted to components of edge points, in some places the lines overshoot the components at their ends. This may be due to noise in the edges near their ends or to the presence of nearby edges with similar directions. To study this effect some experiments have been performed to adjust the length of the fitted lines. The similarity of gray scale along the object side of the segment is used for this type of adjustment. Referring to Figure 88, the average gray level along the object side of the line (here the brighter side) is calculated. Then the average gray level along the object side near each end is calculated. A square of 4*4 is used for this purpose. Let g be the average gray level along the object side and g_{end} be the average gray level in the small neighborhood near the end. If the difference

$$|g-g_{end}| > \text{Threshold}$$

the length is reduced. The new coordinates are

$$x11 = x1 - d\cos\theta \quad x22 = x2 + d\cos\theta$$

$$y11 = y1 - d\sin\theta \quad y22 = y2 + d\sin\theta$$

where d is the width of the strip for calculation of average gray level. This process is continued for both ends until

$$|g - g_{end}| < \text{Threshold}$$

When this inequality is satisfied the corresponding end coordinates are selected as the new end coordinates for the line segments.

The results of this experiment for different thresholds (5,4,3) are shown in Figures 89-91. When the threshold is high (5) only a few changes occur in the lines. When the threshold is 3 or 4 both the overshot lines and some of the other lines become shorter. This shows that a unique threshold cannot be used for all the lines. The best result is obtained when the threshold is dynamically set equal to the standard deviation of the gray level of the object side for each line segment. The result is shown in Figure 92.

From the experiments described in (a-c) above it appears that no improvement results from adjustment of the positions or orientations of the line segments; but there is some improvement when the lengths are adjusted using a dynamic thresholding process as described above. However, these improvements have little effect on the final results. For example, the building and road segments with confidences of 1, 0.75, and 0.5 obtained after maximum-gradient angle adjustment are shown in Figures 93-98. Analogous results for dynamic-threshold length adjustment are shown in Figures 99-104.

7.2 Shadow detection

One of the features that can be used for verification of the recognition of buildings is the shadow of the building. There are cases where a parking lot can be recognized as a building, since they may have the same size or shape. It seems that it is possible to use the shadow for further verification. To study this, some experiments have been performed using the average gray level within a strip along each line segment and the angle of the line segment.

Referring to Figure 105, each line segment with angle θ with respect to the x-axis has two sides. There are two average gray levels associated with each line segment. The average gray levels g1 and g2 are associated with angles θ and $2\pi-\theta$ respectively.

Scatter plots of g1 and g2 with respect to θ are shown in Figure 106 for all of the line segments and in Figure 107 for the line segments after noise cleaning. Figure 107 shows that at dark gray levels, the population of points for $\theta > 180°$ is greater than the population of points for $\theta < 180°$. This shows that in certain orientations along the line segments, there exist dark shadow regions.

To study this effect quantitatively, let us pick the darkest P% of the population. Let

n1 = number of dark points in the interval $(\theta, \theta+\pi)$

and

n2 = number of dark points in the interval $(\theta+\pi, \theta+2\pi)$

for θ = 0,20,40,...,340. The plots of n1/n2 as a function of θ for different values of P and for the line segments after and before noise cleaning are shown in Figure 108 and Figure 109 respectively. These figures show that there is a peak around 180°. The peak is greater for the segments after noise removal. As expected, if P is increased the peak becomes smaller. This effect was tested on several other scenes and similar results were obtained.

These results show that shadow detection is most reliable after noise segments have been eliminated. Shadows could be used to verify the recognition of buildings (which may have shadows) and roads (which should not).

8. Concluding remarks

The approach used in this paper is quite elementary and straightforward. It proceeds in an essentially bottom-up fashion, with no provision, as yet, for top-down feedback between levels, and it makes no use of higher-level information, e.g. that buildings are alongside roads, or that roads form a connected network. It uses less knowledge than the road-finding systems of Fischler et al. [10], and handles fewer types of objects than the aerial photographic interpretation system of Nagao et al. [11]. Nevertheless, it serves to illustrate the level of performance that can be achieved by a straightforward hierarchical system. It is expected that this performance will continue to improve as additional levels of knowledge, and a more flexible control structure, are incorporated into the system.

It would be of interest to investigate a relaxation-like (or MSYS-like) scheme for classifying the feature segments. Initially, each individual segment would be probabilistically classified, on the basis of its properties, as being (part of) a road, building, etc. These probabilities would then be adjusted based on their compatibilities with those of nearby or otherwise related segments. One should not expect that a simple algebraic formula can be used to compute the probability adjustments; rather, they would be computed by a probabilistic "decision tree" associated with each segment. This approach should result in a generally consistent classification (which, of course, may still be ambiguous). If inconsistencies remain, they would probably reflect errors in the feature segment extraction process, assuming that the compatibility models are adequate.

References

1. R. B. Eberlein, An iterative gradient edge detection algorithm, Computer Graphics Image Processing 5, 1976, 245-253.

2. S. Peleg and A. Rosenfeld, Straight edge enhancement and mapping, Computer Science TR-694, University of Maryland, College Park, MD, September 1978.

3. G. J. VanderBrug, Experiments in iterative enhancement of linear features, Computer Graphics Image Processing 6, 1977, 25-42.

4. B. J. Schachter, A. Lev, S. W. Zucker, and A. Rosenfeld, An application of relaxation methods to edge reinforcement, IEEE Trans. Systems, Man, Cybernetics 7, 1977, 813-816.

5. R. Nevatia and K. Babu, Linear feature extraction, Proceedings, Image Understanding Workshop, November 1978, 73-78.

6. G. J. VanderBrug and A. Rosenfeld, Linear feature mapping, IEEE Trans. Systems, Man, Cybernetics 8, 1978, 768-774.

7. A. Scher, M. Shneier, and A. Rosenfeld, Clustering of collinear line segments, TR-888, Computer Vision Laboratory, Computer Science Center, University of Maryland, College Park, MD, April 1980.

8. R. Brooks, Global directed edge linking and ribbon finding, Proceedings, Image Understanding Workshop, April 1979, 72-78.

9. A. Scher, M. Shneier, and A. Rosenfeld, A method for finding pairs of anti-parallel straight lines, TR-845, Computer Vision Laboratory, Computer Science Center, University of Maryland, College Park, MD, December 1979.

10. M. J. Fischler, G. J. Agin, H. G. Barrow, R. C. Bolles, L. H. Quam, J. M. Tenenbaum, and H. C. Wolf, The SRI road expert: an overview. Proceedings, Image Understanding Workshop, November 1978, 13-19.

11. M. Nagao, T. Matsuyama, and Y. Ikeda, Region extraction and shape analysis in aerial photographs, Computer Graphics Image Processing 10, 1979, 195-223.

# of cases	Segment A case	Segment A side	Segment B case	Segment B side	Similar to:
1	a	1	a	1	--
2	a	1	a	2	--
3	a	1	b	1	--
4	a	1	b	2	--
5	a	2	a	1	#2
6	a	2	a	2	#1
7	a	2	b	1	#4 rotated 180°
8	a	2	b	2	#3 rotated 180°
9	b	1	a	1	#3
10	b	1	a	2	#7
11	b	1	b	1	#1
12	b	1	b	2	#2 rotated 90°
13	b	2	a	1	#4
14	b	2	a	2	#8
15	b	2	b	1	#12
16	b	2	b	2	#6

Table 1. Different cases of pairs of line segments according to the conventions of Figure 5.

Case	Geometrical conditions	Similarity conditions for the line a_2b_1
1	$a_2b_1 < a_2b_2/m$ $a_2b_1 < a_1b_1/m$	If $a_2b_1 < d$ or $x_pb_1 < d$ no check or $x_pa_2 < d$
	$\theta_A \neq \theta_B$	
(a)	$x_{a_2} \leq x_p < x_{a_1}$ $x_{b_2} < x_p \leq x_{b_1}$	no check
(b)	$x_{a_2} < x_{b_1}$ $y_{a_2} \leq y_{b_1}$	check side 2
(c)	$x_{a_2} > x_{b_1}$ $y_{a_2} \geq y_{b_1}$	check side 1
(d)	$x_{a_2} < x_{b_1}$ $y_{a_2} > y_{b_1}$	check side 1
(e)	$x_{a_2} \geq x_{b_1}$ $y_{a_2} < y_{b_1}$	check side 2

Table 2. Geometrical and Similarity conditions for case 1.

	Geometrical conditions	Similarity conditions for line a_1b_1
Case 2	$a_1b_1 < a_2b_2/m$ $a_1b_1 < a_1b_2/m$ $a_1b_1 < a_2b_1/m$	If $a_1b_1 < d$ no check
(a)	$\theta_A \neq \theta_B$ $x_{a_2} < x_p \leq x_{a_1}$ $x_{b_2} < x_p \leq x_{b_1}$ $x_pa_1 < x_pa_2/m$, $x_pb_1 < x_pb_2/m$	no check
(b)	$y_{a_2} < y_0$ $x_{a_1} < x_{b_1}, y_{b_1} > y_{a_1}$	If $\theta_A \neq \theta_B$ and $x_pa_1 < d$ no check else check side 1
(c)	$y_{a_2} < y_0$ $x_{a_1} > x_{b_1}$, $y_{b_1} \leq y_{a_1}$	If $\theta_A \neq \theta_B$ and $x_pb_1 < d$ no check else check side 2
(d)	$y_{a_2} < y_0$ $x_{a_1} \geq x_{b_1}, y_{b_1} > y_{a_1}$	check side 1
(e)	$y_{a_2} > y_0$ $x_{a_1} > x_{b_1}, y_{a_1} > y_{b_1}$	If $\theta_A \neq \theta_B$ and $x_pb_1 < d$ no check else check side 2
(f)	$y_{a_2} > y_0$ $x_{a_1} < x_{b_1}, y_{a_1} \leq y_{b_1}$	If $\theta_A \neq \theta_B$ and $x_pa_1 < d$ no check else check side 1
(g)	$y_{a_2} > y_0$ $x_{a_1} \leq x_{b_1}, y_{a_1} > y_{b_1}$	check side 2

Table 3. Geometrical and similarity conditions for Case 2.

	Geometrical conditions	Similarity conditions for line a_1b_2
Case 3 end 1	$a_1b_2 < a_2b_1/m$	If $a_1b_2 < d$
	$a_1b_2 < a_2b_2/m$	no check
	$a_1b_2 < a_1b_1/m$	
(a)	$x_{a_2} < x_p \le x_{a_1}$	no check
	$x_pa_1 < x_pa_2/m$	
	$x_pb_2 < x_pb_1/m$	
	If $\theta_B \neq 90°$	
	$x_{b_1} < x_p \le x_{b_2}$	
	else $y_{b_2} < y_p < y_{b_1}$	
(b)	$x_{a_1} \ge x_{b_2}$	check side 1
	$y_{a_1} < y_{b_2}$	
(c)	$x_{a_1} < x_{b_2}$	check side 1
	$y_{a_1} \le y_{b_2}$	
(d)	$x_{a_1} < x_{b_2}$	If $x_pa_1 < d$ no check
	$y_{a_1} > y_{b_2}$	else check side 2
(e)	$x_{a_1} > x_{b_2}$	If $x_pb_2 < d$ no check
	$y_{a_1} \ge y_{b_2}$	else check side 2

Table 4. Geometrical and similarity conditions for case 3: end 1 of line A.

	Geometrical conditions	Similarity conditions for line a_2b_1
Case 3 end 2	$a_2b_1 < a_1b_2/m$	If $a_2b_1 < d$
	$a_2b_1 < a_2b_2/m$	no check
	$a_2b_1 < a_1b_1/m$	
	$x_pa_2 < x_pa_1/m$	
(a)	$x_pb_1 < x_pb_2/m$	no check
	$x_{a_2} \le x_p < x_{a_1}$	
	If $\theta_B \ne 90°$	
	$x_{b_1} \le x_p < x_{b_2}$	
	else $y_{b_2} < y_p \le y_{b_1}$	
(b)	$y_{b_1} \le y_{a_2}$	If $x_pa_2 < d$ no check
	$x_{a_2} > x_{b_1}$	else check side 1
(c)	$y_{b_1} < y_{a_2}$	check side 1
	$x_{a_2} \le x_{b_1}$	
(d)	$y_{a_2} \le y_{b_1}$	If $x_pb_1 < d$ no check
	$x_{a_2} < x_{b_1}$	else check side 2
(e)	$y_{a_2} \le y_{b_1}$	If $x_pa_2 < d$ no check
	$x_{a_2} > x_{b_1}$	else check side 2

Table 5. Geometrical and similarity conditions for case 3: end 2 of line A.

	Geometrical conditions	Similarity conditions for line a_1b_1
Case 4 end 1	$a_1b_1 < a_2b_2/m$	If $a_1b_1 < d$ no check
	$a_1b_1 < a_2b_1/m$	
	$a_1b_1 < a_1b_2/m$	
	$x_pa_1 < x_pa_2/m$	
	$x_pb_1 < x_pb_2/m$	
(a)	$x_{a_2} < x_p \le x_{a_1}$	no check
	If $\theta_B \neq 90°$	
	$x_{b_1} \le x_p < x_{b_2}$	
	else $y_{b_2} < y_p < y_{b_1}$	
(b)	$x_{a_1} \ge x_{b_1}$	check side 2
	$y_{a_1} > y_{b_1}$	
(c)	$x_{a_1} < x_{b_1}$	check side 1
	$y_{a_1} \le y_{b_1}$	
(d)	$x_{a_1} > x_{b_1}$	If $x_pb_1 < d$ no check
	$y_{a_1} > y_{b_1}$	else check side 2
(e)	$y_{a_1} < y_{b_1}$	If $x_pa_1 < d$ no check
	$x_{a_1} \ge x_{b_1}$	else check side 1

Table 6. Geometrical and similarity conditions for Case 4: end 1 of line A.

	Geometrical conditions	Similarity conditions for line a_2b_2
Case 4 end 2	$a_2b_2 < a_1b_1/m$	If $a_2b_2 < d$ no check
	$a_2b_2 < a_2b_1/m$	
	$a_2b_2 < a_1b_2/m$	
	$x_pa_2 < x_pa_1/m$	
	$x_pb_2 < x_pb_1/m$	
(a)	$x_pa_2 \leq x_p < x_{a_1}$	no check
	If $\theta_B \neq 90°$	
	$x_{b_1} < x_p \leq x_{b_2}$	
	else $y_{b_1} \leq y_p < y_{b_2}$	
(b)	$x_{a_2} > x_{b_2}$	If $x_pa_2 < d$ no check
	$y_{a_2} \geq y_{b_2}$	else check side 1
(c)	$x_{a_2} \leq x_{b_2}$	If $x_pa_2 < d$ no check
	$y_{a_2} > y_{b_2}$	else check side 1
(d)	$x_{a_2} \geq x_{b_2}$	If $x_pb_2 < d$ no check
	$y_{a_2} < y_{b_2}$	else check side 2
(e)	$x_{a_2} < x_{b_2}$	If $x_pb_2 < d$ no check
	$y_{a_2} < y_{b_2}$	else check side 2

Table 7. Geometrical and similarity conditions for Case 4: end 2 of line A.

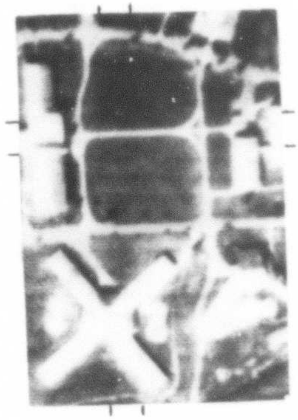

Figure 1. (a) Window of the Occoquan photograph, showing parts of Lorton reformatory

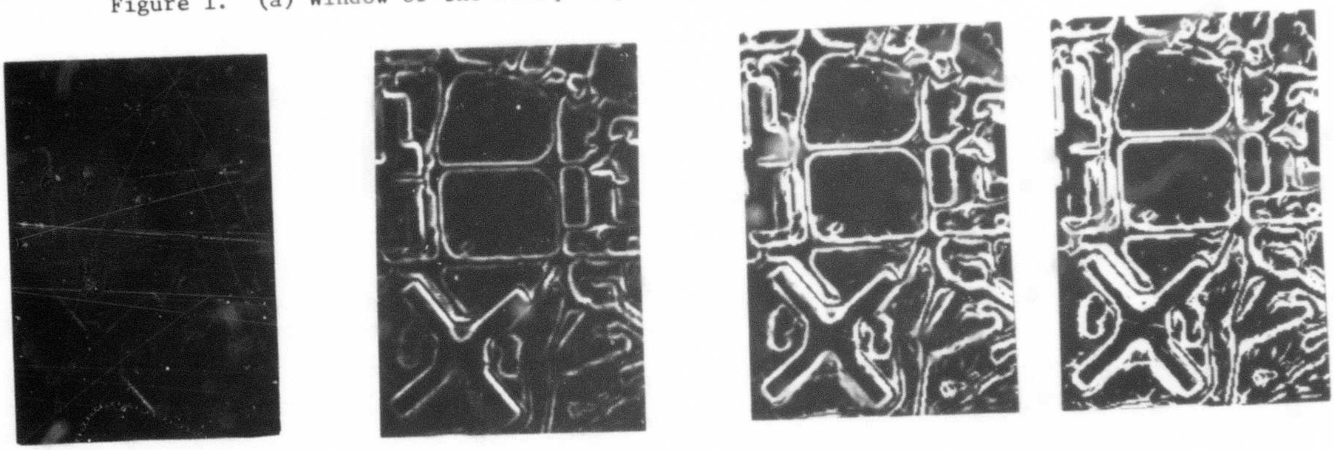

Figure 1. (b) Original Sobel gradient magnitudes and three iterations of the enhancement process

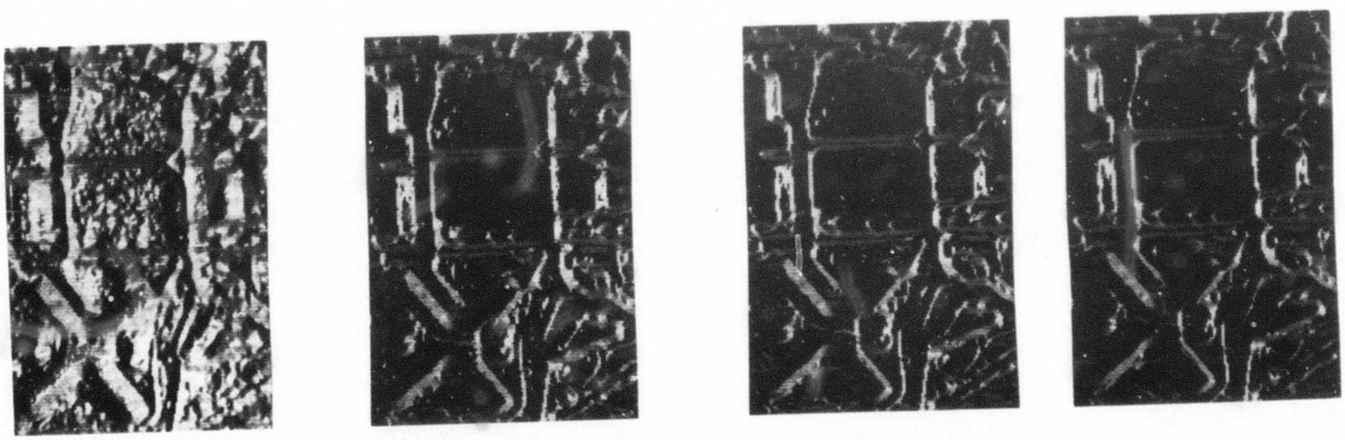

Figure 1. (c) Gradient directions, displayed as gray levels ranging from black to white as the direction (from dark to light) varies from 0° to ±180°; originals and three iterations of enhancement

(d1)

20	19	18	18	17	18	19	20	20	20	19	18	18	19	19	19	19	19	19	19
20	20	19	18	19	19	20	20	20	20	19	19	19	19	19	19	18	18	19	20
20	20	20	20	21	21	20	20	20	20	20	20	19	19	19	19	18	18	19	19
20	20	21	22	22	21	21	20	20	21	21	20	20	20	20	19	19	19	19	19
21	21	22	22	23	22	21	21	21	22	22	22	21	20	21	20	20	20	21	20
24	23	23	24	24	23	23	23	24	24	25	24	23	22	23	23	23	23	24	23
28	28	28	28	28	28	29	29	30	30	30	30	29	29	29	29	29	30	30	30
34	34	34	35	35	35	35	36	36	36	36	36	36	36	36	36	36	36	36	36
38	38	38	38	38	38	38	38	39	39	38	39	38	38	38	38	38	38	38	38
36	36	36	36	36	36	36	36	36	35	35	35	35	35	35	35	35	35	34	34
30	30	31	30	29	29	29	29	29	28	28	28	29	29	29	29	29	29	28	27
25	26	26	25	25	25	24	25	24	23	23	24	24	25	26	25	26	25	24	24
24	23	23	23	23	23	23	23	22	22	22	22	23	24	24	23	23	23	22	23
23	22	22	21	22	21	21	21	21	21	22	22	23	23	22	22	22	22	22	22
22	21	21	20	20	20	20	20	21	21	21	22	22	22	21	21	21	21	21	21
21	20	21	20	20	20	20	20	20	21	21	21	21	21	20	20	20	20	21	21
20	20	20	20	20	20	20	20	20	20	20	20	20	20	20	20	20	20	21	20
20	20	19	19	19	19	20	20	20	19	19	19	19	19	19	19	20	20	20	19
20	19	18	18	18	19	19	19	19	19	19	19	19	19	19	20	20	19	19	19
20	19	19	18	18	19	18	18	18	19	19	19	19	19	19	20	19	19	19	19

(d2)

1	2	2	2	2	2	2	1	1	2	2	2	2	1	1	1	1	0	1	2
1	1	2	3	4	3	2	1	0	1	1	2	1	1	0	1	1	0	1	0
1	1	2	4	3	2	1	1	1	1	2	2	1	1	1	1	1	1	1	0
1	2	2	2	2	2	1	1	2	2	2	2	2	2	2	2	2	2	2	2
4	3	3	2	2	2	3	3	4	4	4	4	3	3	3	4	4	5	5	5
7	7	7	6	6	7	8	9	9	9	8	8	9	9	9	9	10	10	10	10
11	11	11	11	12	12	13	13	13	12	12	12	13	14	14	13	13	13	13	13
10	10	10	10	10	10	10	9	9	9	9	9	9	9	9	9	9	9	8	8
3	2	2	2	1	1	1	1	0	1	1	1	1	1	1	1	1	1	1	2
7	7	7	8	8	9	9	9	10	10	10	10	9	9	9	9	9	9	10	10
10	10	10	10	11	11	11	11	11	12	11	11	10	10	9	9	9	9	10	10
6	7	7	7	6	6	6	6	6	6	6	6	5	5	5	5	6	6	5	4
2	3	4	3	3	3	3	3	3	2	1	1	1	2	3	3	3	3	2	2
2	2	2	2	3	3	3	2	1	1	0	1	1	2	2	2	2	1	1	1
2	1	1	1	1	1	1	1	0	0	0	1	1	2	2	2	2	1	1	1
1	1	1	1	0	0	0	0	0	1	1	1	2	1	1	1	1	0	0	1
1	1	1	1	1	0	0	0	0	1	2	2	2	1	1	0	0	0	1	1
2	1	1	2	1	1	1	1	1	1	1	1	1	1	0	0	0	1	1	1
2	2	1	1	0	0	1	2	1	0	0	0	0	0	1	1	1	1	1	1
2	2	1	1	1	1	1	0	0	0	0	0	0	0	0	0	1	1	1	1

(d3)

0	0	0	0	0	0	0	0	0	0	0	0	0	0	0	0	0	0	0	0
0	0	0	7	8	7	0	0	0	0	0	0	0	0	0	0	0	0	0	0
0	0	0	7	8	0	0	0	0	0	0	0	0	0	0	0	0	0	0	0
0	0	0	0	0	0	0	0	0	0	0	0	0	0	0	0	0	0	0	0
10	0	0	0	0	0	0	0	0	12	12	11	10	0	0	0	0	0	0	14
19	19	17	17	16	19	21	23	23	22	21	22	22	23	23	24	25	25	25	25
26	26	26	26	26	28	28	30	29	28	27	28	29	30	30	30	30	30	29	29
22	22	22	22	22	23	22	22	21	20	19	20	20	20	20	20	20	20	19	18
0	0	0	0	0	0	0	0	0	0	0	0	0	0	0	0	0	0	0	0
14	14	15	16	17	18	19	19	20	22	21	20	20	19	19	19	18	19	20	21
22	22	23	23	23	24	25	24	26	25	26	24	24	21	21	22	21	22	22	22
17	17	18	18	17	17	17	17	17	16	16	15	15	13	14	15	16	15	14	13
0	9	10	10	0	9	10	10	8	0	0	0	0	0	8	9	9	0	0	0
0	0	0	0	5	6	6	0	0	0	0	0	0	0	0	0	0	0	0	0
0	0	0	0	0	0	0	0	0	0	0	0	0	0	0	0	0	0	0	0
0	0	0	0	0	0	0	0	0	0	0	0	0	0	0	0	0	0	0	0
0	0	0	0	0	0	0	0	0	0	0	0	0	0	0	0	0	0	0	0
0	0	0	0	0	0	0	0	0	0	0	0	0	0	0	0	0	0	0	0
0	0	0	0	0	0	0	0	0	0	0	0	0	0	0	0	0	0	0	0
0	0	0	0	0	0	0	0	0	0	0	0	0	0	0	0	0	0	0	0

Figure 1. (d) Gradient magnitudes displayed numerically on a scale of 0–63 for a small subwindow, indicated by tick marks in (a): (d1) subwindow gray levels; (d2) original gradient magnitudes; (d3-5) results of three iterations

(d4)

0	0	0	0	0	0	0	0	0	0	0	0	0	0	0	0	0	0	0	0
0	0	0	0	12	8	0	0	0	0	0	0	0	0	0	0	0	0	0	0
0	0	0	0	0	0	0	0	0	0	0	0	0	0	0	0	0	0	0	0
0	0	0	0	0	0	0	0	0	0	0	0	0	0	0	0	0	0	0	0
0	0	0	0	0	0	0	0	0	0	31	28	0	0	0	0	0	0	0	0
46	45	41	40	42	42	47	49	55	52	54	53	54	54	51	52	53	53	57	58
61	62	61	60	63	63	63	63	63	63	63	63	63	63	63	63	63	63	63	63
48	47	47	46	48	48	50	47	47	45	45	45	46	47	47	47	47	46	45	45
0	0	0	0	0	0	0	0	0	0	0	0	0	0	0	0	0	0	0	0
30	35	34	36	39	41	41	42	43	45	45	44	41	41	40	38	39	39	42	43
49	51	51	53	54	56	56	58	57	60	58	58	53	52	49	50	51	51	53	48
38	40	45	43	45	41	44	46	43	42	36	37	34	37	35	40	39	39	32	0
0	0	24	0	0	0	26	26	0	0	0	0	0	0	0	21	0	0	0	0
0	0	0	0	0	11	0	0	0	0	0	0	0	0	0	0	0	0	0	0
0	0	0	0	0	0	0	0	0	0	0	0	0	0	0	0	0	0	0	0
0	0	0	0	0	0	0	0	0	0	0	0	0	0	0	0	0	0	0	0
0	0	0	0	0	0	0	0	0	0	0	0	0	0	0	0	0	0	0	0
0	0	0	0	0	0	0	0	0	0	0	0	0	0	0	0	0	0	0	0
0	0	0	0	0	0	0	0	0	0	0	0	0	0	0	0	0	0	0	0
0	0	0	0	0	0	0	0	0	0	0	0	0	0	0	0	0	0	0	0

(d5)

0	0	0	0	0	0	0	0	0	0	0	0	0	0	0	0	0	0	0	0
0	0	0	0	0	8	0	0	0	0	0	0	0	0	0	0	0	0	0	0
0	0	0	0	0	0	0	0	0	0	0	0	0	0	0	0	0	0	0	0
0	0	0	0	0	0	0	0	0	0	0	0	0	0	0	0	0	0	0	0
0	0	0	0	0	0	0	0	0	0	0	0	0	0	0	0	0	0	0	0
63	63	63	63	63	63	63	63	63	63	63	63	63	63	63	63	63	63	63	63
63	63	63	63	63	63	63	63	63	63	63	63	63	63	63	63	63	63	63	63
63	63	63	63	63	63	63	63	63	63	63	63	63	63	63	63	63	63	63	63
0	0	0	0	0	0	0	0	0	0	0	0	0	0	0	0	0	0	0	0
63	63	63	63	63	63	63	63	63	63	63	63	63	63	63	63	63	63	63	63
63	63	63	63	63	63	63	63	63	63	63	63	63	63	63	63	63	63	63	63
63	63	63	63	63	63	63	63	63	63	63	63	63	63	63	63	63	63	0	0
0	0	0	0	0	0	0	0	0	0	0	0	0	0	0	0	0	0	0	0
0	0	0	0	0	0	0	0	0	0	0	0	0	0	0	0	0	0	0	0
0	0	0	0	0	0	0	0	0	0	0	0	0	0	0	0	0	0	0	0
0	0	0	0	0	0	0	0	0	0	0	0	0	0	0	0	0	0	0	0
0	0	0	0	0	0	0	0	0	0	0	0	0	0	0	0	0	0	0	0
0	0	0	0	0	0	0	0	0	0	0	0	0	0	0	0	0	0	0	0
0	0	0	0	0	0	0	0	0	0	0	0	0	0	0	0	0	0	0	0
0	0	0	0	0	0	0	0	0	0	0	0	0	0	0	0	0	0	0	0

Figure 1(d), continued

(e1)

225	207	207	243	270	297	297	315	270	207	225	243	270	315	270	180	180		270	270
225	225	225	270	270	270	270	270		225	225	243	270	270		180	180		0	
180	270	270	270	270	243	225	225	270	270	243	243	225	270	225	225	225	270	0	
225	270	297	297	243	225	225	225	270	270	243	243	243	270	243	243	243	270	270	243
256	270	288	297	243	225	252	270	284	284	256	243	236	270	270	256	270	270	270	259
262	262	270	270	260	262	270	270	277	270	270	256	257	270	270	263	270	276	270	264
264	264	270	270	266	270	270	274	270	270	270	266	266	270	270	270	270	270	270	266
270	270	270	270	270	270	270	277	270	263	270	263	263	270	270	270	270	270	270	270
252	270	270	270	270	270	270	270		180	90	90	135	90	90	90	90	135	135	90
98	90	90	97	97	90	90	90	96	96	90	90	90	90	90	90	90	97	96	90
101	90	96	101	96	96	90	90	100	94	90	90	90	90	90	90	90	103	101	90
100	90	98	98	100	100	90	100	108	100	90	80	79	79	101	101	90	108	101	90
117	108	104	108	90	108	90	108	108	90	90	45	45	90	108	108	90	108	117	90
117	117	117	117	90	108	90	90	90	90		0	45	117	117	117	90	135	90	90
117	135	135	135	90	135	90	90				90	90	117	117	90	90	90	90	135
135	135	180	180						90	90	90	90	135	135	90	90			180
180	180	135	135	90					90	90	90	90	135	135				90	135
180	135	135	90	90	90	90	90	135	135	90	90	90	90				90	135	135
180	180	180	180			90	90	90						270	270	180	135	180	180
180	207	225	225	270	270	180										180	225	225	225

Figure 1. (e) Gradient directions displayed in degrees for the subwindow: original

(e2)

			267	273	276														
			273	270															
260									278	262	252	249							264
264	266	270	269	266	266	271	271	276	271	269	262	262	269	271	270	271	273	270	269
267	269	270	270	269	271	273	274	270	271	267	269	269	269	270	271	271	271	271	270
269	270	270	271	271	271	271	274	270	269	270	267	269	270	270	270	270	270	270	271
98	94	91	93	94	90	90	91	93	93	91	90	90	91	90	90	91	93	93	93
97	91	93	96	94	93	90	91	94	93	90	89	89	90	90	89	91	97	97	91
96	91	96	97	98	94	91	96	100	97	90	84	82	82	93	94	93	101	100	91
	105	100	98		100	96	103	103						101	101	100			
				98	96	96													

(e3)

				280	287														
										266	262								
264	264	270	270	269	269	271	271	277	274	270	264	263	266	271	271	271	273	274	274
269	269	270	270	270	273	273	274	271	271	269	269	270	270	271	271	271	271	271	270
271	270	270	271	271	271	273	273	271	269	270	270	270	271	270	271	271	271	270	271
98	91	90	91	91	89	90	90	90	91	90	90	90	90	89	90	90	91	91	91
94	91	91	94	93	91	90	91	93	91	90	89	89	89	89	89	91	94	94	96
90	89	94	97	96	89	91	94	98	96	89	86	84	82	87	91	96	98	94	
		96				97	100								96				
					105														

(e4)

					270														
264	269	271	270	270	271	273	271	274	276	274	264	264	270	271	271	271	271	273	276
270	270	270	271	271	273	273	274	273	273	270	270	270	270	271	271	271	273	273	271
271	270	270	271	271	271	273	273	271	270	270	270	270	271	271	271	271	271	271	271
94	90	90	90	90	89	90	90	90	90	90	90	90	90	89	89	90	90	91	91
93	90	90	93	91	91	89	91	91	91	90	89	87	87	87	89	91	93	97	96
91	87	91	97	93	86	87	96	97	91	89	87	86	86	84	90	96	93		

Figure 1. (e) Gradient directions displayed in degrees for the subwindow: three iterations

Figure 2. (a) Edge components extracted from the subwindow in Figure 1

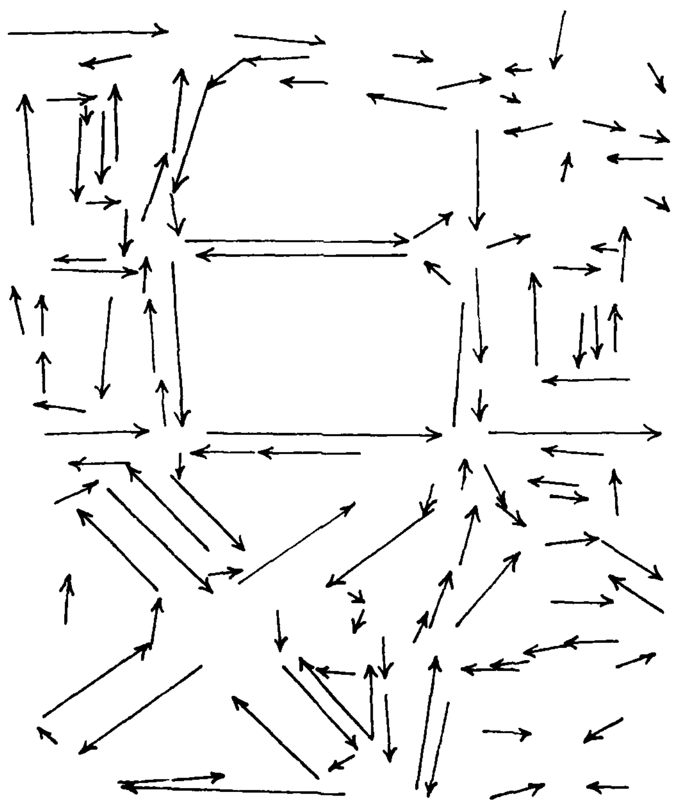

Figure 2. (b) Line segments fitted to the edge components in the window of Figure 1

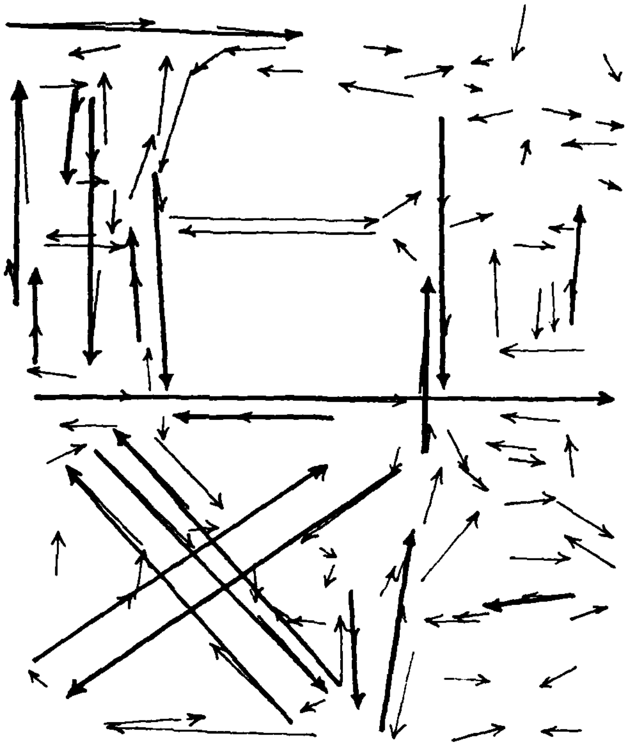

Figure 3. Results of collinear linking (heavy lines) for the window of Figure 1

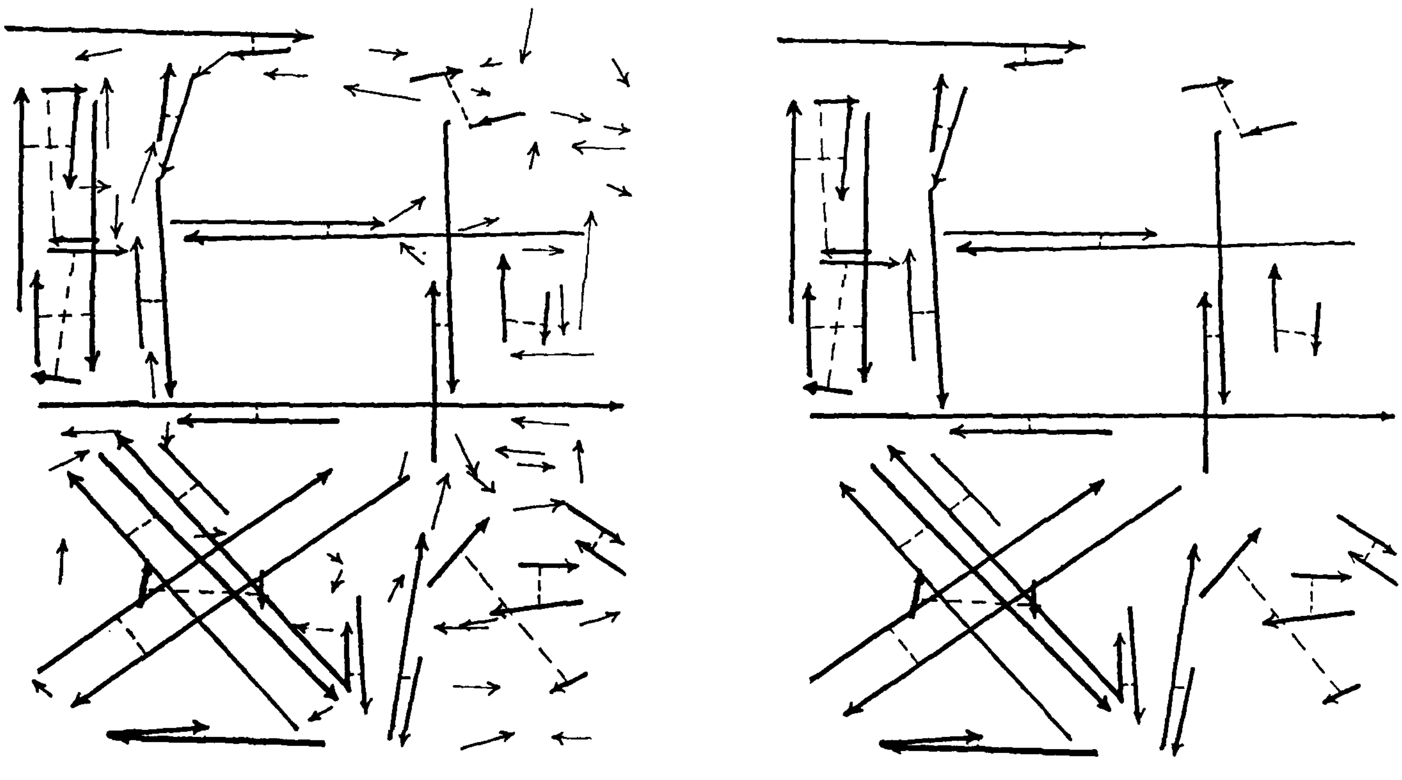

(a)

(b)

Figure 4. (a) Results of antiparallel linking (heavy lines, joined by dashed lines) for the window of Figure 3. (b) The antiparallel pairs only

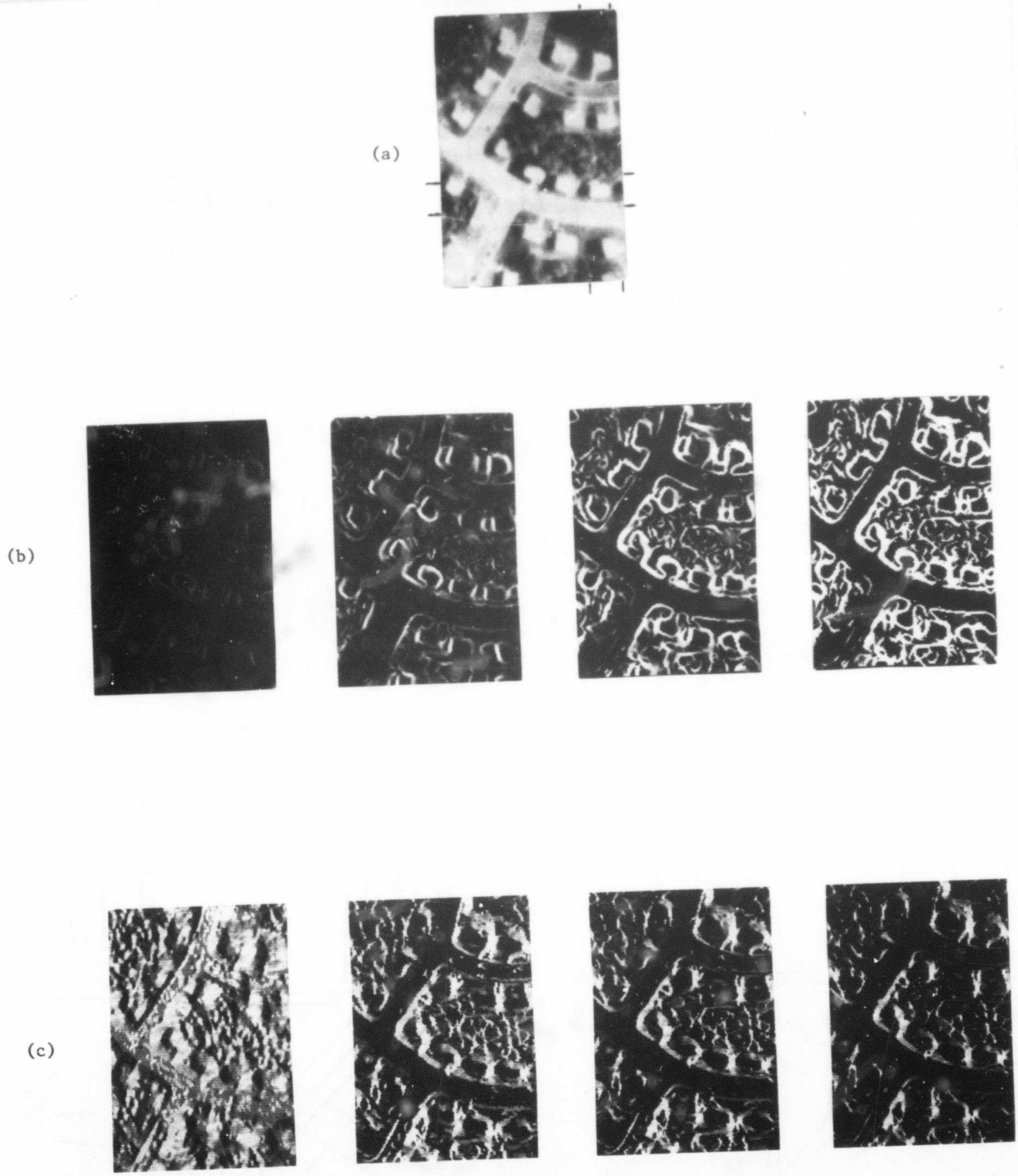

Figure 1'. Analogous to Figure 1 for a second window showing part of a new suburban area

(d1)

28	27	26	28	29	29	26	21	20	20	22	25	28	29	29	28	26	23	22	22	24	24	25	26
27	25	23	23	25	27	26	24	23	24	25	27	28	29	28	27	25	23	23	24	23	23	24	26
24	22	21	23	25	27	30	31	30	30	29	28	27	27	26	24	23	22	23	25	25	24	24	25
21	21	23	26	28	31	34	35	35	35	33	29	27	26	26	24	23	22	23	25	26	25	25	26
19	21	26	31	34	35	36	37	38	37	35	31	29	28	28	27	25	24	24	26	27	27	25	26
19	21	27	31	35	37	38	38	39	39	38	34	32	31	32	31	29	28	27	28	29	28	26	27
19	20	22	27	33	38	39	40	40	41	40	37	35	35	36	36	34	31	30	30	30	29	26	24
19	18	19	23	32	39	41	41	41	41	41	40	40	39	40	39	38	36	33	31	30	28	23	18
18	19	19	23	33	40	42	42	42	42	42	42	42	42	42	41	41	40	37	33	30	26	19	14
17	18	19	23	33	40	42	43	43	43	43	43	43	43	43	42	42	41	39	35	30	25	18	13
14	16	18	24	34	41	43	43	43	43	43	43	43	43	43	43	42	42	40	36	29	25	18	13
12	13	18	25	35	41	43	43	44	43	43	43	44	44	43	43	43	42	40	36	30	25	18	13
12	13	18	25	36	42	43	43	43	44	44	44	44	44	43	43	43	42	41	36	31	26	19	14
15	15	18	25	35	42	43	43	43	44	43	43	43	43	43	43	43	42	40	37	31	26	20	17
19	20	20	25	35	41	43	43	43	43	43	43	43	43	43	43	42	42	40	36	30	26	22	20
24	24	23	27	35	39	42	42	42	42	42	42	42	43	42	42	42	40	39	34	29	26	24	22
27	27	27	28	31	35	39	39	39	38	39	39	40	41	40	40	39	38	36	33	29	26	25	24
29	29	28	29	31	34	36	35	34	34	34	36	36	37	37	36	34	33	32	31	29	28	25	24
30	30	31	34	36	37	36	33	31	31	32	33	33	34	35	35	32	30	30	30	29	28	25	23
34	34	36	39	40	40	37	34	32	33	33	33	32	34	36	36	33	31	30	30	30	28	25	23
39	40	40	41	42	42	40	38	36	36	36	36	36	37	38	38	36	34	33	33	33	32	29	28
42	42	43	43	43	43	42	41	40	40	40	40	40	40	40	40	39	39	38	38	38	37	36	35
40	42	43	43	44	43	43	42	42	42	42	42	42	42	41	41	41	41	41	41	41	40	39	38
38	40	42	43	43	43	43	43	43	43	42	43	43	43	42	42	42	42	42	42	42	42	41	39

(d2)

1	2	4	6	5	4	7	6	4	5	6	6	4	1	1	4	6	4	3	3	1	1	2	1
3	5	5	4	4	1	5	9	10	10	7	3	1	2	3	4	4	2	1	2	2	0	2	2
5	3	1	4	5	6	8	11	12	11	8	3	1	2	3	3	3	1	2	2	3	2	1	2
3	2	7	9	9	8	7	7	8	7	7	6	3	2	2	4	4	2	2	2	2	3	2	2
1	6	8	9	8	6	5	4	4	5	7	7	5	6	6	7	7	6	5	4	3	3	2	2
2	6	9	8	6	3	3	3	3	4	7	8	7	7	8	9	9	8	6	5	3	3	2	2
2	4	9	11	11	6	3	3	3	3	5	7	8	8	8	9	9	8	6	4	2	5	6	8
2	1	5	12	15	8	3	3	2	2	3	5	7	7	6	6	7	9	8	5	4	8	11	11
3	1	4	13	16	9	2	2	2	2	3	3	4	4	4	4	4	6	9	8	7	11	12	8
4	2	5	14	17	9	2	1	1	1	1	1	1	1	2	2	2	3	7	9	10	12	12	7
4	5	8	15	16	8	2	1	1	1	0	1	1	1	1	1	1	3	6	11	11	12	12	7
1	5	11	17	16	8	1	0	1	1	1	1	1	1	1	1	1	3	6	11	11	12	12	7
3	5	11	17	16	7	1	0	0	1	1	0	0	1	1	0	1	3	6	10	11	12	12	8
7	6	9	16	16	7	1	0	0	0	1	1	1	1	1	1	1	3	6	10	11	11	9	7
9	8	7	14	15	7	2	1	1	1	1	1	0	0	1	1	2	3	6	10	10	8	8	7
8	8	6	10	11	8	5	4	4	4	4	3	3	2	2	3	3	4	6	10	9	6	5	5
5	5	5	5	7	8	6	7	7	8	7	6	6	5	5	6	7	7	7	7	7	5	3	2
3	4	5	6	7	4	2	5	7	7	6	6	6	6	5	5	7	7	5	5	4	4	4	2
6	6	8	10	9	6	4	5	2	1	1	2	3	2	1	3	5	3	1	2	3	5	5	2
10	10	9	8	6	5	7	7	5	5	4	4	3	4	3	5	6	5	4	4	4	6	7	5
8	8	7	5	4	4	6	8	8	8	7	8	8	6	5	5	7	8	8	8	9	10	11	12
2	2	3	3	2	2	4	5	6	6	6	6	6	5	4	4	5	7	8	8	8	9	10	10
4	2	1	0	0	1	1	2	3	3	3	3	3	3	3	3	3	4	4	4	5	5	5	6
3	3	2	1	0	1	1	1	1	1	1	1	1	2	2	2	2	2	2	2	2	2	4	6

(d3)

0	0	0	11	8	0	0	13	10	13	16	15	10	0	0	9	11	8	6	0	0	0	0	0
6	10	8	7	0	0	0	19	24	23	16	10	0	0	7	9	8	0	0	0	0	0	0	0
9	8	0	0	0	12	18	24	28	25	16	10	0	0	4	6	5	0	0	0	5	0	0	0
6	0	0	19	19	20	17	19	20	19	19	14	9	0	0	0	0	0	0	0	0	6	0	0
0	0	18	0	14	15	12	12	12	15	18	18	15	12	15	15	16	14	11	9	8	5	0	0
0	0	20	20	16	12	8	8	8	11	16	19	17	18	20	21	20	18	15	10	8	8	0	0
0	0	20	26	23	15	9	8	7	8	13	17	18	20	20	20	22	21	15	9	0	11	0	20
0	0	15	28	32	21	10	6	0	0	9	12	16	17	16	15	18	21	19	14	0	18	24	25
6	0	0	31	37	24	0	0	0	0	5	8	9	11	10	9	11	17	20	19	0	27	28	22
10	0	0	33	36	23	0	0	0	0	0	0	0	0	0	0	0	11	18	22	27	30	29	19
9	13	0	37	38	23	0	0	0	0	0	0	0	0	0	0	0	8	17	26	30	31	28	19
0	12	0	39	36	21	0	0	0	0	0	0	0	0	0	0	0	8	17	25	30	32	29	19
7	13	29	41	38	21	0	0	0	0	0	0	0	0	0	0	0	8	17	25	29	30	27	18
16	17	22	38	37	0	0	0	0	0	0	0	0	0	0	0	0	8	16	24	28	27	24	20
21	20	0	31	33	20	0	0	0	0	0	0	0	0	0	0	0	9	16	24	26	22	18	16
20	18	17	22	26	20	13	9	11	0	0	0	7	0	0	7	10	13	17	22	21	16	0	10
13	14	0	15	16	0	12	14	17	17	16	14	13	12	11	12	14	16	18	17	17	12	9	0
10	0	14	14	0	0	0	0	14	14	14	14	13	12	10	11	12	14	13	0	11	12	9	0
17	16	19	21	18	0	0	0	0	0	0	0	0	0	0	0	10	8	0	0	8	11	11	0
23	22	22	19	16	13	16	16	12	10	0	8	8	6	7	8	11	10	10	10	12	0	18	14
18	18	16	13	10	10	15	17	18	17	17	16	16	14	10	11	16	17	18	19	19	21	24	24
0	0	0	6	0	0	0	12	15	15	15	15	15	14	10	10	13	16	18	19	19	21	23	21
5	0	0	0	0	0	0	0	0	9	0	0	9	8	7	7	9	10	12	13	12	13	15	17
5	6	0	0	0	0	0	0	0	0	0	0	0	0	0	0	0	0	0	0	0	0	10	14

Figure 1'. (d1-3)

(d4)

0	0	0	0	10	0	0	28	24	29	40	37	23	0	0	19	22	0	10	0	0	0	0	0
0	13	18	0	0	0	0	0	55	54	40	21	0	0	0	15	17	0	0	0	0	0	0	0
24	15	0	0	0	0	41	52	63	59	40	20	0	0	0	0	0	0	0	0	0	0	0	0
18	0	0	0	29	38	44	47	51	48	46	38	22	0	0	0	0	0	0	0	0	0	0	0
0	0	0	0	33	36	35	32	33	39	47	45	35	34	31	34	31	28	23	20	0	0	0	0
0	0	36	30	32	30	26	20	22	29	43	46	42	47	49	52	50	44	34	24	18	0	0	0
0	0	34	55	58	40	26	18	16	19	32	41	45	49	49	51	51	47	38	0	0	21	0	43
0	0	0	63	63	51	24	0	0	0	18	29	39	42	40	39	45	52	49	0	0	30	50	62
0	0	0	63	63	58	0	0	0	0	0	0	23	24	23	22	30	44	51	47	0	62	62	55
18	0	0	63	63	57	0	0	0	0	0	0	0	0	0	0	0	29	47	54	0	63	63	48
0	0	0	63	63	53	0	0	0	0	0	0	0	0	0	0	0	20	43	63	63	63	63	51
0	31	0	63	63	54	0	0	0	0	0	0	0	0	0	0	0	21	45	63	63	63	63	46
19	21	0	63	63	0	0	0	0	0	0	0	0	0	0	0	0	21	43	62	63	63	63	48
42	44	51	63	63	0	0	0	0	0	0	0	0	0	0	0	0	21	43	61	63	63	55	45
52	35	0	63	63	33	0	0	0	0	0	0	0	0	0	0	0	24	43	60	63	50	38	41
47	34	35	46	52	39	31	22	0	0	0	0	0	0	0	0	21	32	42	55	55	42	0	0
33	0	0	32	0	0	0	33	29	36	31	29	25	25	25	28	32	34	41	35	37	32	0	0
21	0	23	29	0	0	0	0	0	29	28	27	26	24	24	21	25	32	27	0	26	29	20	0
38	43	42	40	0	0	0	0	0	0	0	0	0	0	0	0	0	0	0	0	10	25	28	0
54	53	49	43	33	34	23	21	22	0	0	0	18	18	0	17	21	26	24	25	0	0	34	34
41	39	37	28	22	20	32	41	39	38	37	35	35	30	27	25	29	37	41	43	45	49	45	56
0	0	0	0	0	0	0	0	34	32	34	35	33	31	27	25	30	40	44	45	48	51	54	50
0	0	0	0	0	0	0	0	0	0	0	0	0	19	17	17	19	24	27	28	29	34	38	37
0	4	0	0	0	0	0	0	0	0	0	0	0	0	0	0	0	0	0	0	0	0	27	37

(d5)

0	0	0	0	0	0	0	0	54	63	63	63	50	0	0	37	48	0	0	0	0	0	0	0
0	0	17	0	0	0	0	0	0	63	63	51	0	0	0	0	0	0	0	0	0	0	0	0
44	35	0	0	0	0	0	63	63	63	63	49	0	0	0	0	0	0	0	0	0	0	0	0
41	0	0	0	0	63	63	63	63	63	63	63	54	0	0	0	0	0	0	0	0	0	0	0
0	0	0	0	0	63	63	63	63	63	63	63	63	63	63	63	63	61	51	0	0	0	0	0
0	0	0	0	63	63	63	58	56	63	63	63	63	63	63	63	63	63	63	46	31	0	0	0
0	0	0	63	63	63	63	46	29	47	63	63	63	63	63	63	63	63	0	0	0	29	0	0
0	0	0	63	63	63	53	0	0	0	0	63	63	63	63	63	63	63	63	0	0	63	63	63
0	0	0	63	63	63	0	0	0	0	0	0	0	57	55	53	63	63	63	0	0	63	63	63
0	0	0	63	63	63	0	0	0	0	0	0	0	0	0	0	0	63	63	63	0	63	63	63
0	0	0	63	63	63	0	0	0	0	0	0	0	0	0	0	0	52	63	63	63	63	63	63
0	0	0	63	63	0	0	0	0	0	0	0	0	0	0	0	0	53	63	63	63	63	63	63
38	59	0	63	63	0	0	0	0	0	0	0	0	0	0	0	0	55	63	63	63	63	63	63
63	63	63	63	63	0	0	0	0	0	0	0	0	0	0	0	0	54	63	63	63	63	63	63
63	63	0	63	63	63	0	0	0	0	0	0	0	0	0	0	0	60	63	63	63	63	0	0
63	63	54	63	0	0	63	0	0	0	0	0	0	0	0	0	46	63	63	63	63	63	0	0
48	0	0	63	0	0	0	0	63	50	63	55	52	48	47	62	63	63	63	63	63	63	0	0
0	0	59	0	0	0	0	0	0	0	60	54	51	52	50	52	56	58	0	0	54	63	0	0
63	63	63	0	0	0	0	0	0	0	0	0	0	0	0	0	0	0	0	0	0	56	63	0
63	63	63	63	63	59	60	49	0	0	0	0	0	0	0	0	0	39	54	0	0	0	63	63
63	63	63	62	49	49	51	63	63	63	63	63	63	63	62	52	63	63	63	63	63	63	63	63
0	0	0	0	0	0	0	0	0	63	63	63	63	63	63	63	63	63	63	63	63	63	63	0
0	0	0	0	0	0	0	0	0	0	0	0	0	0	42	42	48	56	63	63	63	63	63	63
0	0	0	0	0	0	0	0	0	0	0	0	0	0	0	0	0	0	0	0	0	0	57	63

Figure 1'. (d4-5)

(e1)

315	135	90	72	79	135	180	198	243	281	308	322	315	315	180	180	190	207	252	288	315	45	45	45
108	135	101	63	45	45	233	252	264	276	285	304	0	90	124	135	153	153	315	297	243		0	0
113	124	0	315	315	308	284	264	266	264	256	236	180	117	146	146	146	135	0	297	252	243	315	333
108	0	315	302	294	297	293	278	263	255	231	218	214	243	225	225	225	243	315	315	270	236	270	333
90	350	333	319	300	297	293	284	270	239	219	219	239	260	260	248	248	260	281	297	270	236	243	333
27	10	18	21	0	326	288	288	270	243	225	225	248	270	270	252	246	249	270	281	270	214	207	90
27	45	41	31	15	350	288	270	270	252	225	231	256	270	270	252	246	243	252	256	225	180	153	117
27	45	23	10	0	346	304	270	270	270	236	248	262	270	270	252	248	238	235	225	180	159	149	128
18	0	0	356	356	353	315	270	270	270	252	252	256	270	256	243	243	232	221	210	188	170	162	145
45	45	11	356	357	353	333	270	270	270	270	270	270	270	243	243	243	214	203	193	180	176	176	172
63	45	7	353	353	346	333	270	270	225		270	270	225	225	225	225	198	190	186	186	180	180	180
45	23	0	357	353	353	315		270	225	270	270	270	225	225	225	225	198	190	186	190	190	184	188
270	338	354	0	356	352	315			270	225			180	180		180	180	190	186	186	190	194	210
270	297	342	356	0	0	0				135	90	90	180	180	180	180	180	180	180	180	186	198	231
270	277	309	347	0	8	27	90	90	90	135	90			180	135	153	162	170	169	174	187	210	236
277	263	297	343	10	35	53	90	104	90	90	90	72	90	117	108	124	135	153	169	173	190	217	233
281	259	281	338	15	35	63	98	98	90	82	80	80	90	101	108	113	113	129	158	180	203	214	225
304	256	281	297	315	333	90	121	105	90	80	80	80	80	101	121	124	113	121	143	180	194	194	180
280	270	291	293	288	270	207	180	153	90	45	90	72	45	90	180	169	162	135	180	198	191	180	180
270	276	288	291	280	248	225	225	248	270	270	256	288	315	288	233	218	233	256	256	243	218	225	248
270	277	285	293	270	243	232	240	256	270	270	263	270	288	281	248	236	249	263	270	257	248	250	256
270	297	288	270	270	225	225	239	260	270	270	270	270	270	270	256	248	255	263	270	263	252	253	253
63	45	45			225	225	243	252	252	270	270	270	252	252	252	252	256	256	270	259	248	239	218
34	34	27	45		180	225	225	270	225	270	270	270	243	243	270	270	270	270	243	243	243	225	198

Figure 1'. (e1)

(e2)

			80	87			211	239	285	308	316	31'6			174	186	205	248					
114	125	107	80				243	266	276	294	304			125	139	169							
121	122				294	284	270	269	266	249	240			160	166	172				257			
124			307	293	301	290	280	264	245	231	224	226									235		
		346		293	288	287	281	267	236	222	222	238	257	260	256	255	263	276	287	276	256		
		13	11	354	329	304	283	267	240	226	228	253	267	266	259	256	257	267	274	264	212		
		38	31	6	343	305	277	273	256	228	232	259	270	270	259	242	239	243	246		183		122
		27	11	0	350	307	276			236	242	263	267	267	259	242	236	232	224		170	145	129
25			0	359	354					267	267	266	266	259	255	250	231	222	214		172	165	143
41			356	356	354												218	208	203	181	177	176	170
55	42		354	356	352												198	191	187	184	181	181	181
	25		357	356	353												193	187	186	187	187	186	188
284	328	356	0	359	356												183	186	184	186	186	190	215
276	305	333	359	0													177	179	180	180	184	195	226
273	281		353	3	13												163	172	173	176	186	214	235
274	270	304	346	8	34	55	82	96				79			120	128	135	146	170	177	187		245
276	267		336	3		68	87	91	91	86	82	83	89	98	103	104	118	131	153	181	197	201	
304		277	288					101	90	82	79	83	86	100	108	110	110	122		187	197	193	
277	280	285	287	283												173	165			204	201	193	
271	278	285	298	276	252	229	226	252	267		263	285	295	278	246	207	245	255	257	248		225	252
271	274	278	283	269	252	233	238	259	267	269	269	273	280	276	257	238	245	263	267	260	256	257	260
			269				238	260	267	269	271	269	267	266	260	257	260	266	267	264	260	259	257
75									262			266	257	257	259	263	264	263	267	262	255	233	221
21	38																					222	211

(e3)

				103			203	250	295	308	315	315			170	183		235					
	110	110						267	277	295	304				159	174							
124	128					283	277	270	266	248	242												
127				278	291	287	280	266	243	231	226	228											
				312	302	287	280	264	235	225	225	238	256	264	263	263	269	276	280				
		17	23	350	328	308	295	266	238	226	229	253	264	267	262	260	260	266	276	262			
		18	18	1	343	311	290	276	252	231	233	259	269	270	262	242	239	240			191		128
			13	1	350	309				232	255	264	269	267	260	240	233	231			188	139	131
			4	359	353							269	267	263	260	243	229	224	214		170	155	143
31			359	357	357												217	212	207		173	·176	169
			359	356	356												195	194	187	184	181	181	181
	23		354	357	357												190	186	184	186	186	186	191
288	346		356	356													183	184	183	184	184	190	215
278	307	328	3	0													179	179	180	180	184	194	226
274	300		354	8	30												153	172	174	177	180	217	233
273	269	300	352	0	38	58	80									121	134	145	170	177	198		
280			338				80	77	86	87	89	86	86	100	103	104	111	132	146	188	195		
309		300	308						89	84	83	84	87	93	104	105	108	129		190	197	190	
274	281	287	277																	180	215	204	
271	277	283	285	267	255	250	250	257				280	285		245	201	233	255	260			224	256
271	274	274	276	274	259	238	238	257	263	269	274	271	277	274	257	252	256	264	266	262	259	267	263
								259	267	273	267	266	267	266	263	262	263	266	267	266	263	260	260
													262	262	266	270	270	269	269	266	257	235	225
	53																					218	215

(e4)

								242	297	309	314	314			176	184							
		114							278	297	304												
122	124						280	277	267	246	242												
129					295	288	280	269	242	232	229	231											
					307	288	280	263	235	226	226	239	256	266	266	267	271	277					
				349	328	311	298	264	238	228	231	255	264	267	264	263	262	271	270	249			
			21	0	343	315	293	271	252	231	235	260	269	270	263	242	238				195		
			8	1	352	318					246	263	269	269	260	239	233	225			188	138	131
			0	0	354								269	266	262	240	229	224			176	149	142
			0	359	359												217	215	208		170	176	166
			0	357	359												195	194	194	205	176	181	181
			359	353													188	184	184	184	184	186	193
300	349		352	353													183	183	183	184	184	188	215
281	288	308	0	3													179	179	180	180	183	205	224
277	305		354	10	35												152	172	176	179	177		
277	269	297	350			62										124	131	146	158	179	187		
298			339					75	80	89	89	87	89	94	101	104	110	134	145	191	195		
		309								84	84	86	89	93	98	100	104			190	205		
271	281	287																			217	210	
271	276	278	274	264	262	255	255										248	260				226	259
271	273	273	271	270	262	255	252	256	263	269	276	276	270	271	262	257	260	264	263	262	264	271	273
									267	270	270	266	264	267	266	266	267	267	269	267	264	263	
														264	269	273	273	270	270	269	257	235	224
																						224	219

Figure 1'. (e2-4)

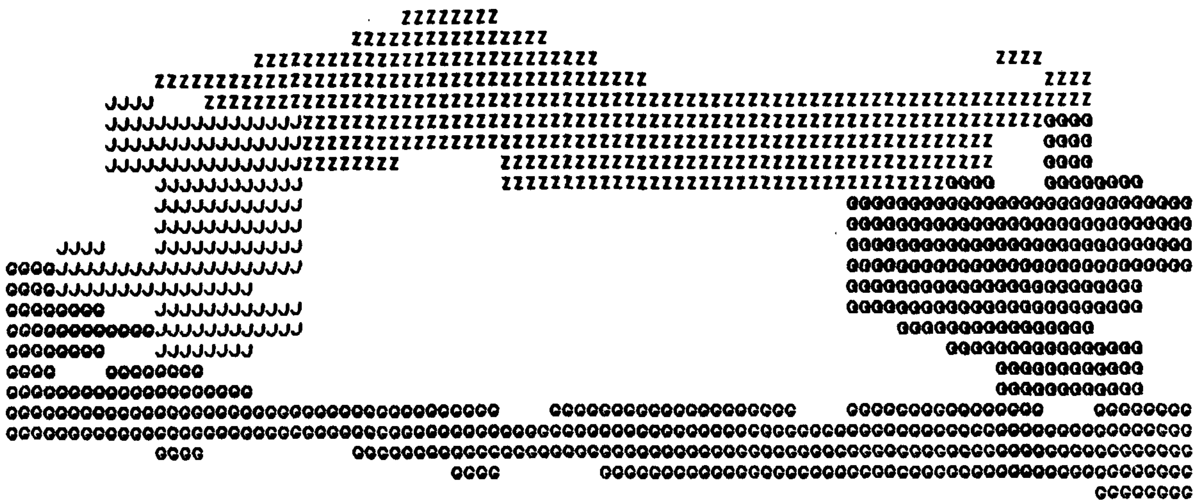

(a)

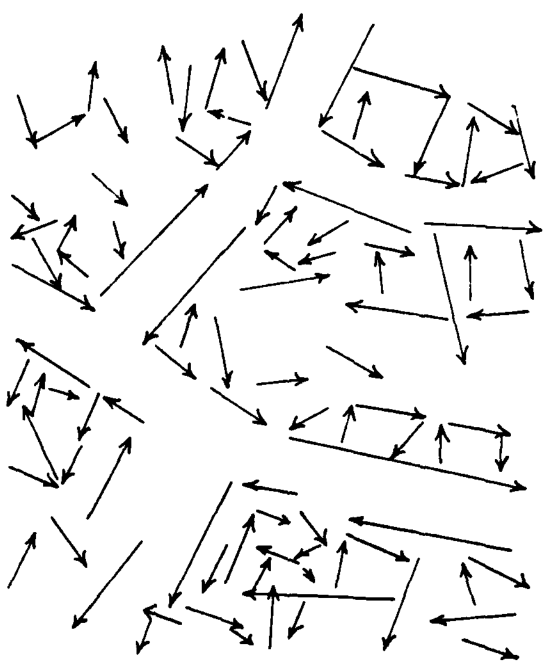

(b)

Figure 2'. Analogous to Figure 2 for the second (sub)window

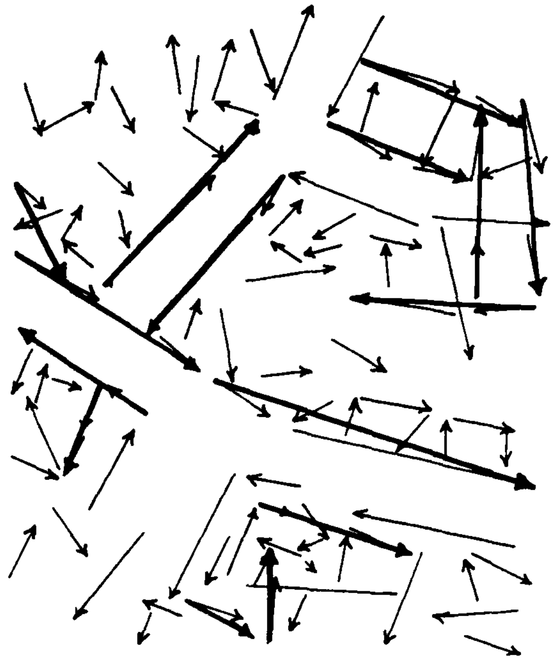

Figure 3'. Analogous to Figure 3 for the window of Figure 1'.

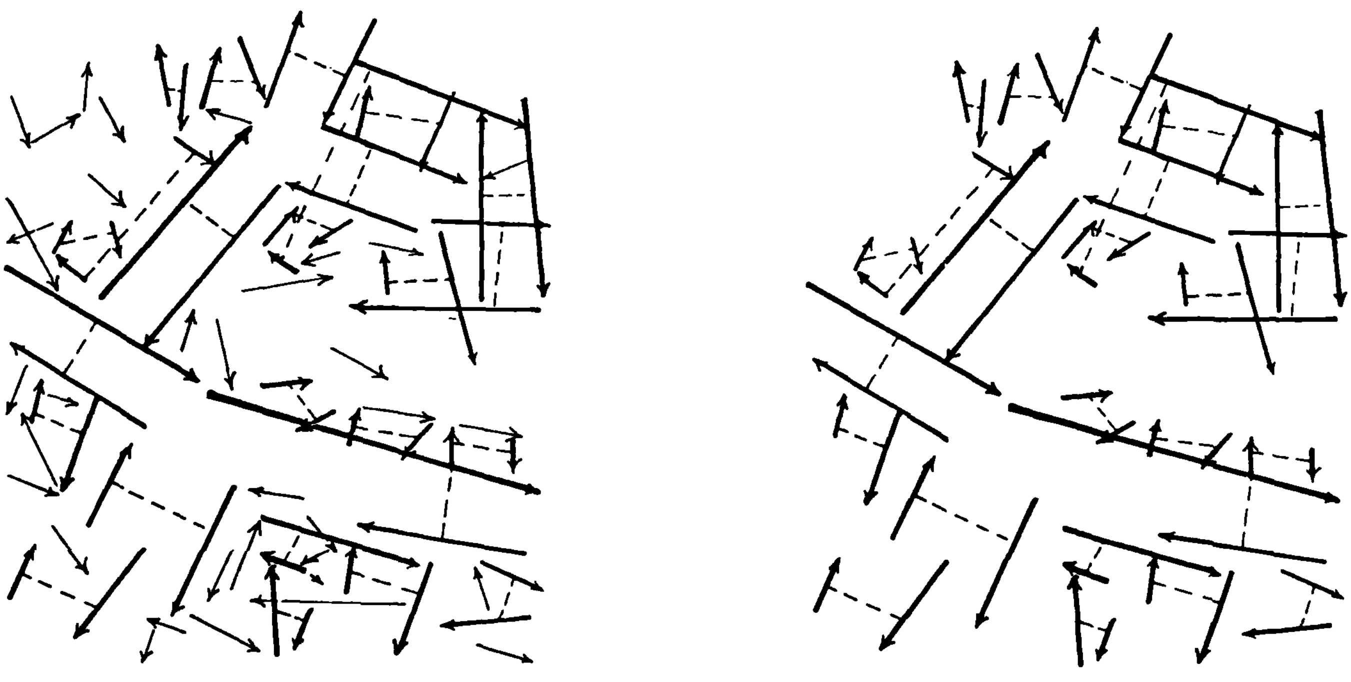

(a)

(b)

Figure 4'. Analogous to Figure 4 for the window of Figure 3'.

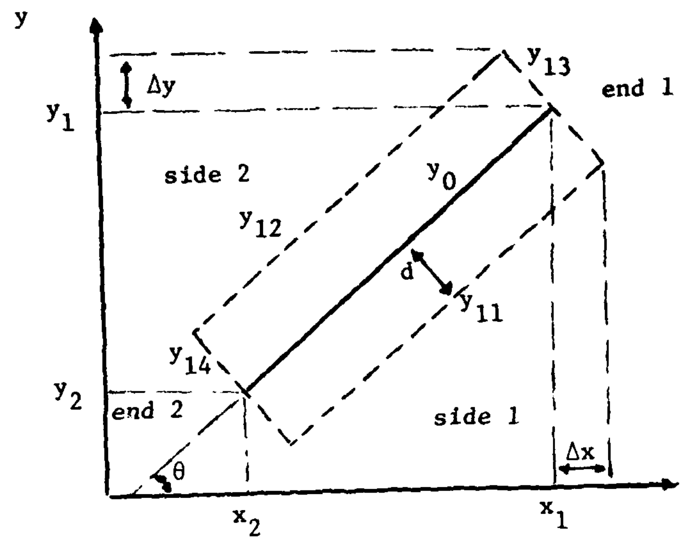

(a)

$0 \leq \theta < 90$

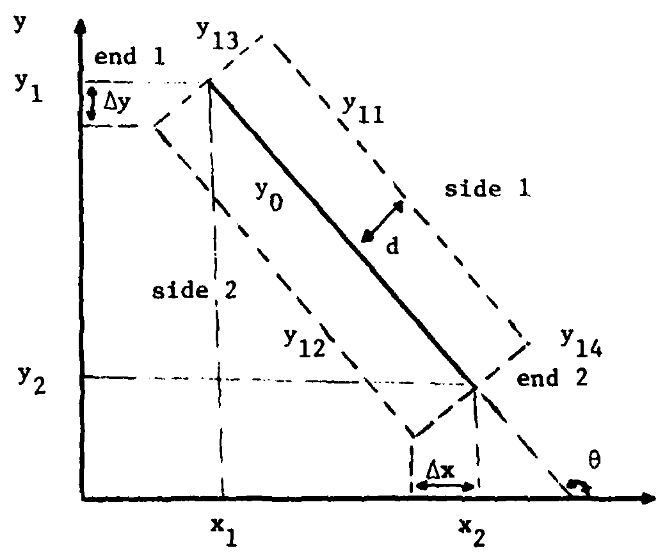

(b)

$90 < \theta < 180$

Figure 5. End and side conventions.

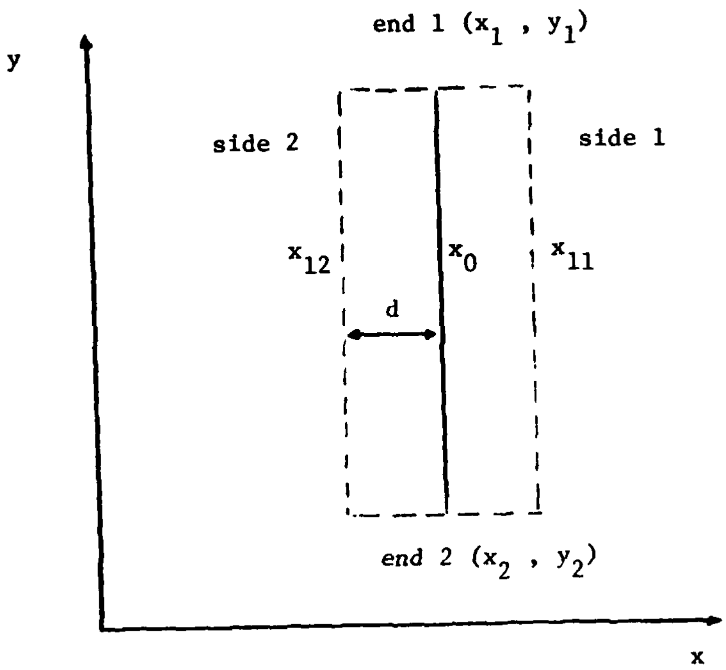

Figure 6. θ=90°

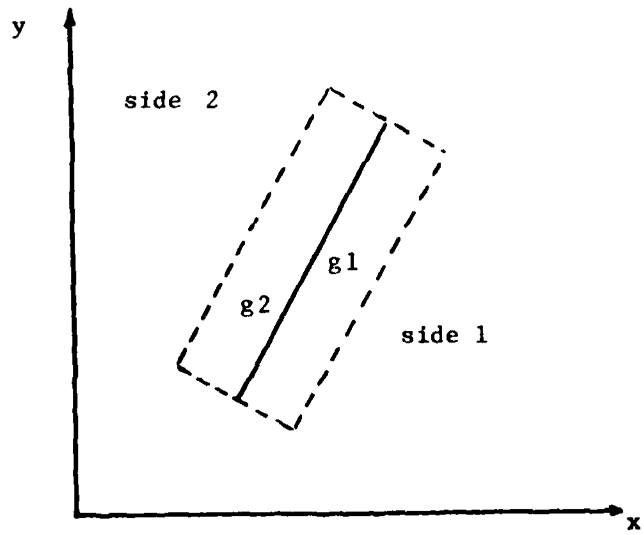

Figure 7. A line segment and strips along each side of it

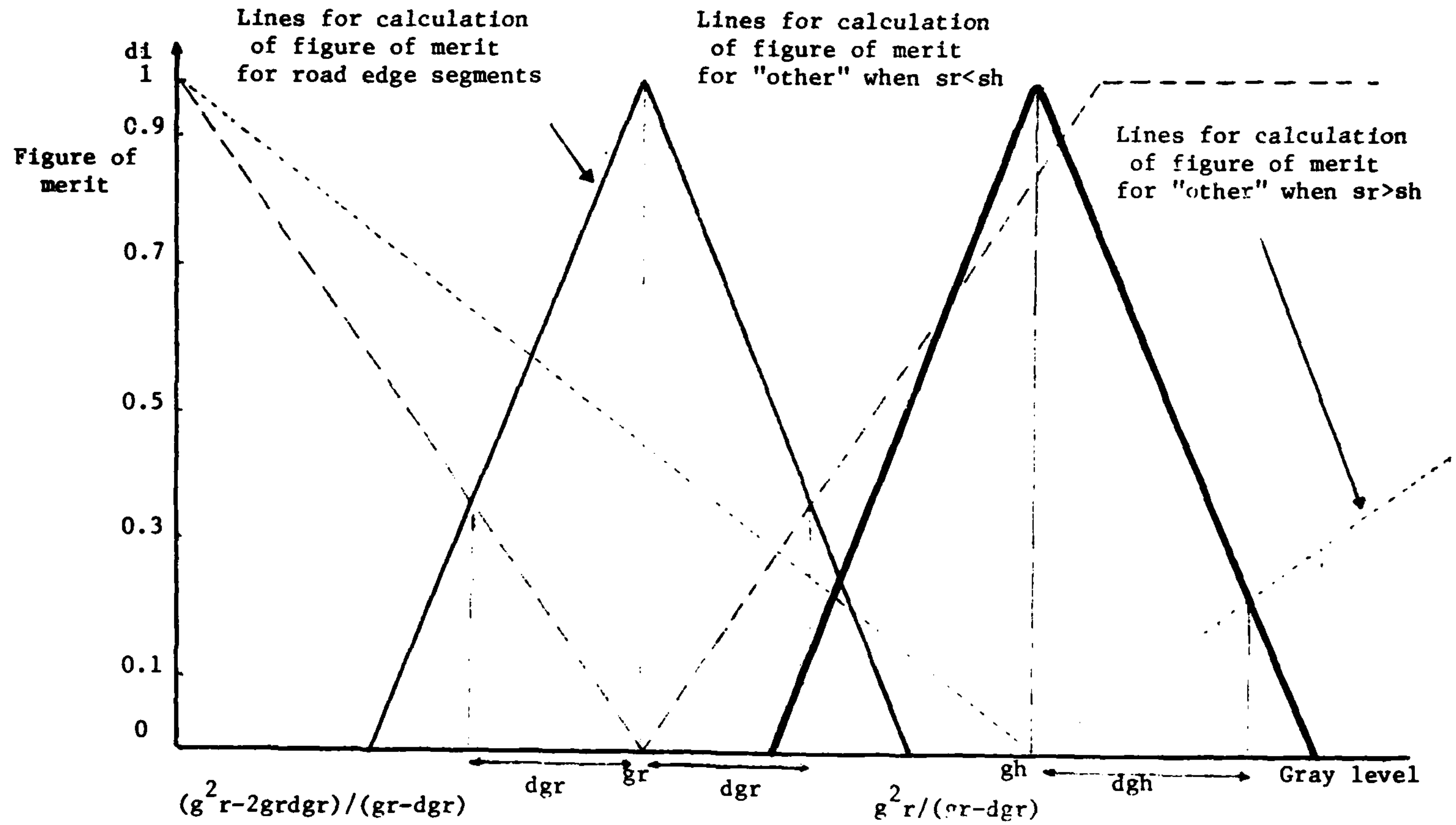

Figure 8. Linear functions for calculation of figures of merit

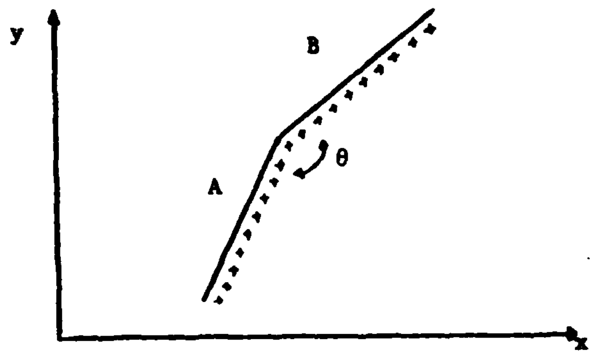

(a)

$$\theta = \pi + |\theta_A - \theta_B| \text{ if } \theta_B \geq \theta_A$$

$$\theta = \pi - |\theta_A - \theta_B| \text{ if } \theta_B \leq \theta_A$$

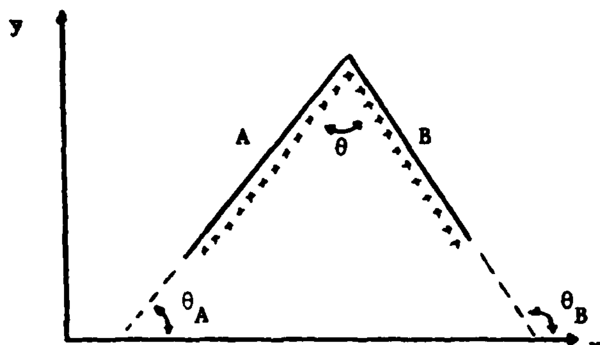

(b)

$$\theta = |\theta_A - \theta_B|$$

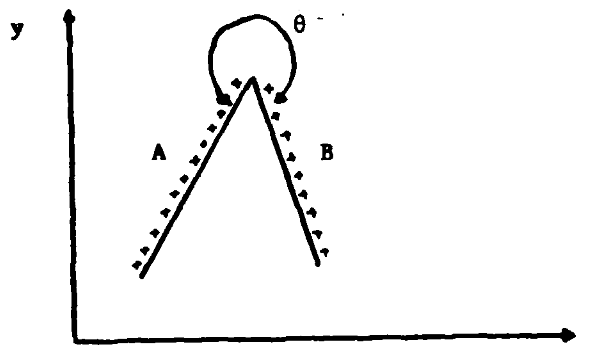

(c)

$$\theta = 2\pi - |\theta_A - \theta_B|$$

Figure 9. The angle between two lines in different orientations

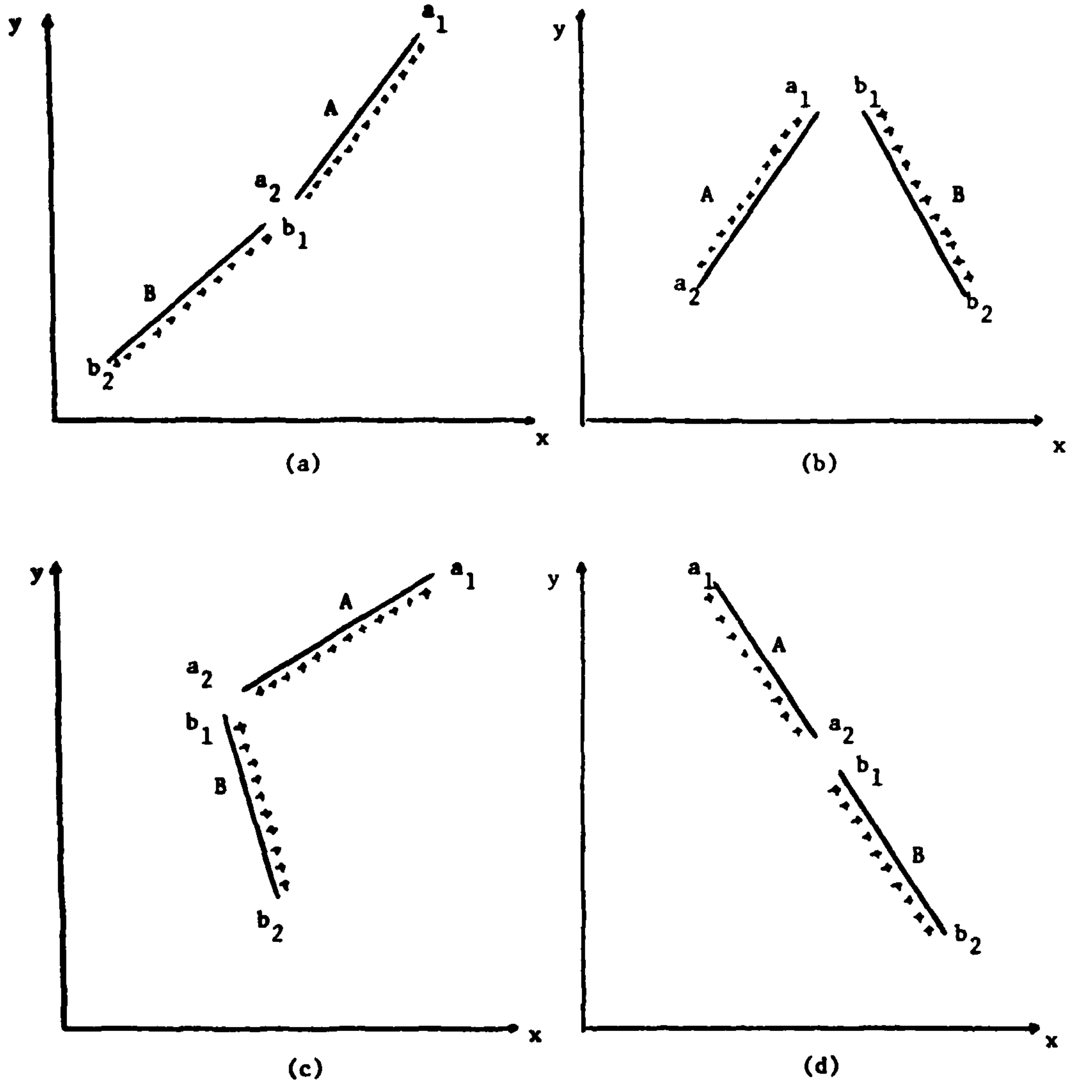

Figure 10. Examples of geometrically compatible candidate pairs.

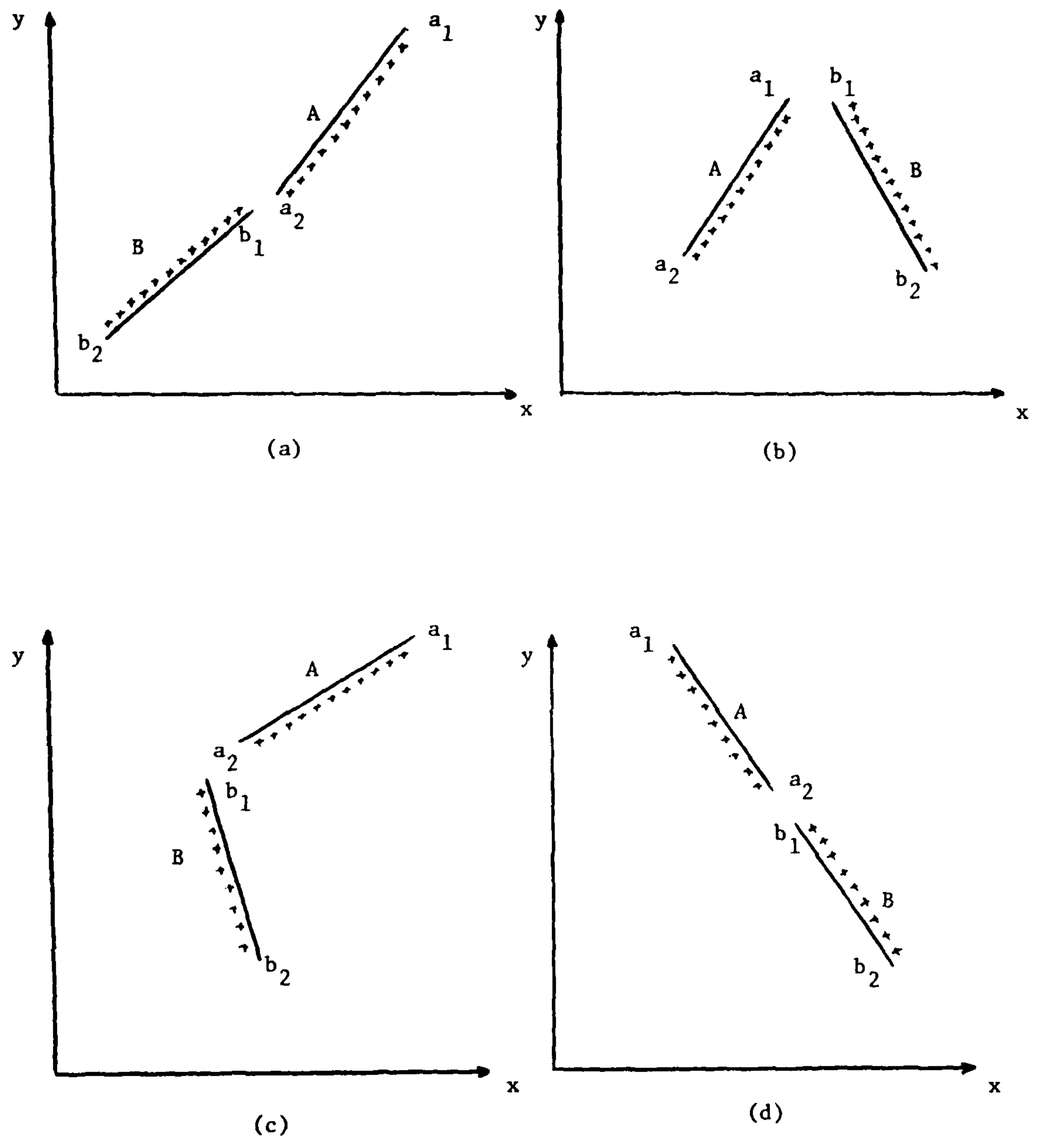

Figure 11. Examples of geometrically incompatible candidate pairs.

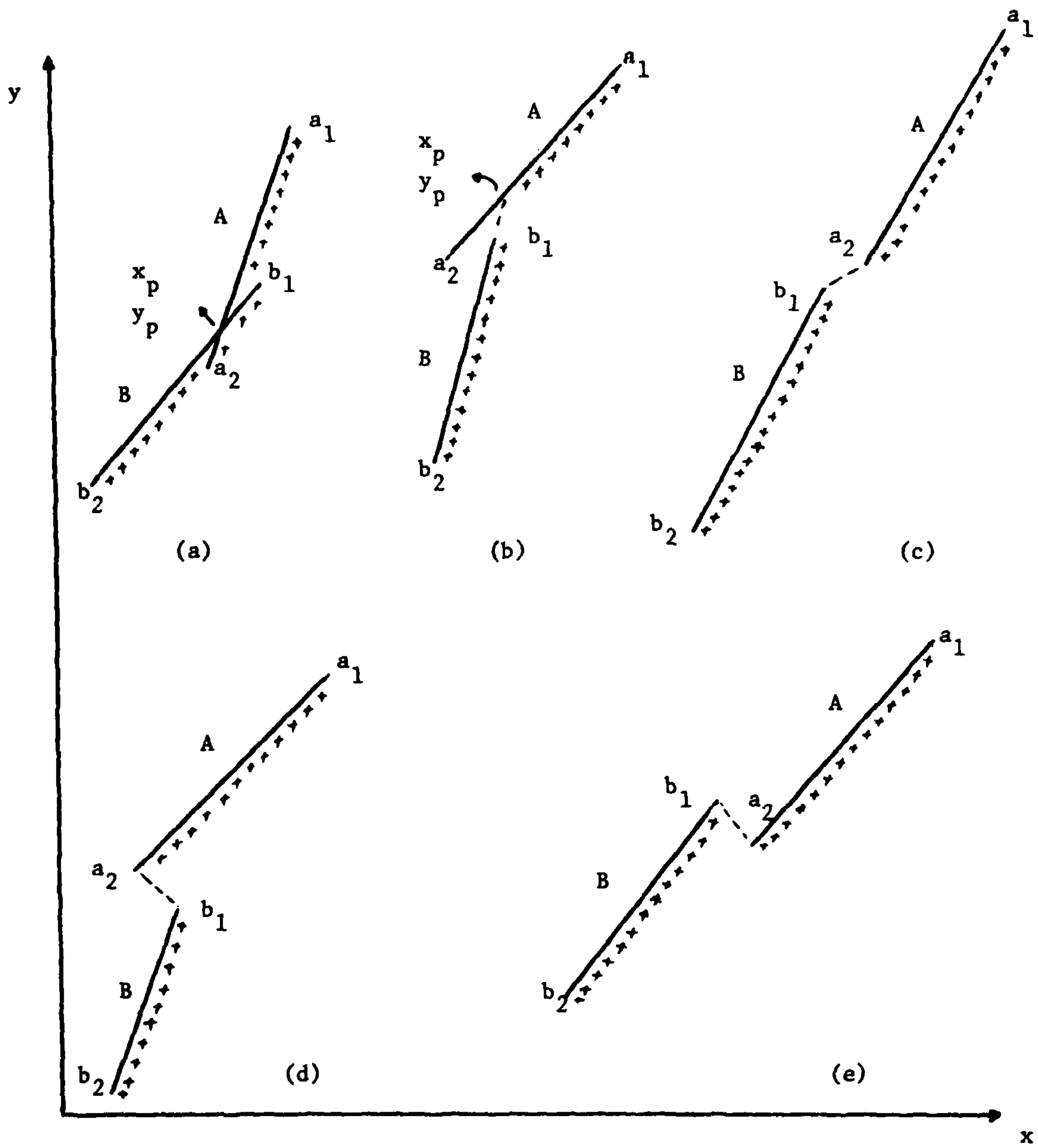

Figure 12. Configurations in Case 1

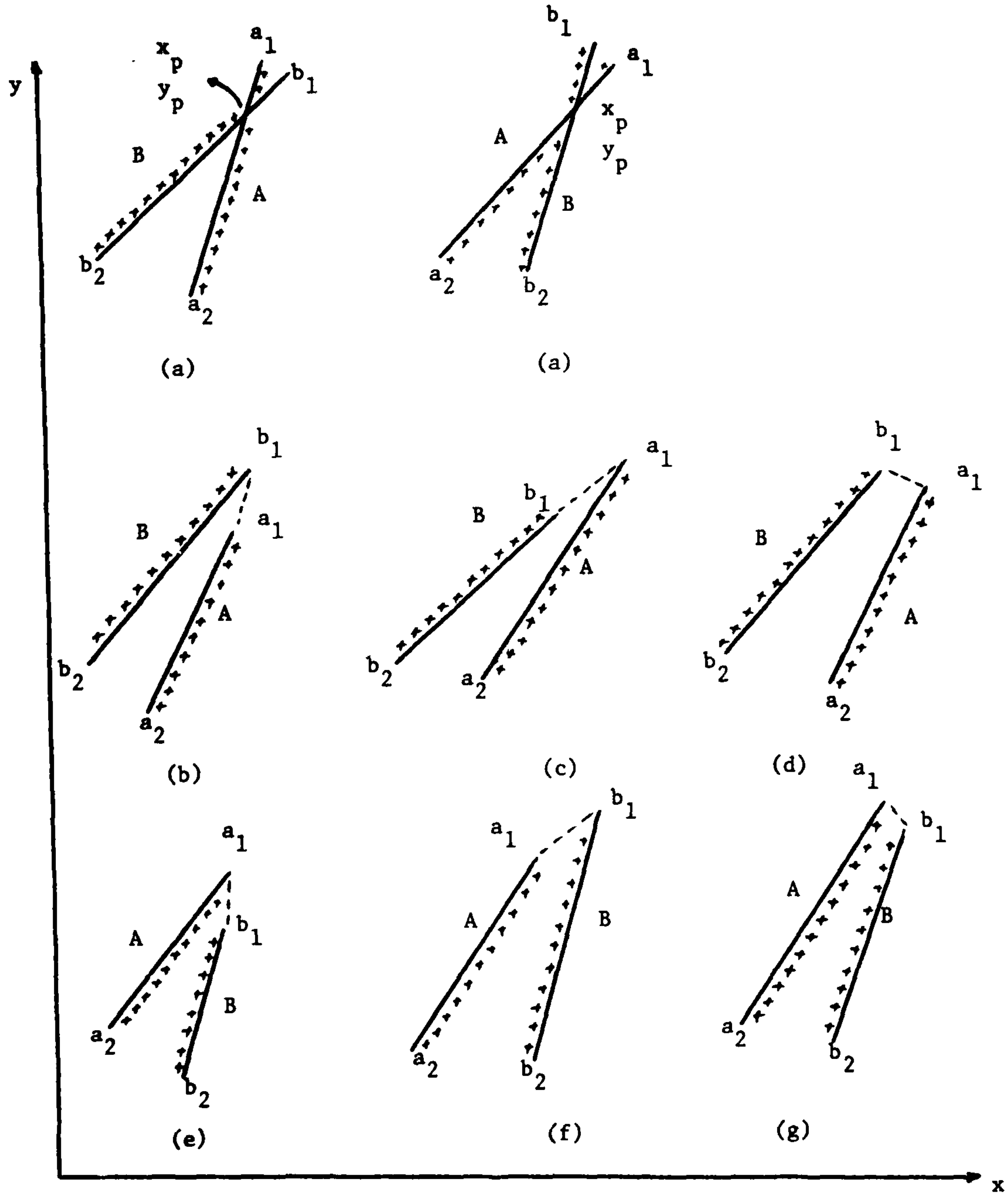

Figure 13. Configurations in Case 2

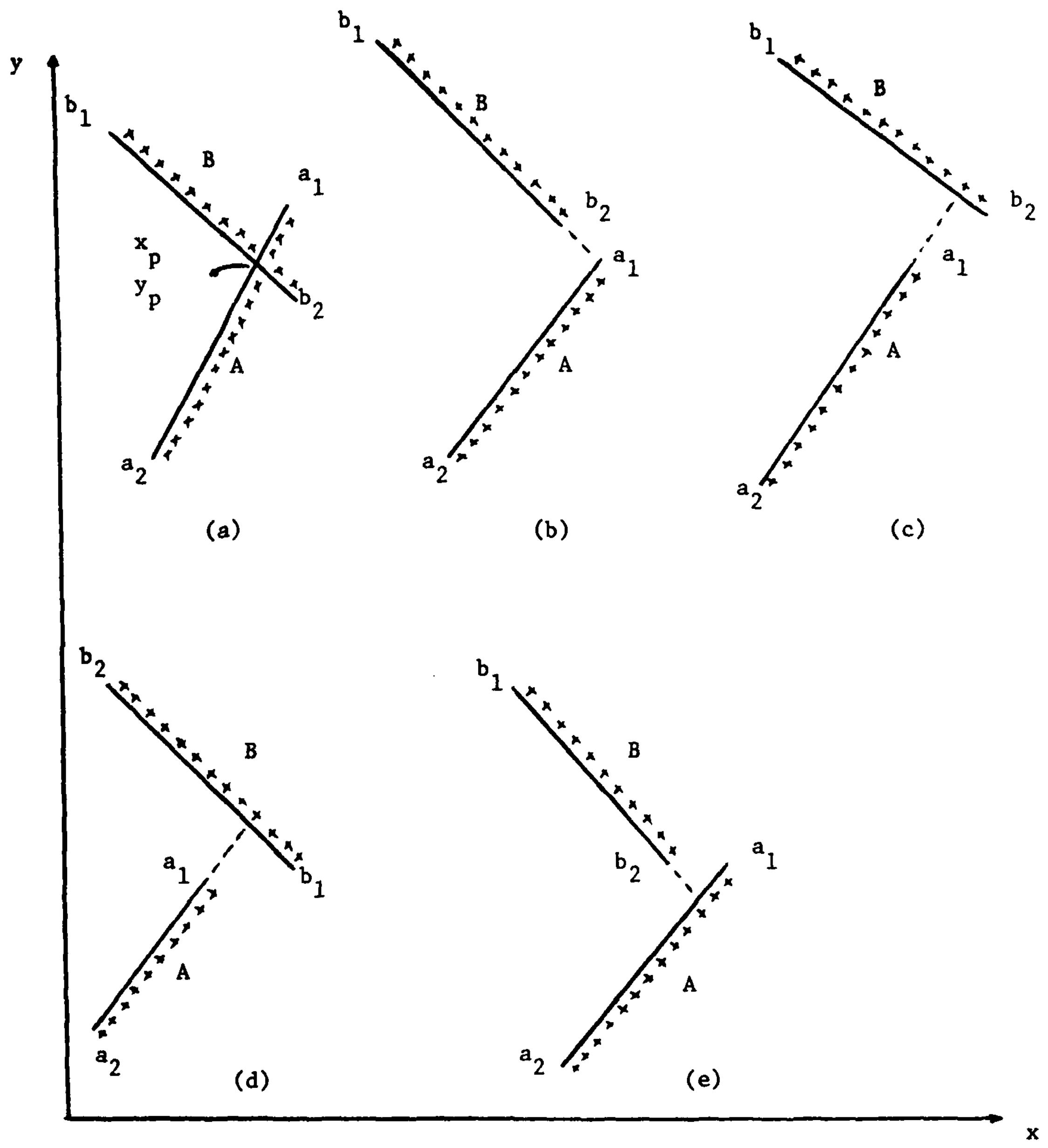

Figure 14. Configurations in Case 3: end 1 of line A

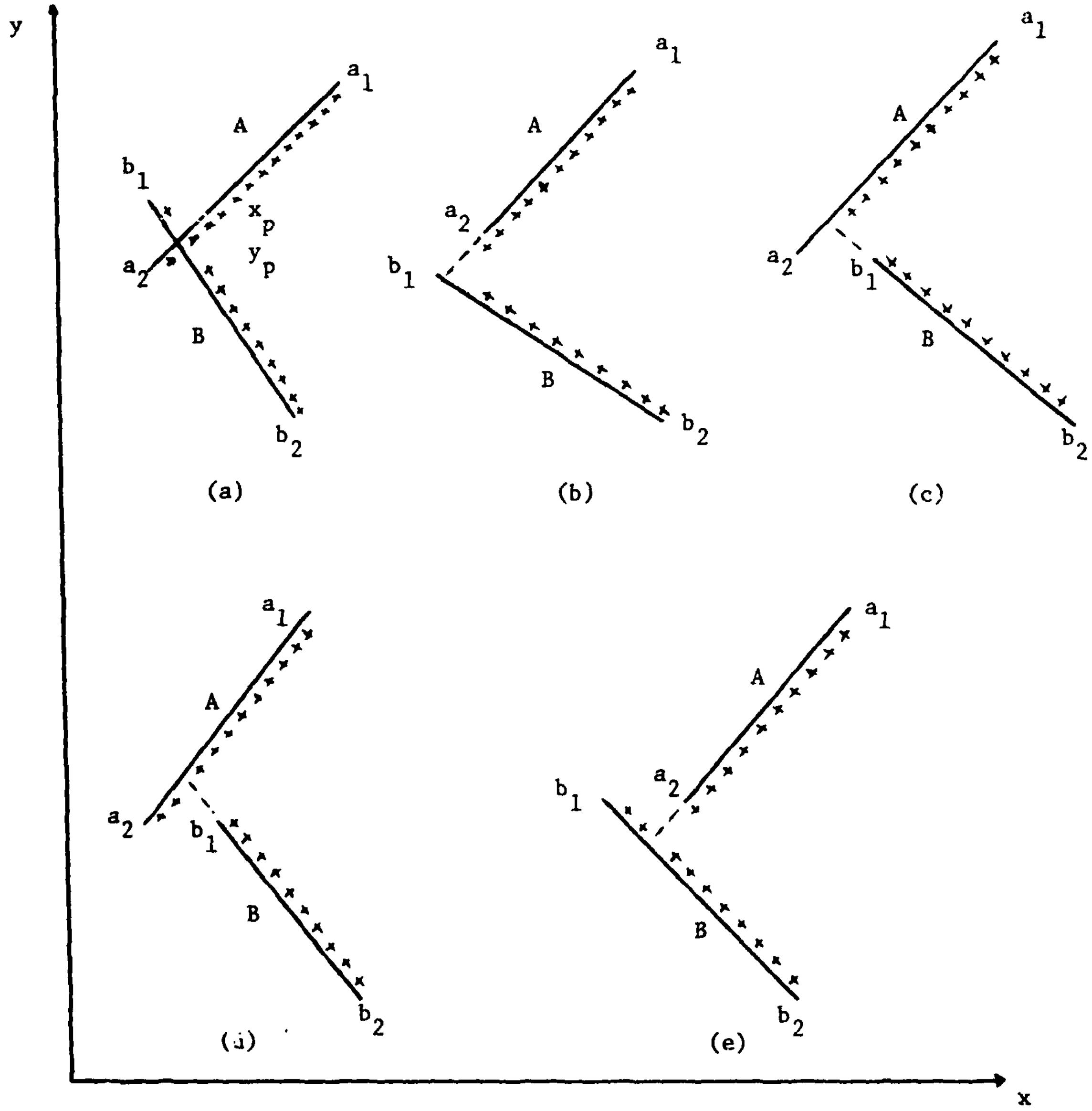

Figure 15. Configurations in Case 3: end 2 of line A

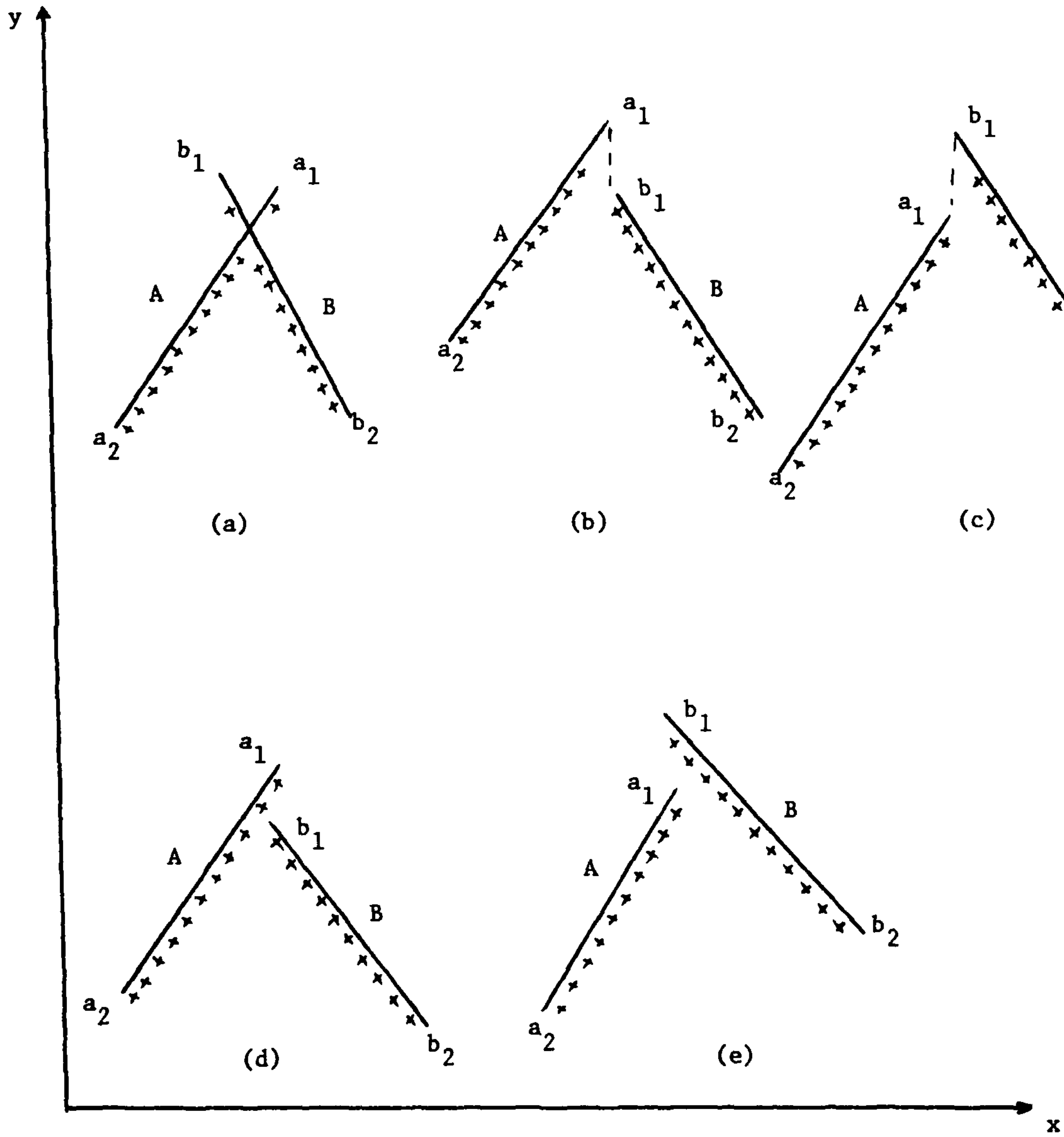

Figure 16. Configurations in Case 4: end 1 of line A

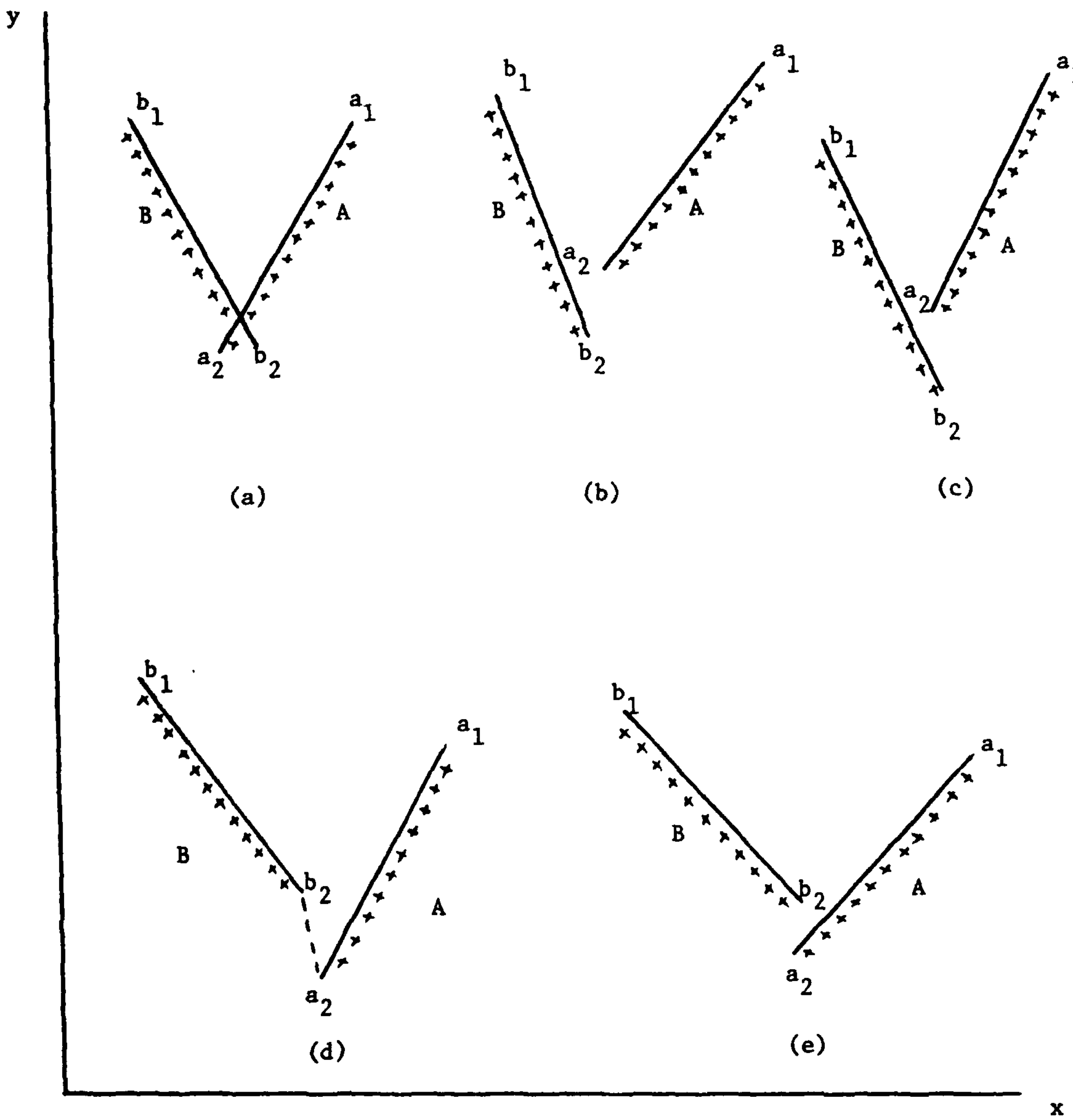

Figure 17. Configurations in Case 4: end 2 of line A.

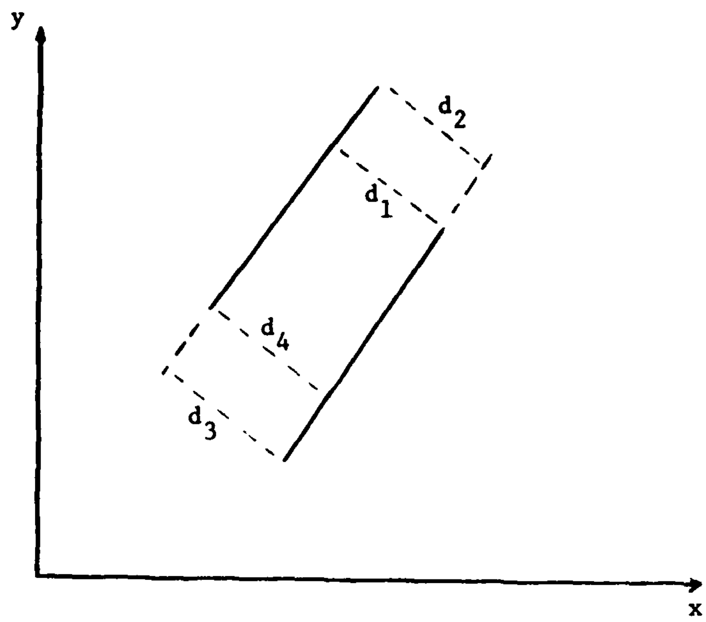

Figure 18. Calculation of the distances between two lines.

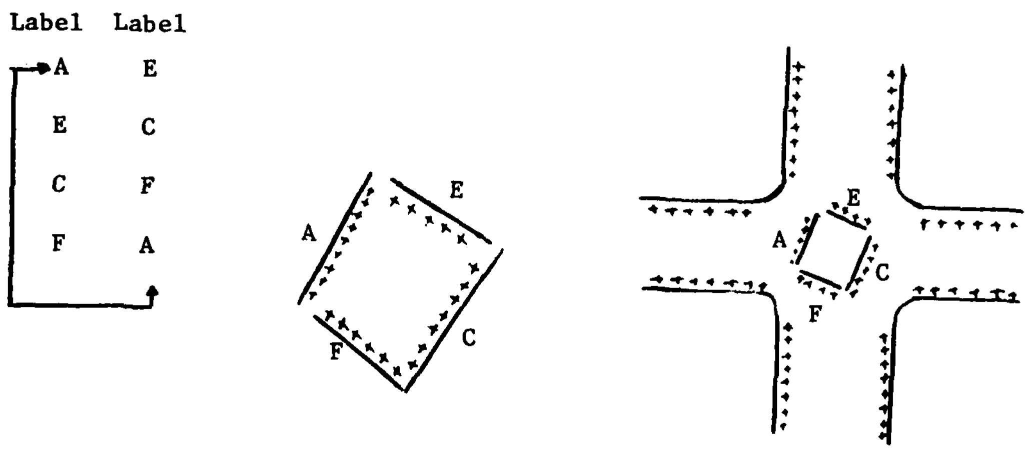

a) A group b) A house c) An intersection

Figure 19. Examples of closed groups.

Label	Label
A	E
E	C
C	D

a) A group

Label	Label
E	C
C	D
E	A

b) A group

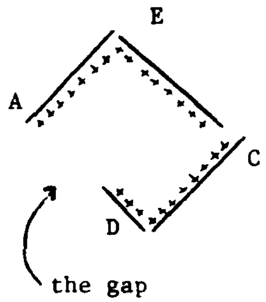

c) A house with missing edge.

Figure 20. Examples of semiclosed groups.

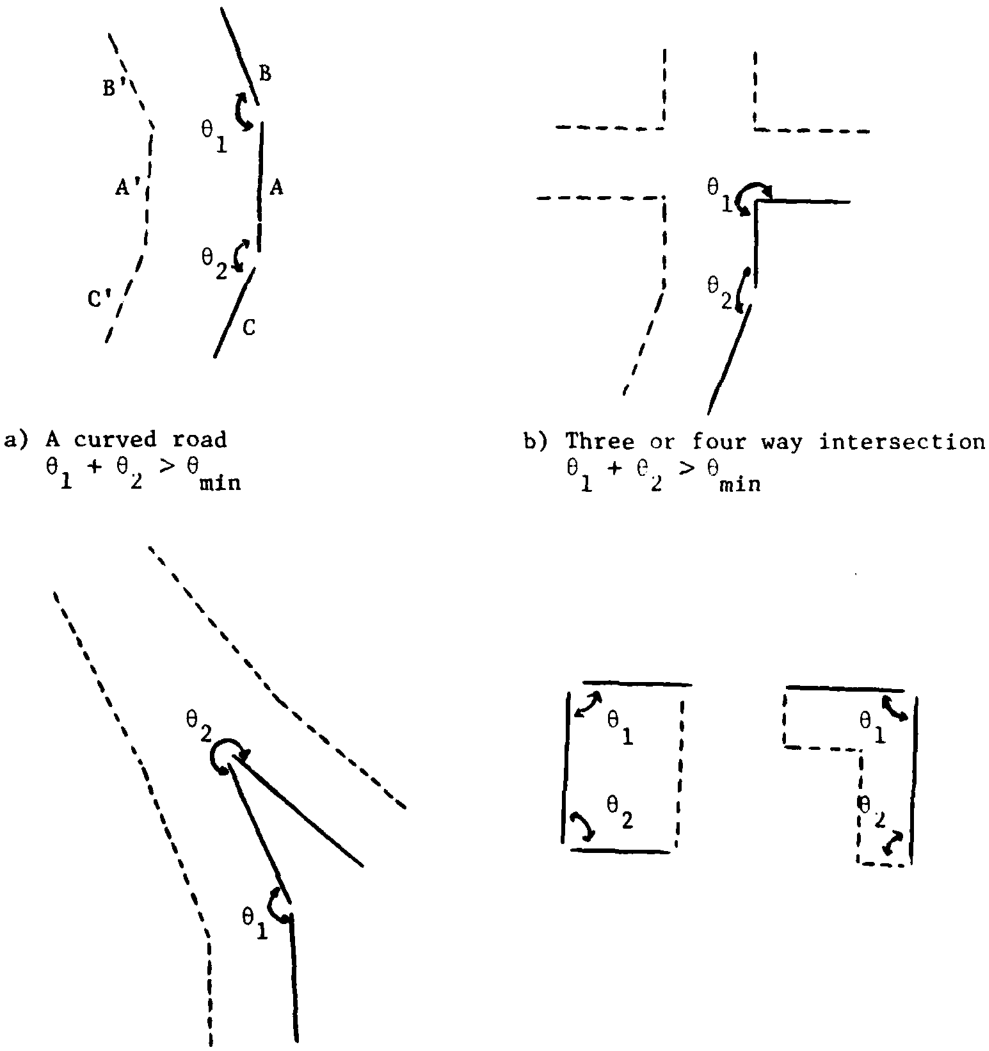

a) A curved road
$\theta_1 + \theta_2 > \theta_{min}$

b) Three or four way intersection
$\theta_1 + \theta_2 > \theta_{min}$

c) Merging roads
$\theta_1 + \theta_2 > \theta_{min}$

d) Single houses
$\theta_1 + \theta_2 < \theta_{min}$

Figure 21. Examples of possible cases of roads and buildings.

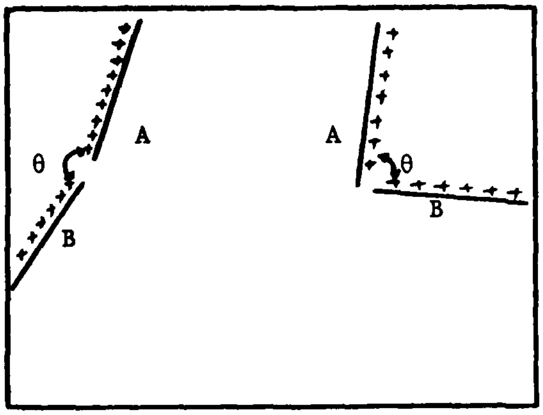

Figure 22. Case (a) of two compatible lines.

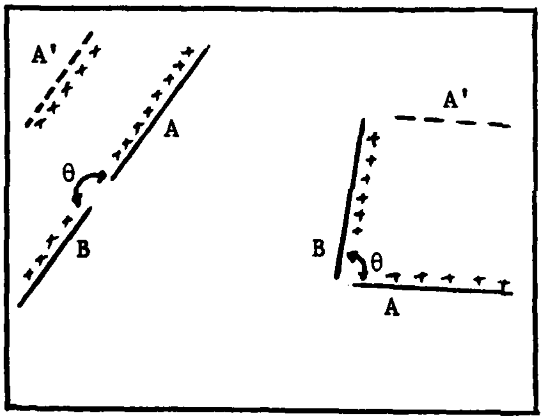

Figure 23. Case (b) of two compatible lines.

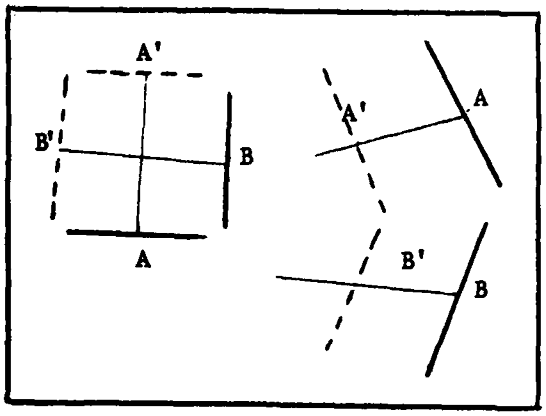

Figure 24. Case (c) of two compatible lines.

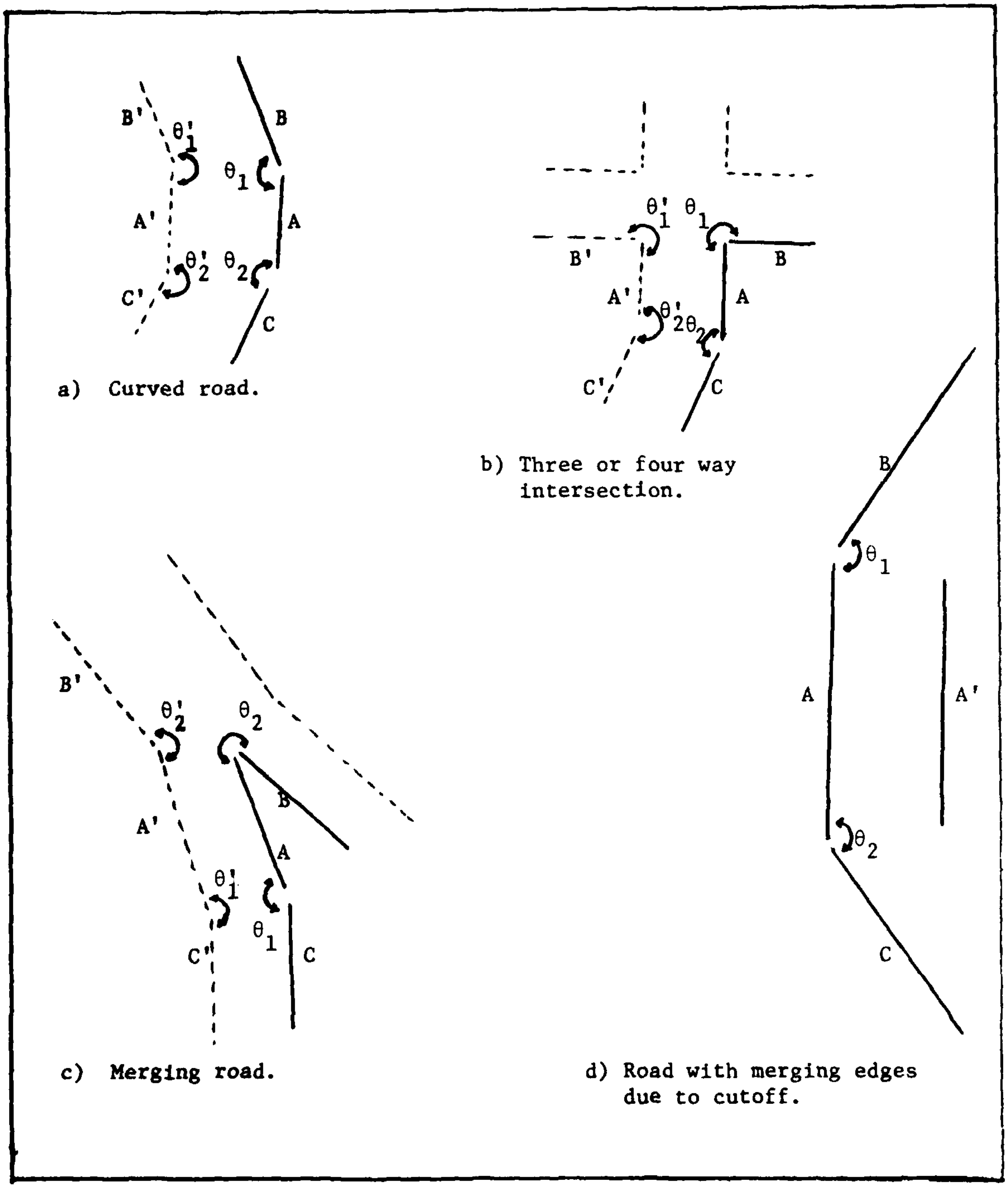

Figure 25. Examples of possible roads with high confidence.

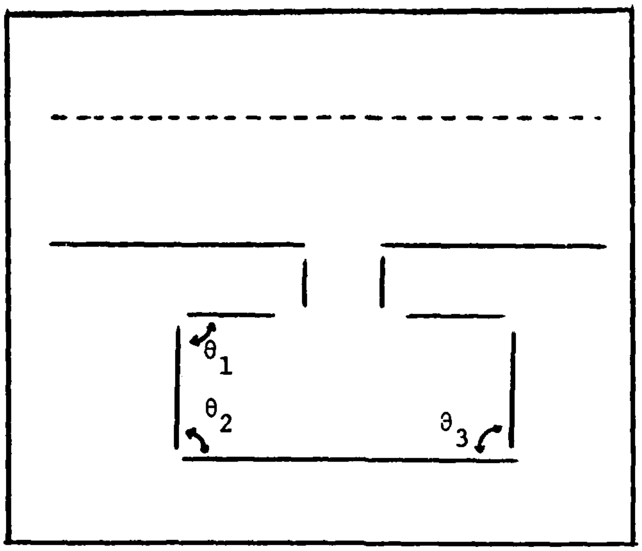

Figure 26. Example of a possible building connected to a road via a driveway (semiclosed within a group).

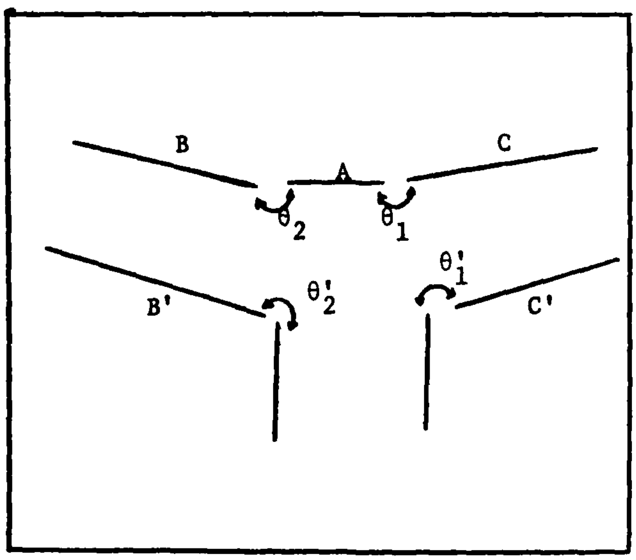

Figure 27. A special case where a line such as A has no anti-parallel, but both of its compatible neighbors are roads with high confidence.

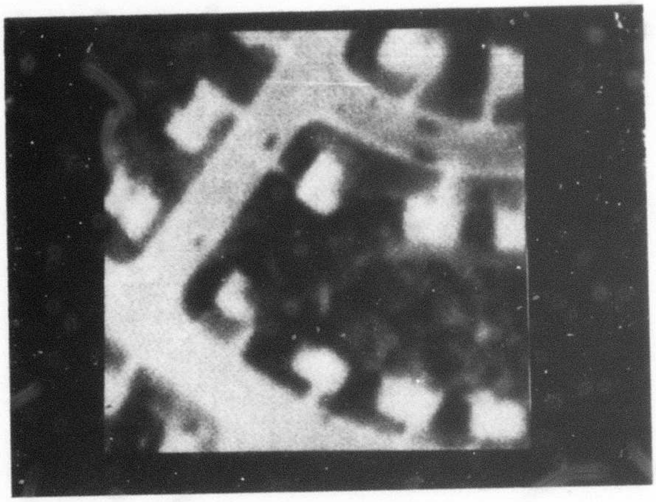

Figure 28 . A suburban scene.

Figure 29. Line segments fitted to the edge components of the scene of Figure 23.

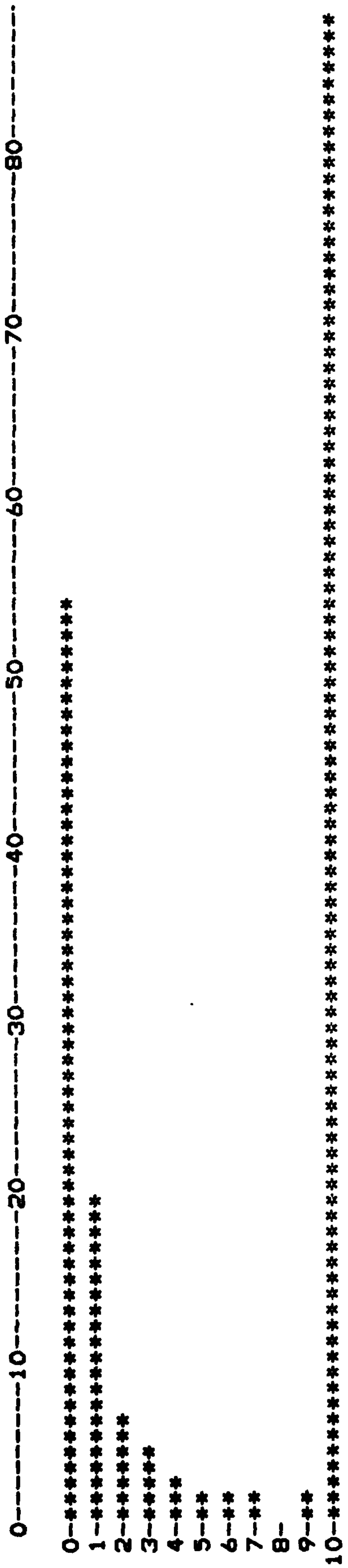

Figure 30. Histogram of the probability of "other".

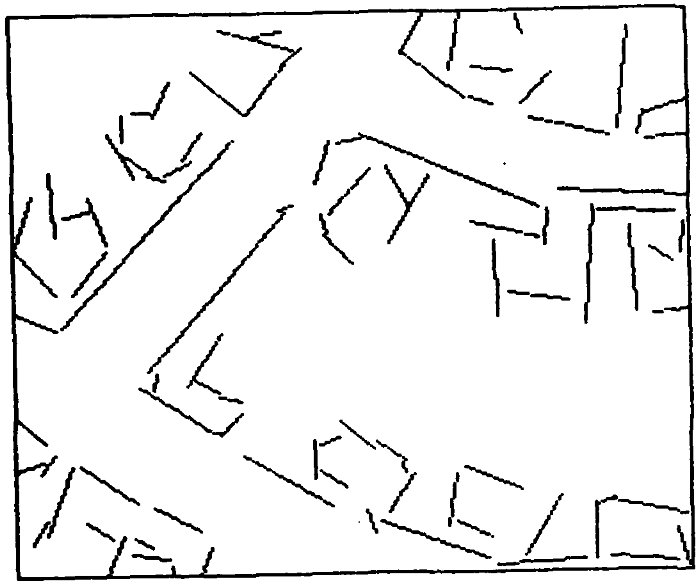

Figure 31. The line segments whose probabilities of being a piece of a road or building are not equal to zero.

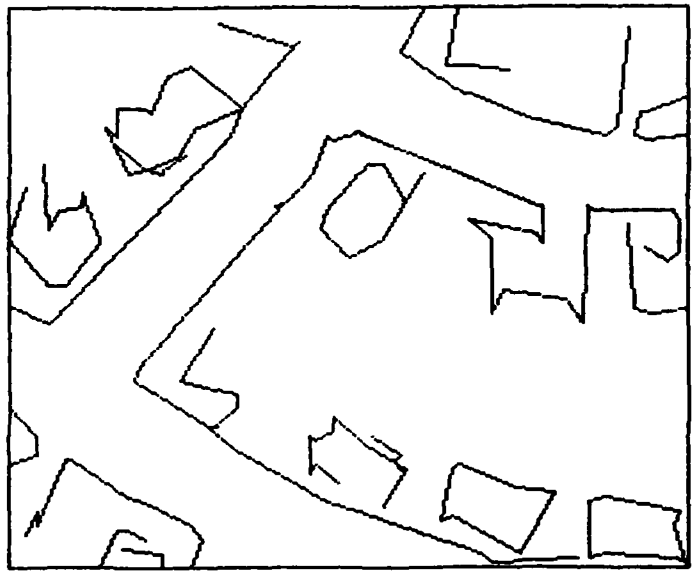

Figure 32. Results of linking compatible lines.

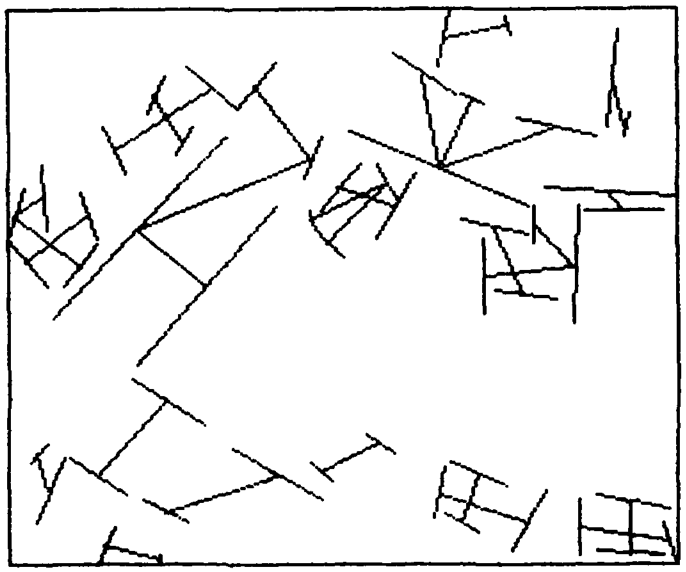

Figure 33. Antiparallel lines.

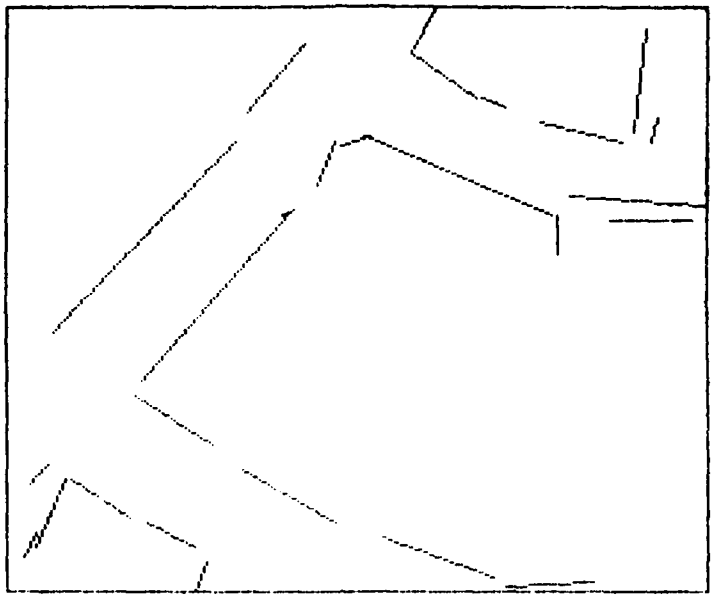

Figure 34. High confidence roads.

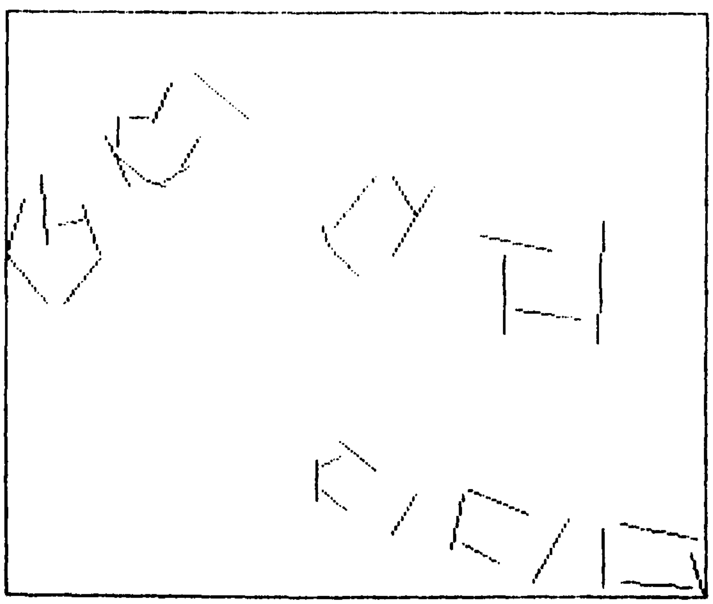

Figure 35. High confidence buildings.

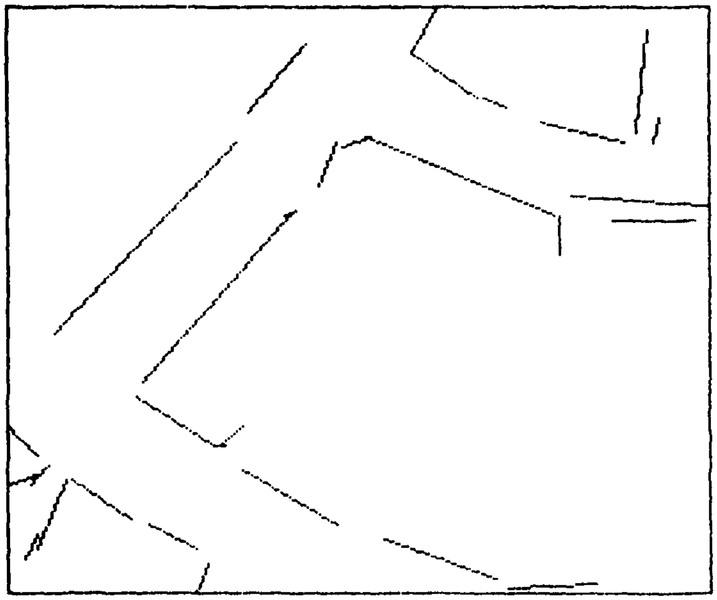

Figure 36. Roads with probability ≥ 0.75.

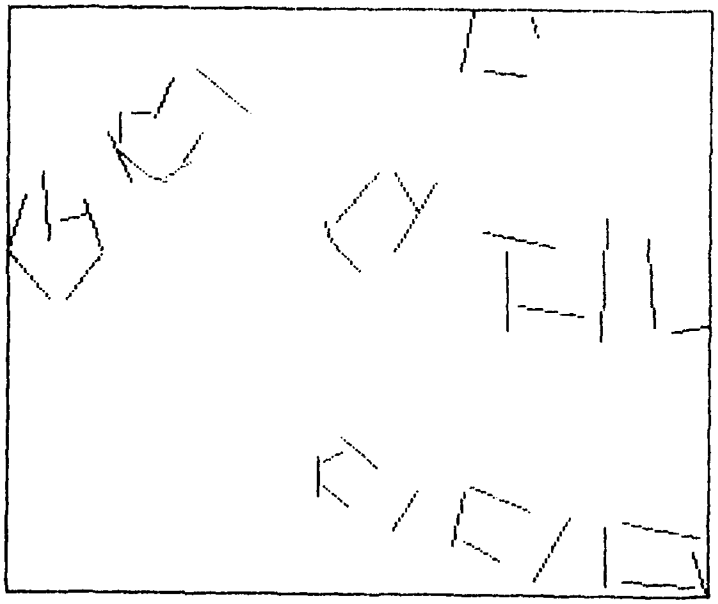

Figure 37. Buildings with probability ≥ 0.75.

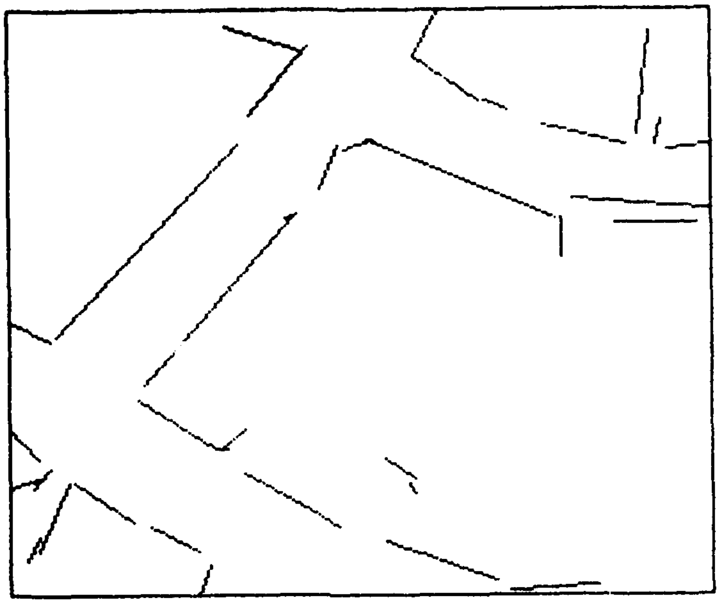

Figure 38. Roads with probability ≥0.5.

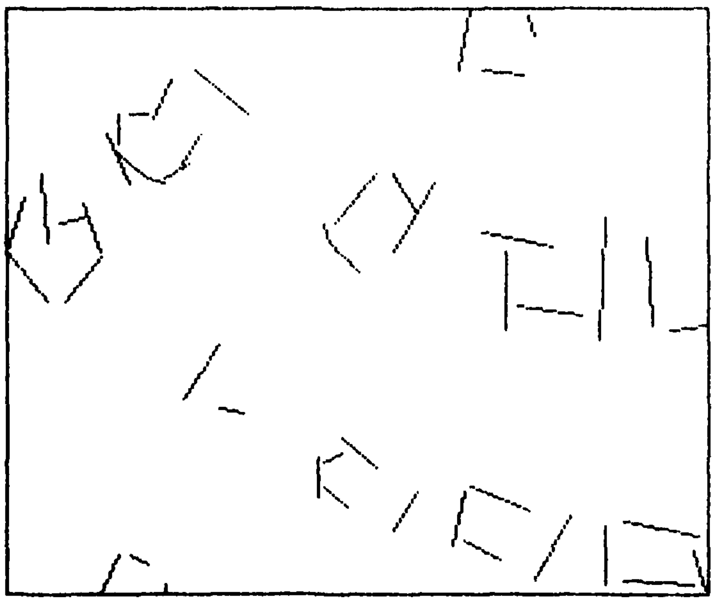

Figure 39. Buildings with probability ≥0.5.

Figure 40. Another suburban scene

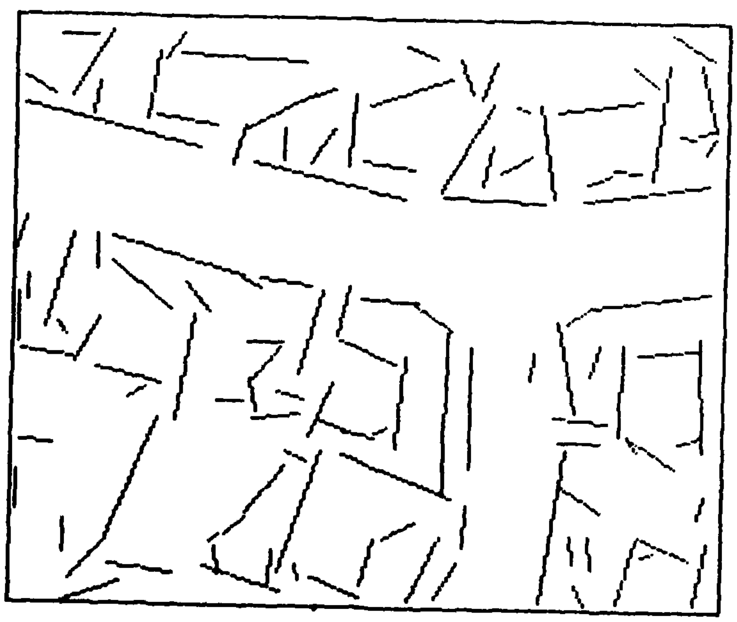

Figure 41. Line segments fitted to the edge components

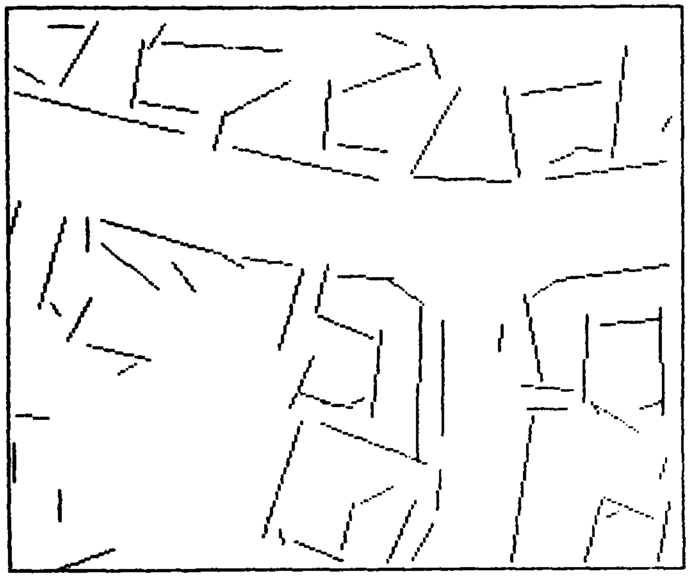

Figure 42. Line segments whose probabilities of being a piece of road or building are nonzero.

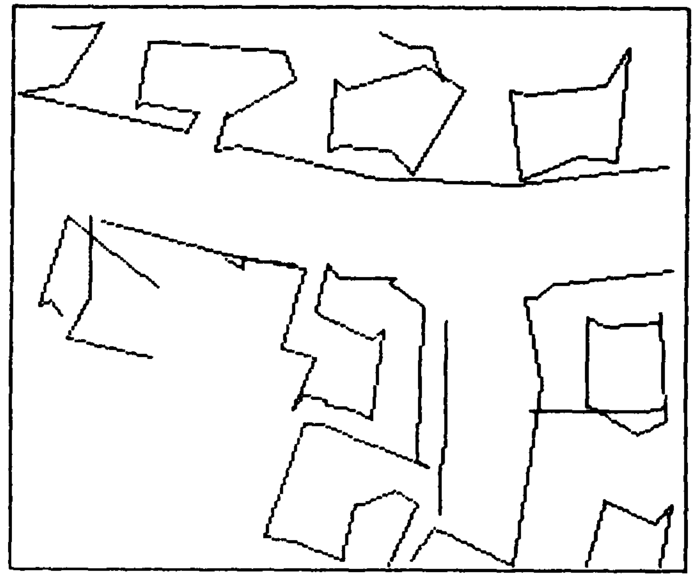

Figure 43. Compatible lines.

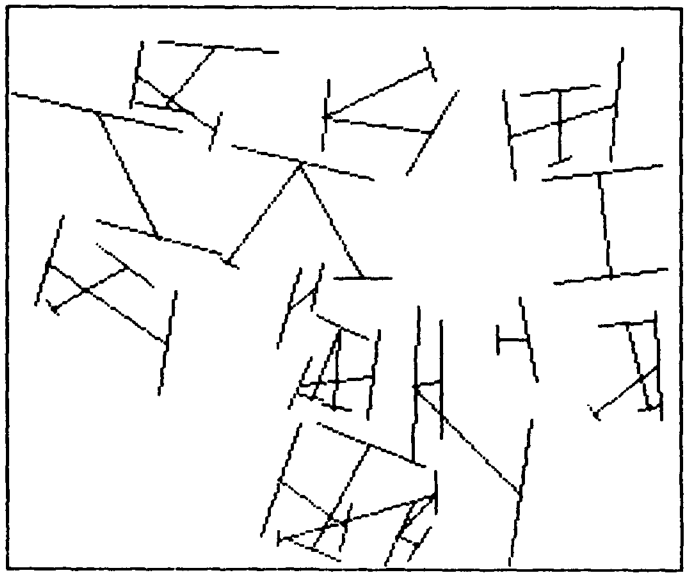

Figure 44. Antiparallel lines.

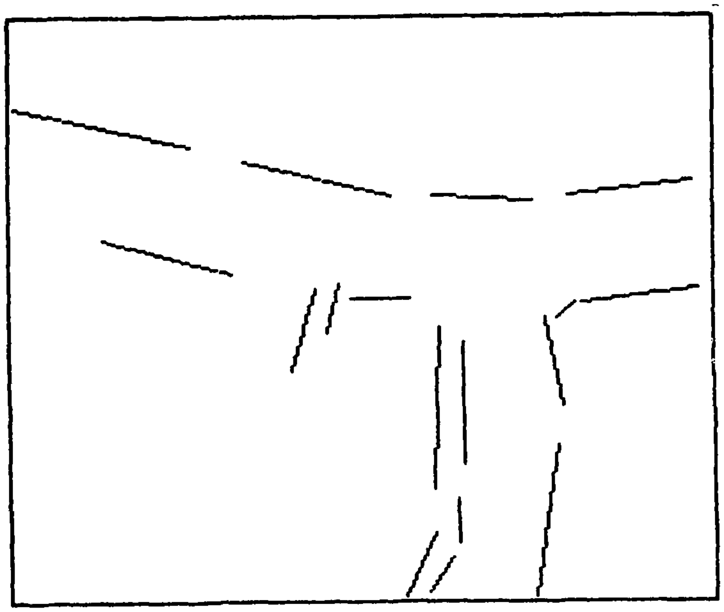

Figure 45. High confidence roads.

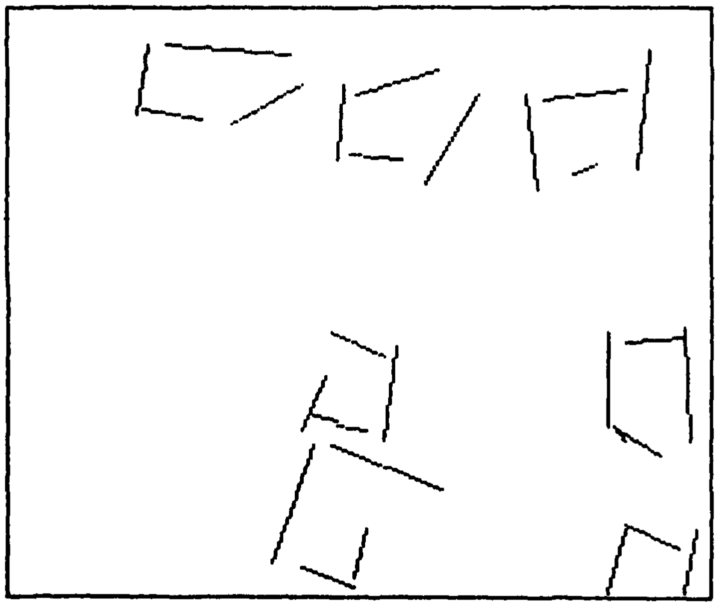

Figure 46. High confidence buildings.

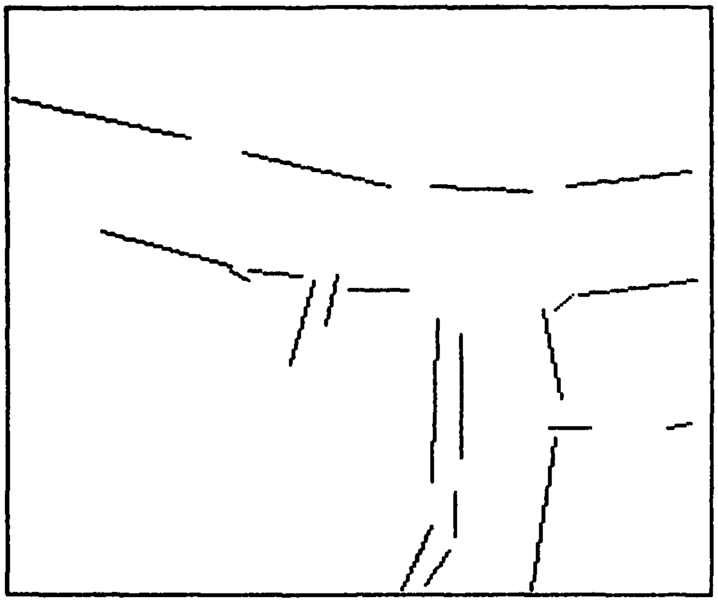

Figure 47. Roads with probability ≥0.75.

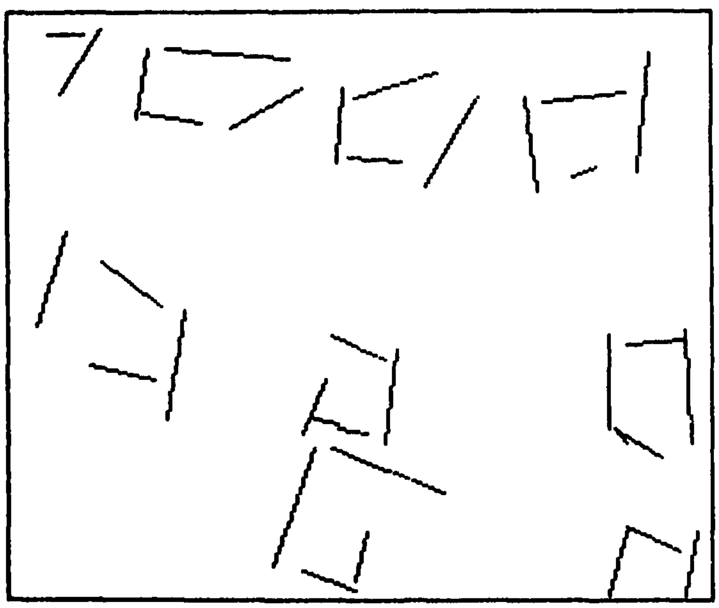

Figure 48. Buildings with probability ≥0.75.

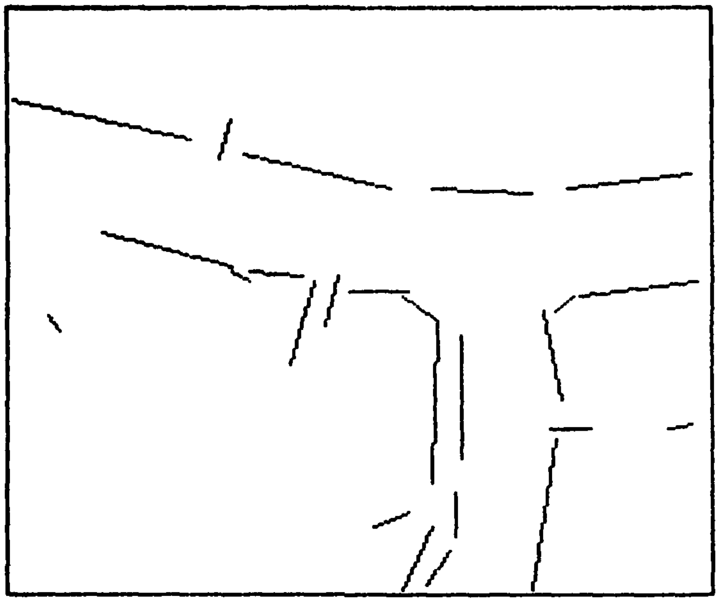

Figure 49. Roads with probability ≥0.5.

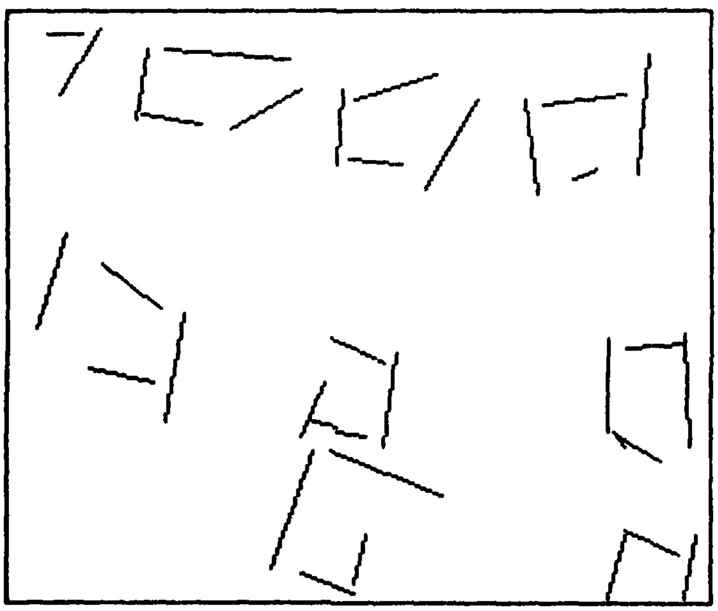

Figure 50. Buildings with probability ≥0.5.

Figure 51. Another suburban scene.

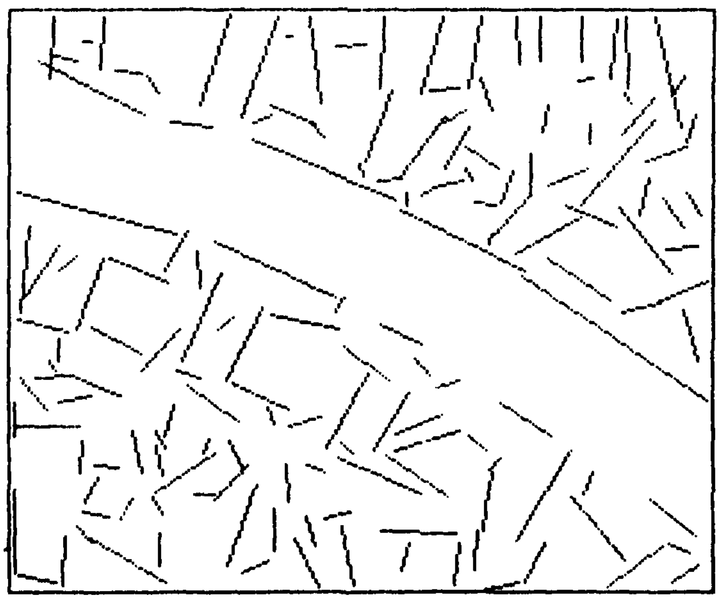

Figure 52. Line segments fitted to the edge components.

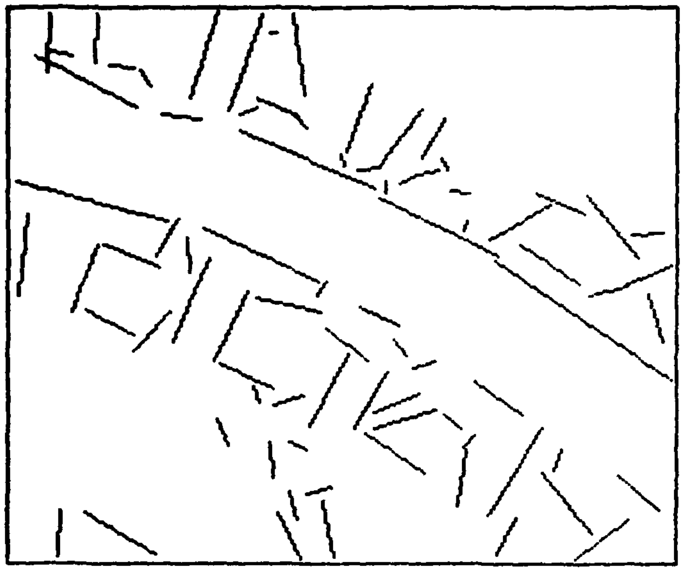

Figure 53. Line segments whose probabilities of being a piece of road or building are nonzero.

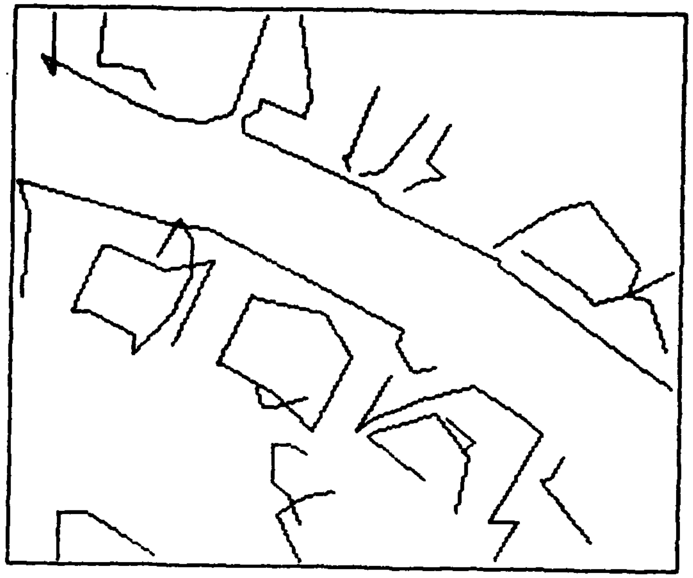

Figure 54. Compatible lines.

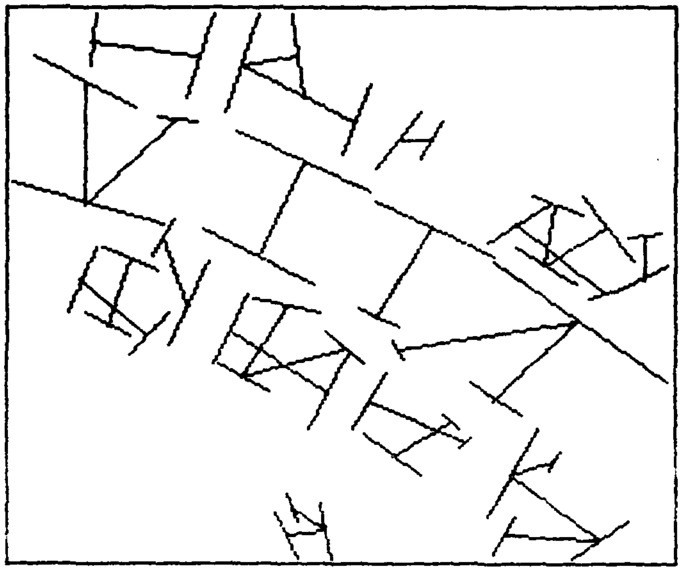

Figure 55. Antiparallel lines.

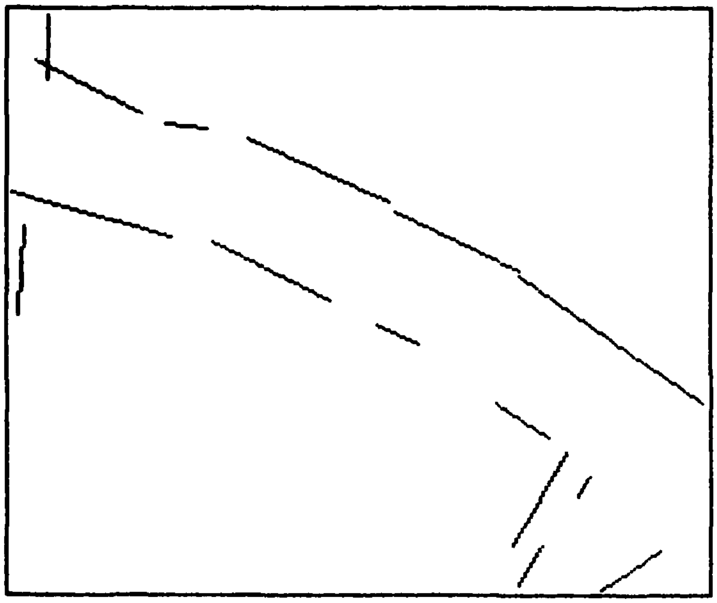

Figure 56. High confidence roads.

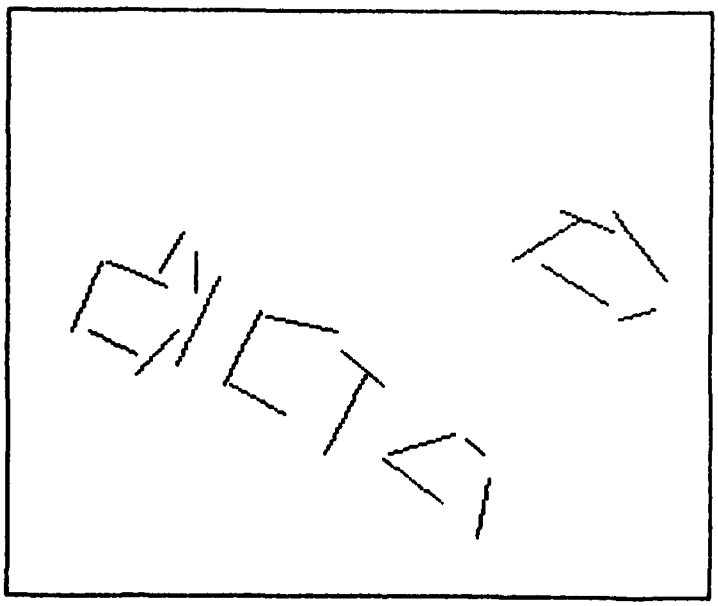

Figure 57. High confidence buildings.

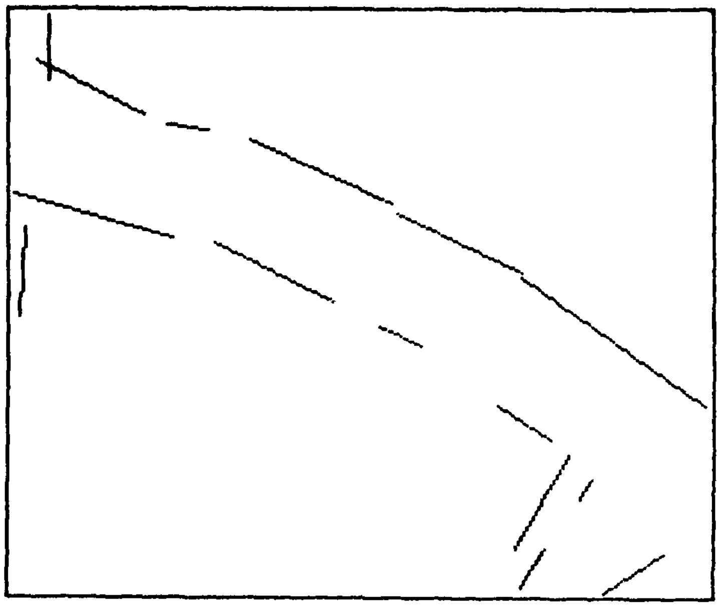

Figure 58. Road with probability ≥0.75.

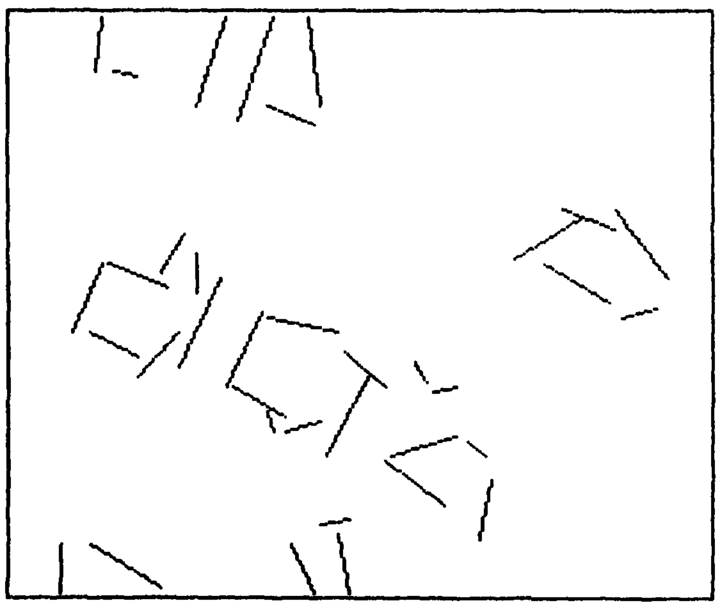

Figure 59. Buildings with probability ≥0.75.

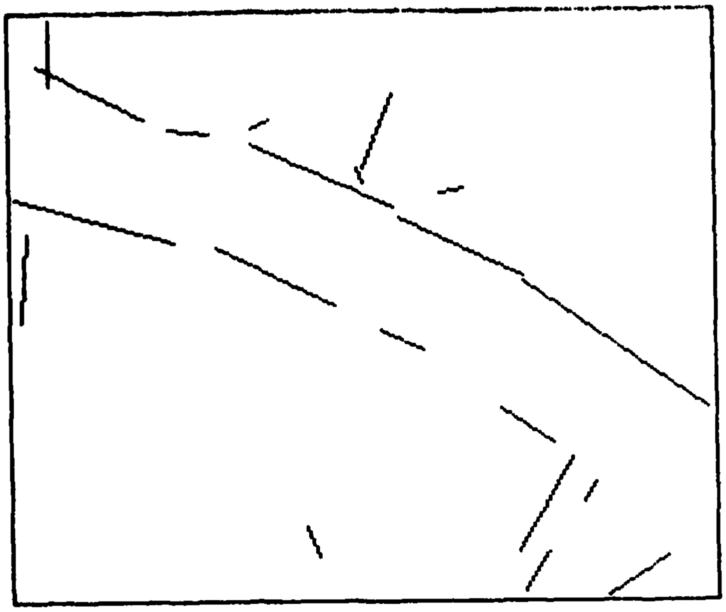

Figure 60. Roads with probability ≥0.5.

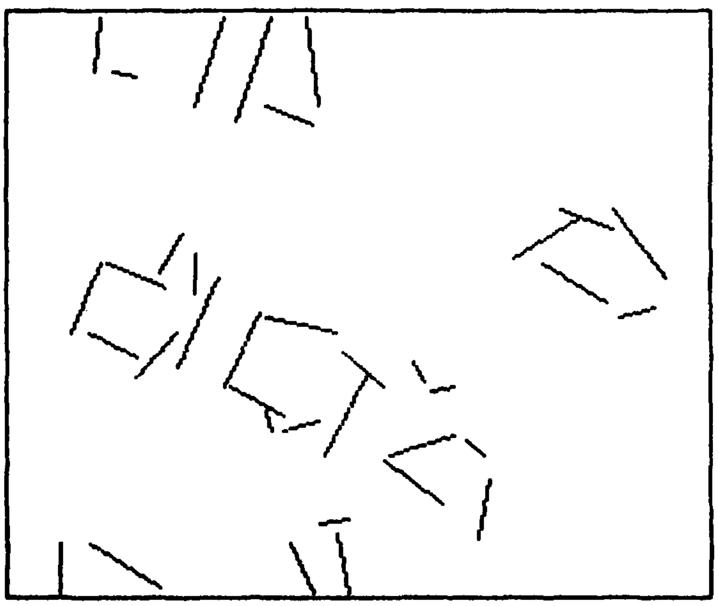

' ~~re 6' Buildings with probability ≥0.5.

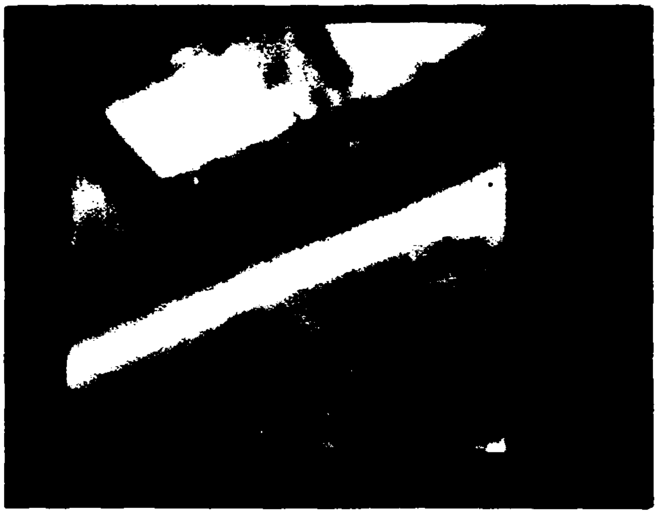

Figure 62. A non-residential scene.

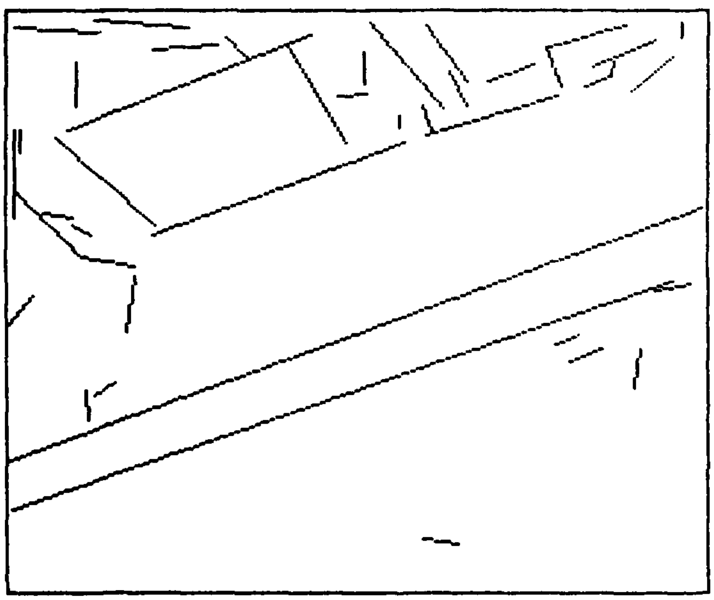

Figure 63. Line segments fitted to the edge components.

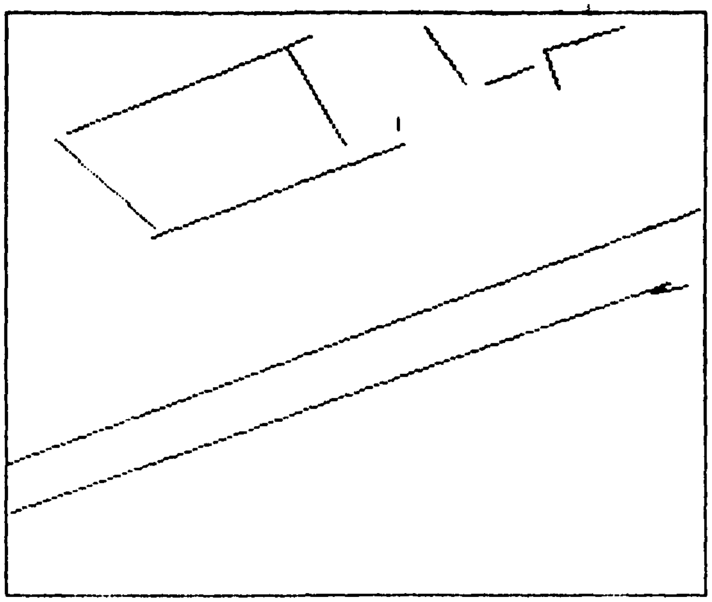

Figure 64. Line segments whose probability of being a piece of road or building are nonzero.

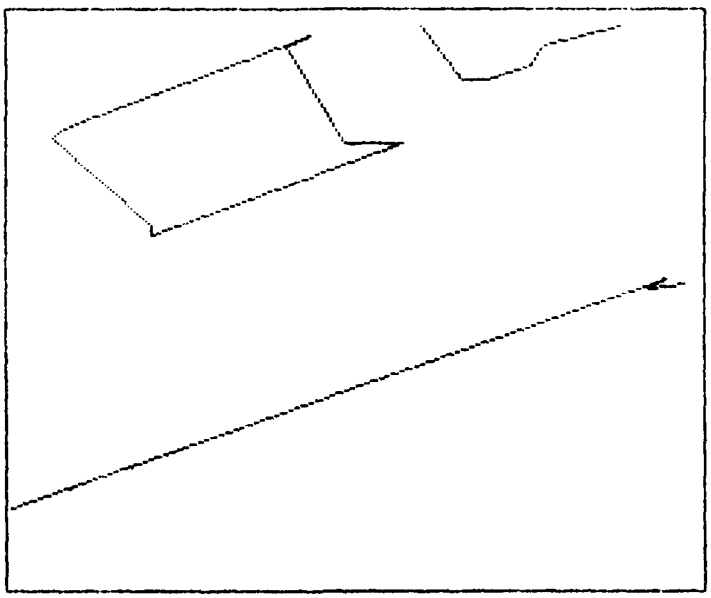

Figure 65. Compatible lines.

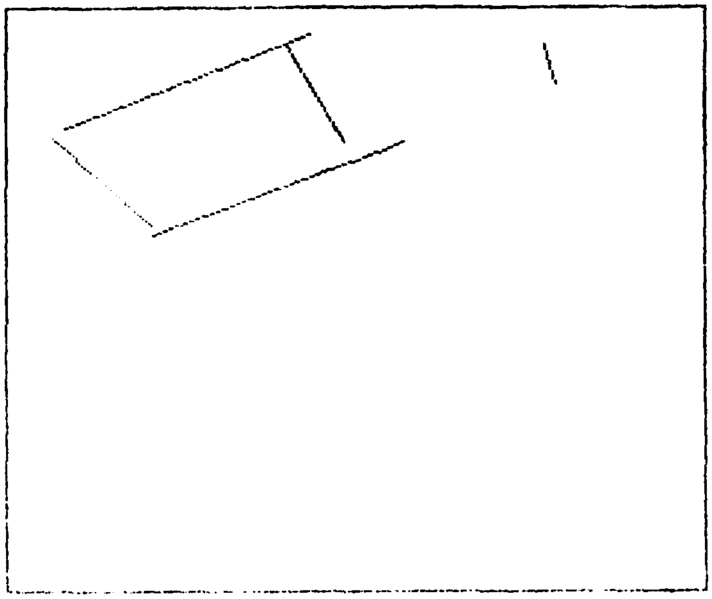

Figure 66. High confidence buildings.

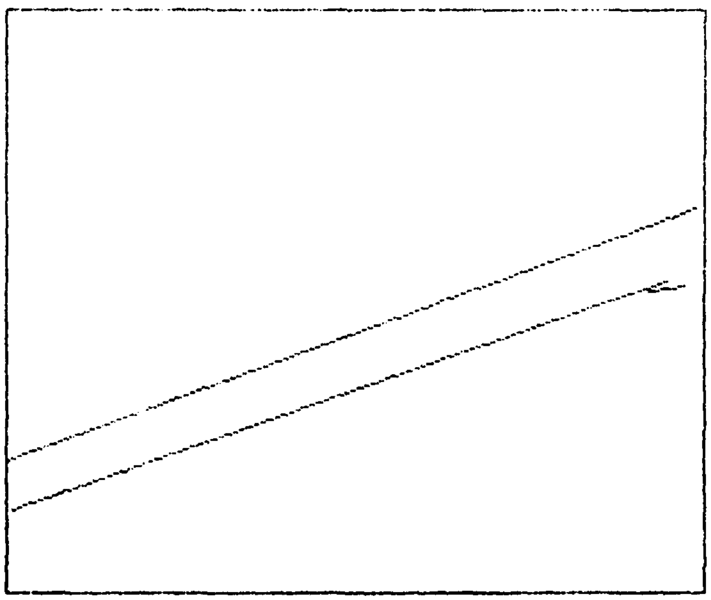

Figure 67. High confidence roads.

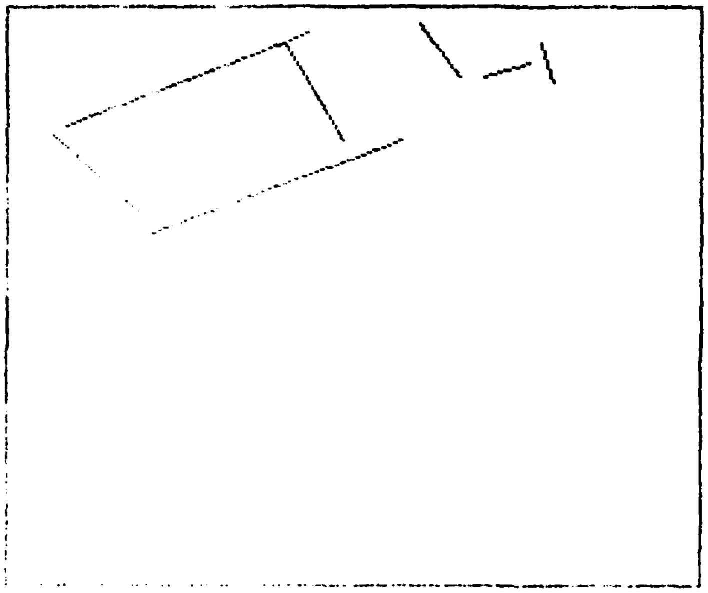

Figure 68. Buildings with probability ≥0.75 or ≥.5.

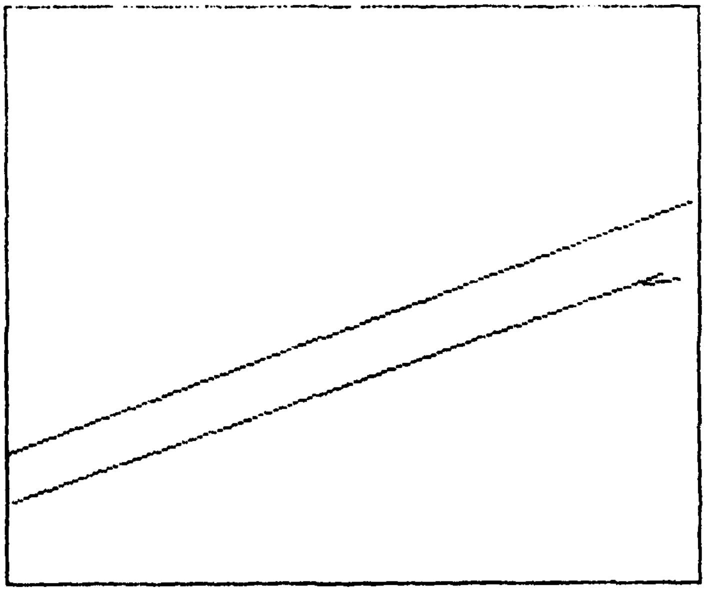

Figure 69. Roads with probability ≥0.75 or ≥.5.

Figure 70. A non-residential scene.

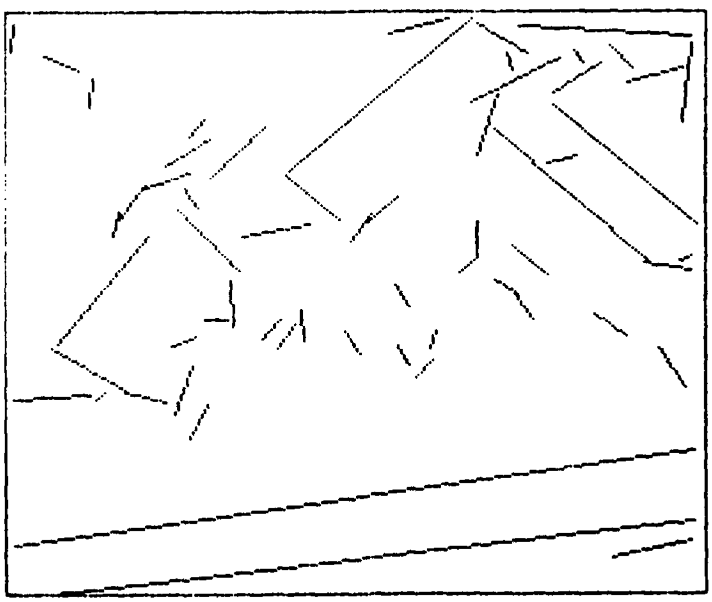

Figure 71. Line segments fitted to the edge components.

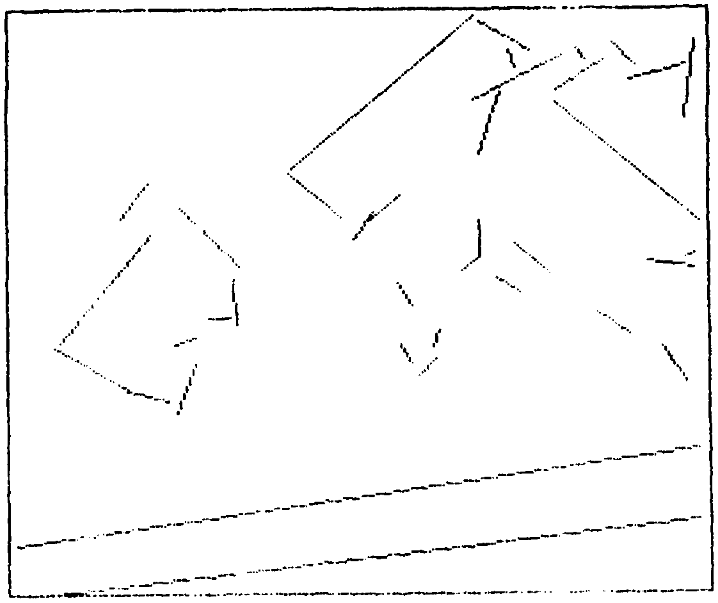

Figure 72. Line segments whose probability of being a piece of road or building are nonzero.

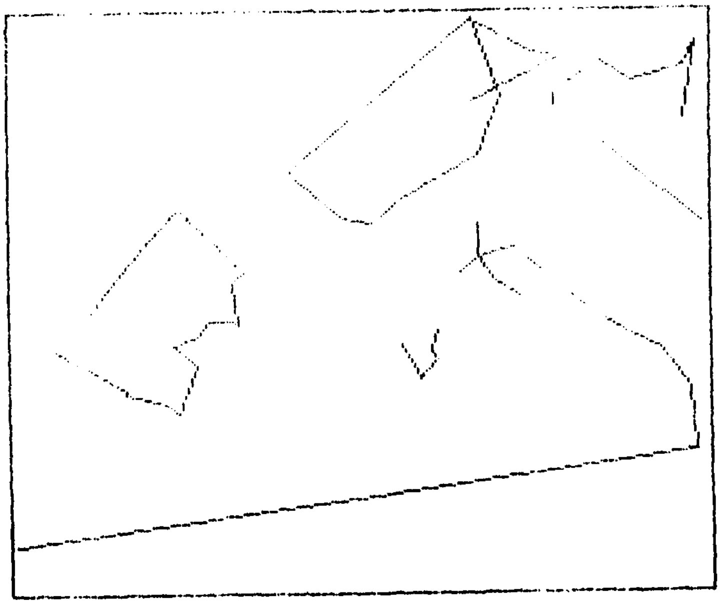

Figure 73. Compatible lines.

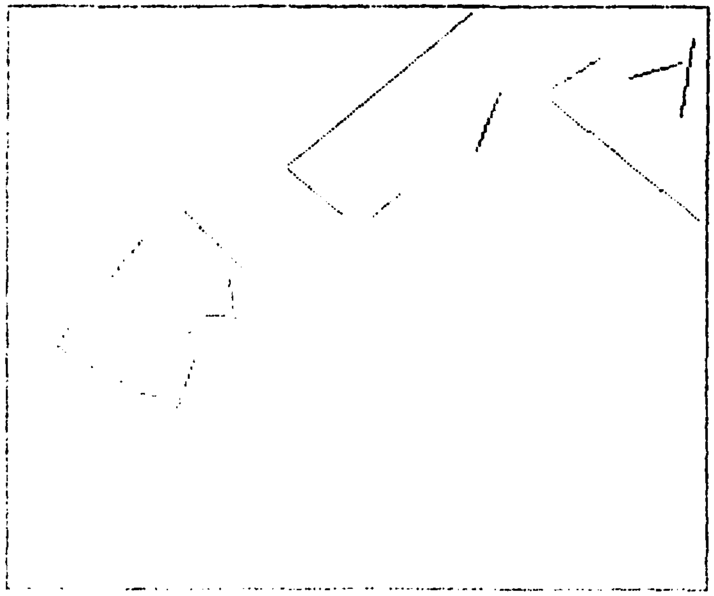

Figure 74. High confidence buildings.

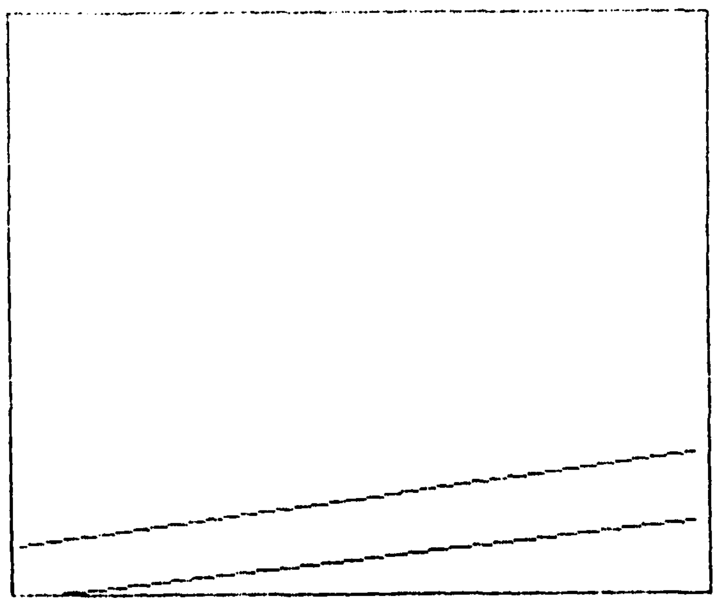

Figure 75. High confidence roads.

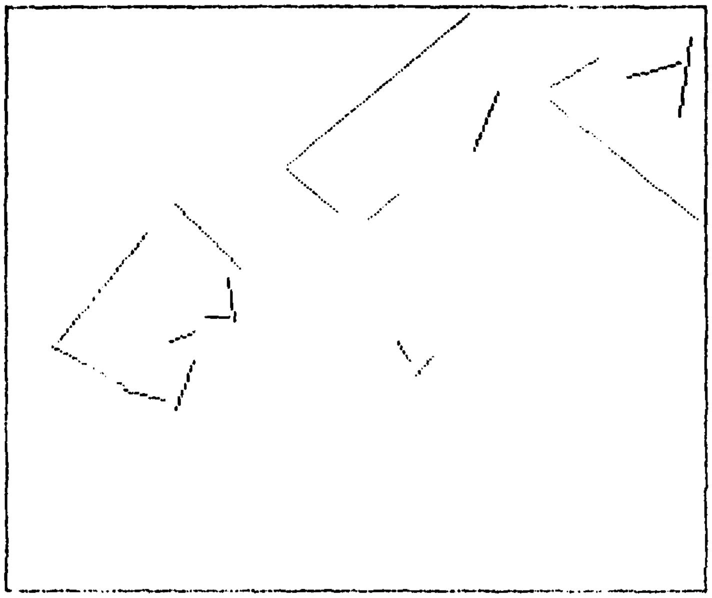

Figure 76. Buildings with probability ≥0.75 or ≥.5

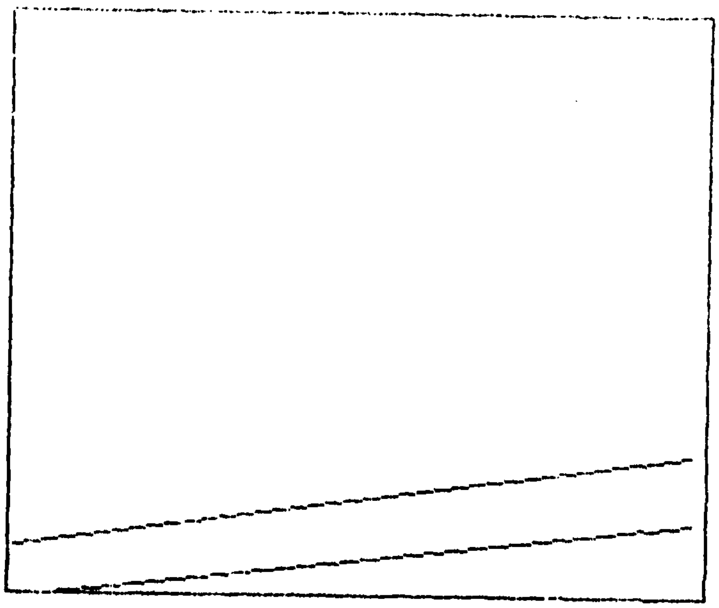

Figure 77. Roads with probability ≥0.75 or ≥ .5

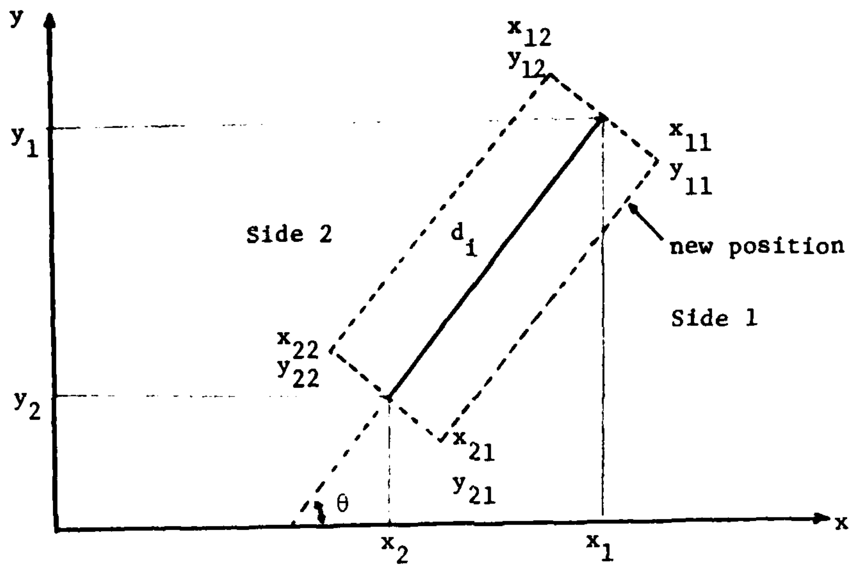

Figure 78. Displacement of the line segment.

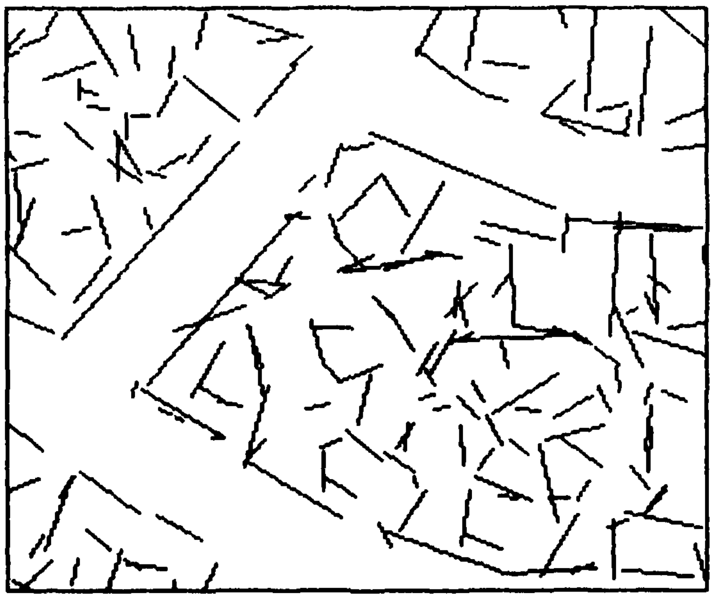

Figure 79. Relocating the lines at the maximum gradient position.

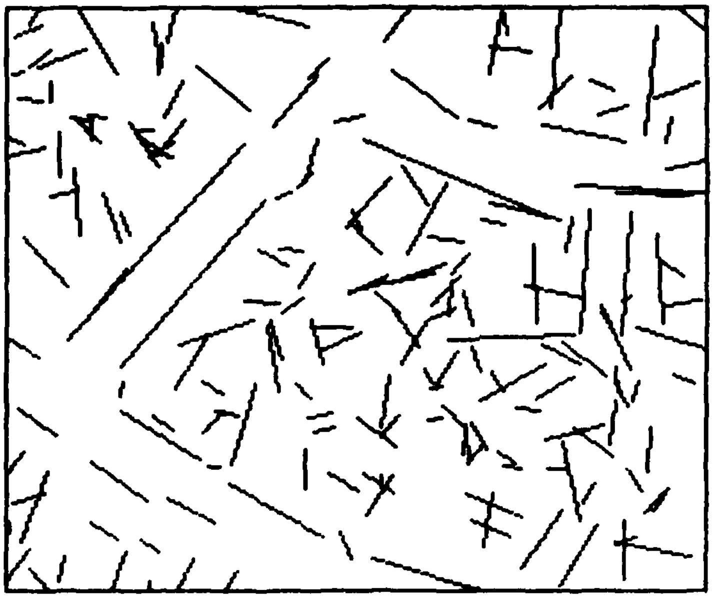

Figure 80. Relocating the lines at the minimum standard deviation position.

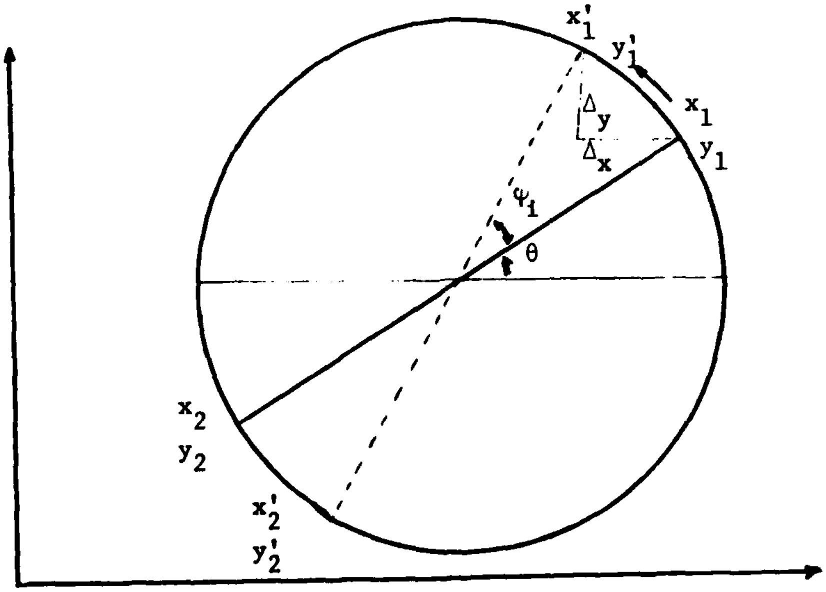

Figure 81. Changing the angle of the line segment.

Figure 82. Rotating the lines and relocating them at the maximum gradient position.

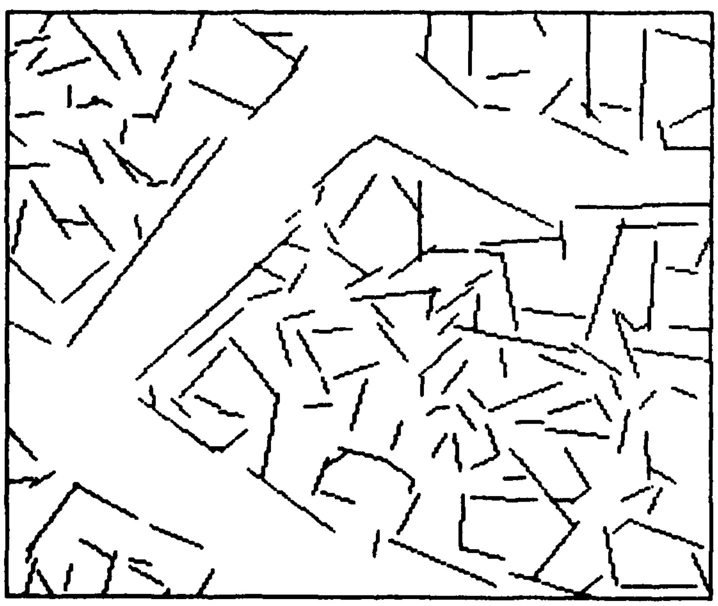

Figure 83. Rotating the lines and relocating them at the minimum standard deviation position.

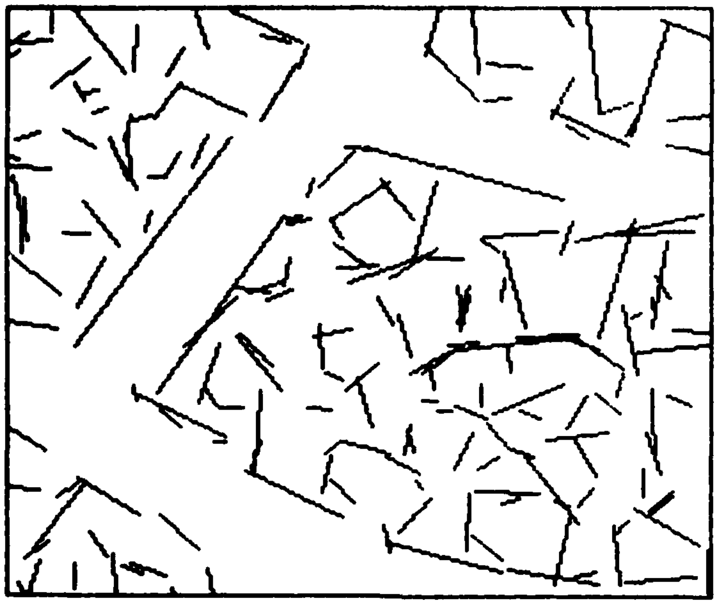

Figure 84. First translation then rotation and relocating at the maximum gradient position.

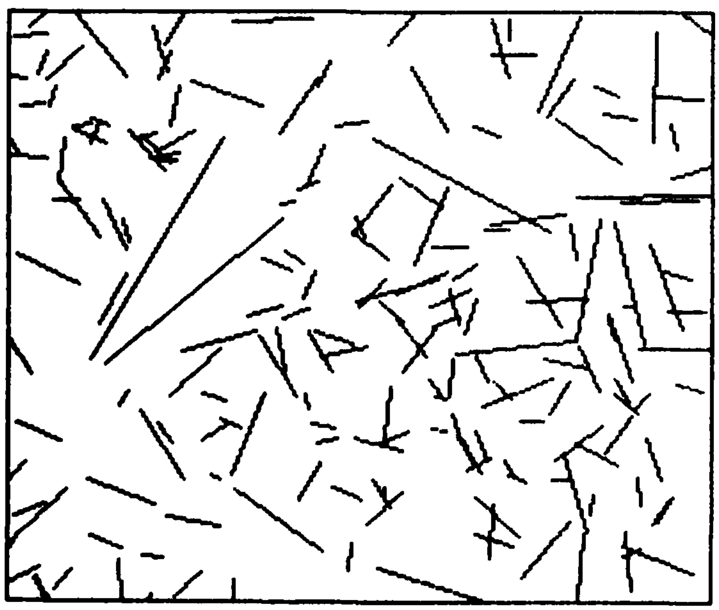

Figure 85. First translation then rotation and relocating at the minimum standard deviation position.

Figure 86. First rotation then translation and relocating at the maximum gradient position.

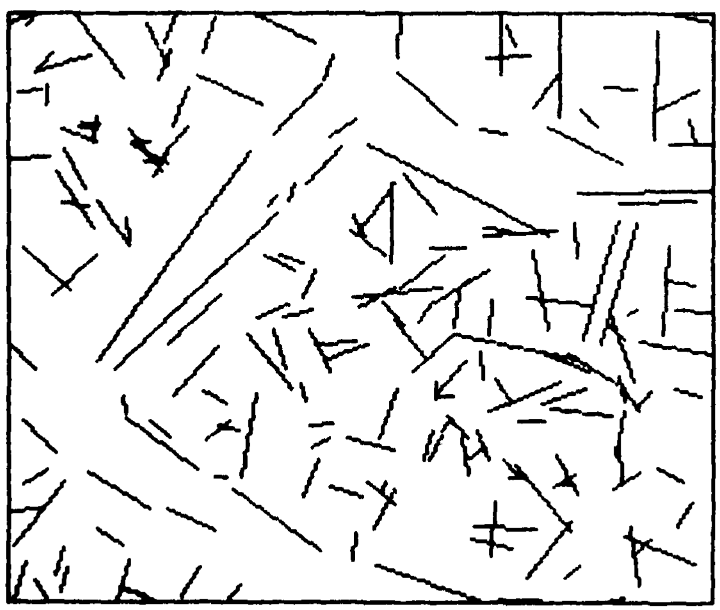

Figure 87. First rotation then translation and relocating at the minimum standard deviation position.

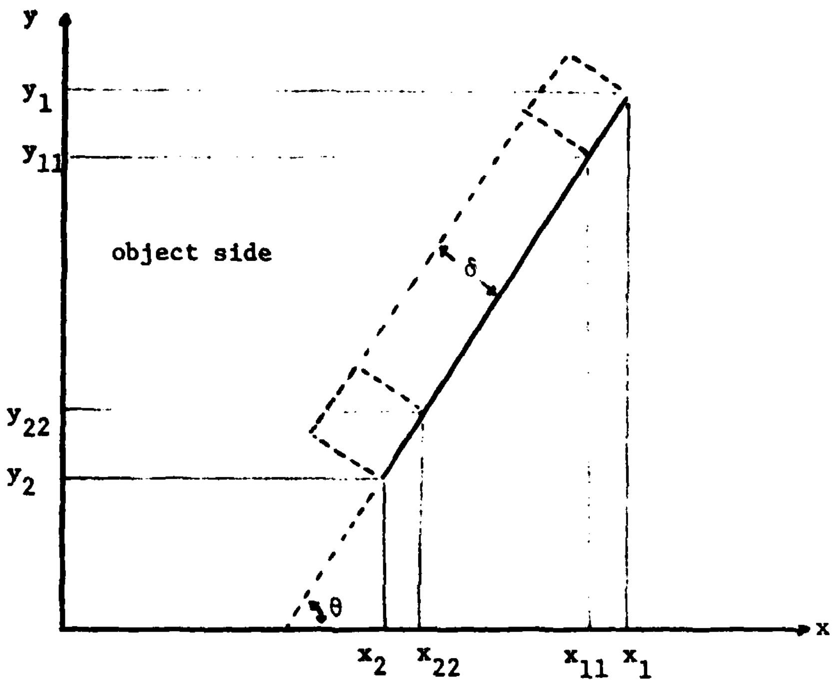

Figure 88. Length adjustment.

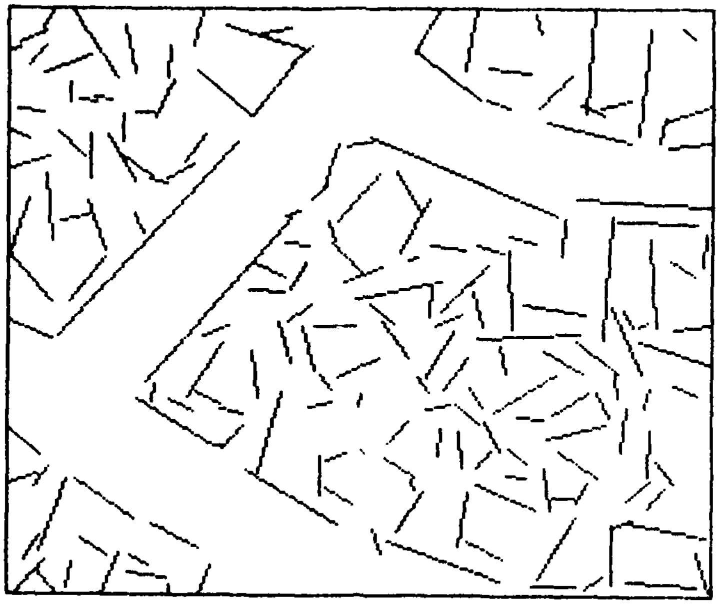

Figure 89. Threshold = 5 in length adjustment.

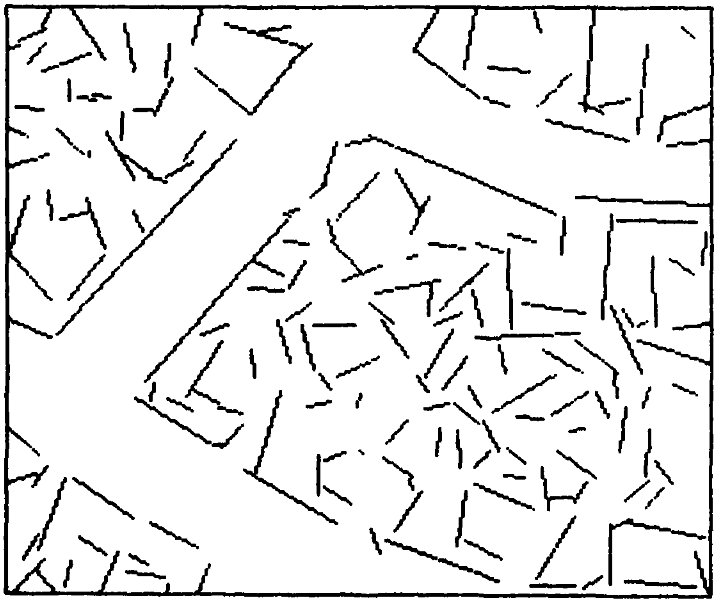

Figure 90. Threshold = 4 in length adjustment.

Figure 91. Threshold = 3 in length adjustment.

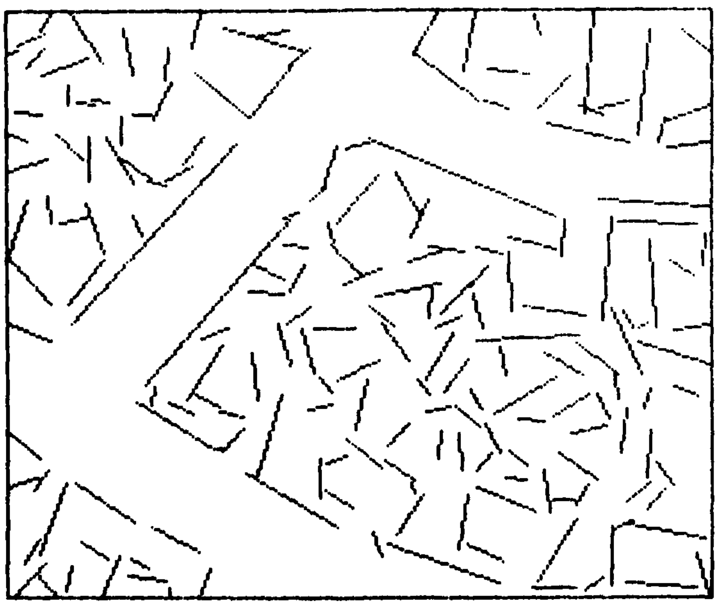

Figure 92. Length adjustment with threshold = standard deviation of the gray level on the object side of the line segment.

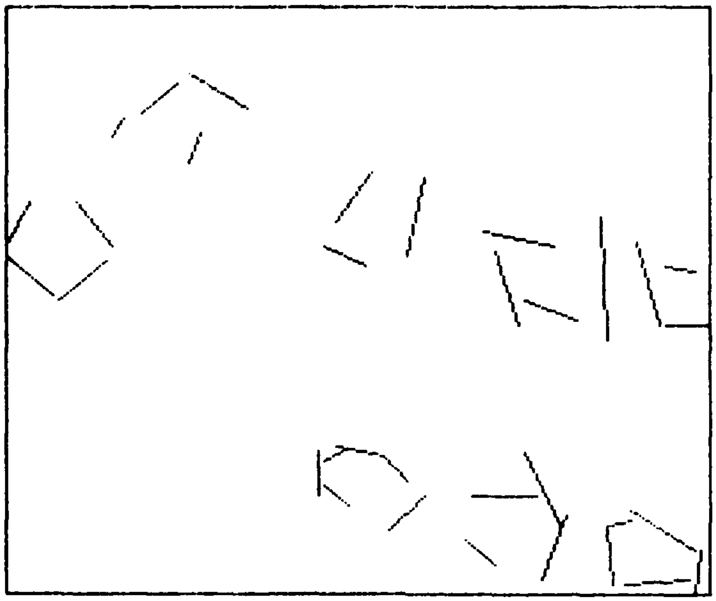

Figure 93. Buildings with confidence 1 after maximum gradient angle adjustment.

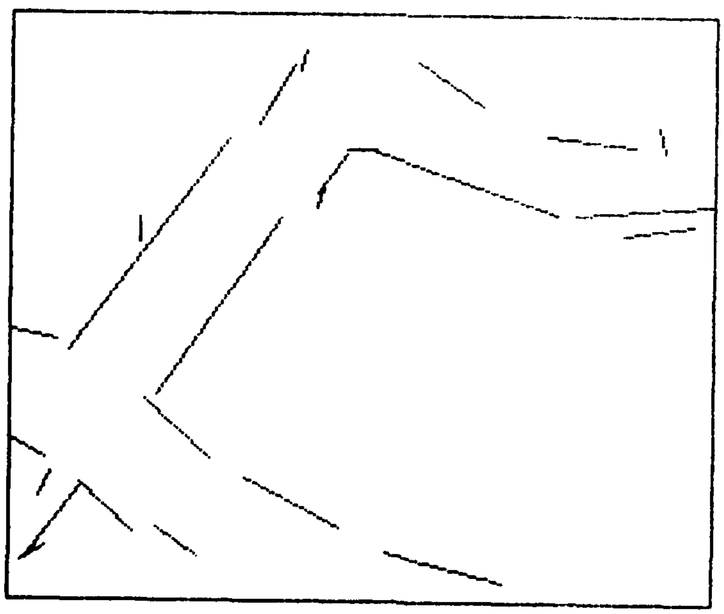

Figure 94. Roads with confidence 1 after maximum gradient angle adjustment.

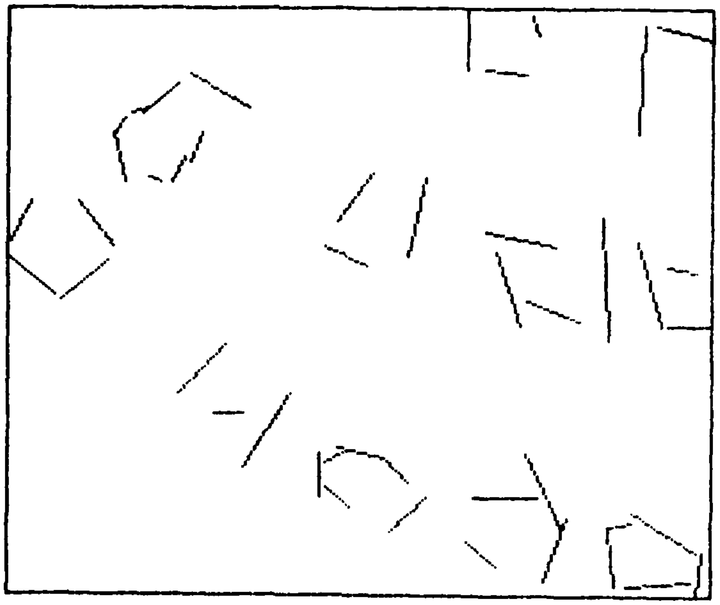

Figure 95. Buildings with *confidence* .75 after maximum gradient angle adjustment.

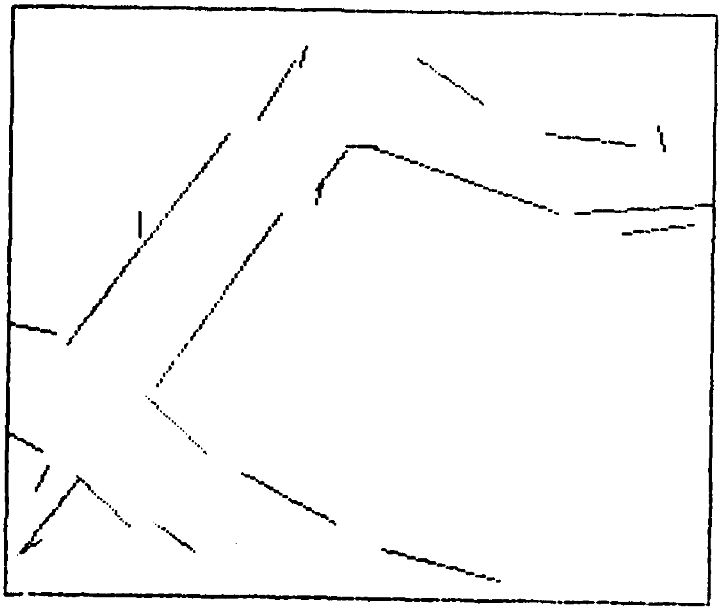

Figure 96. Roads with confidence .75 after maximum gradient angle adjustment.

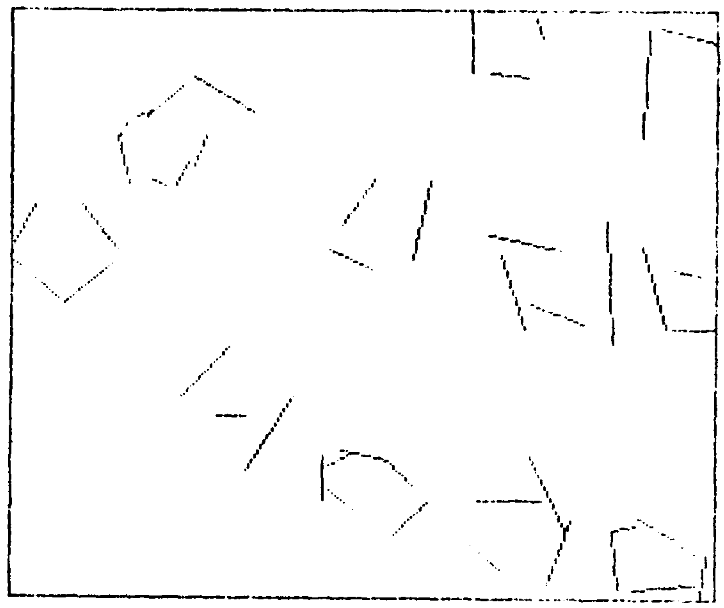

Figure 97. Buildings with confidence .5 after maximum gradient angle adjustment.

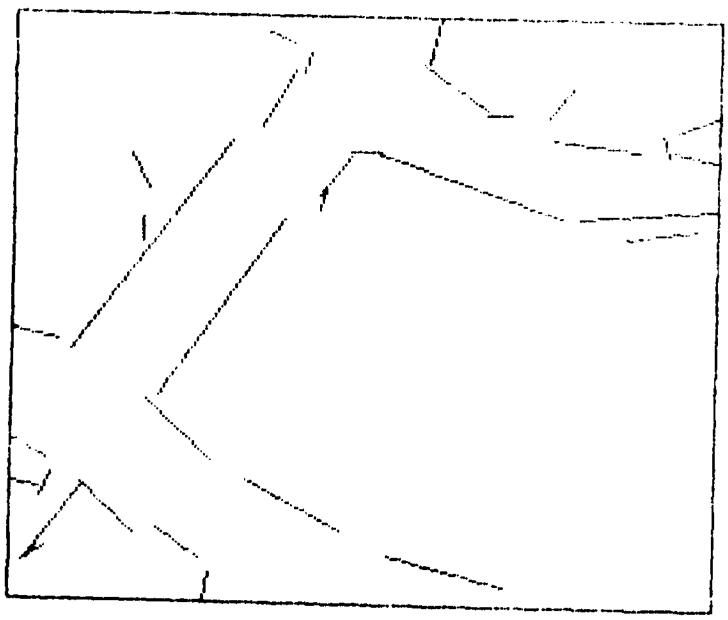

Figure 98. Roads with confidence .5 after maximum gradient angle adjustment.

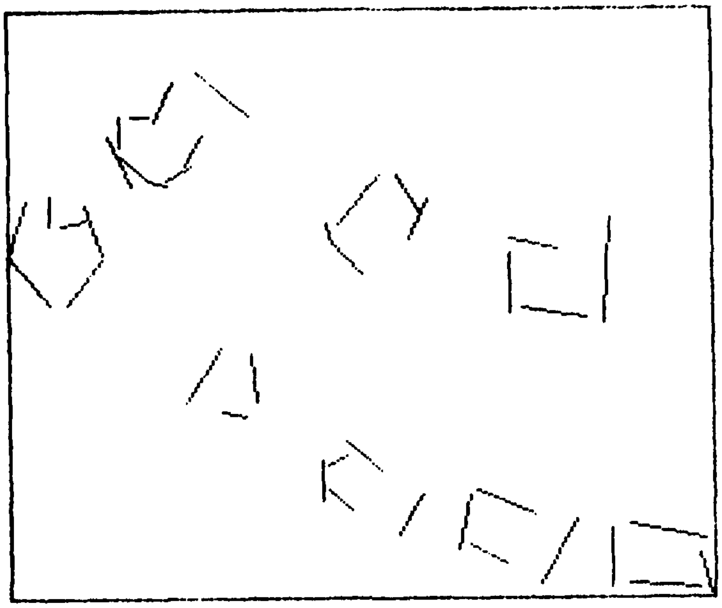

Figure 99. Buildings with confidence 1 after dynamic-threshold length adjustment.

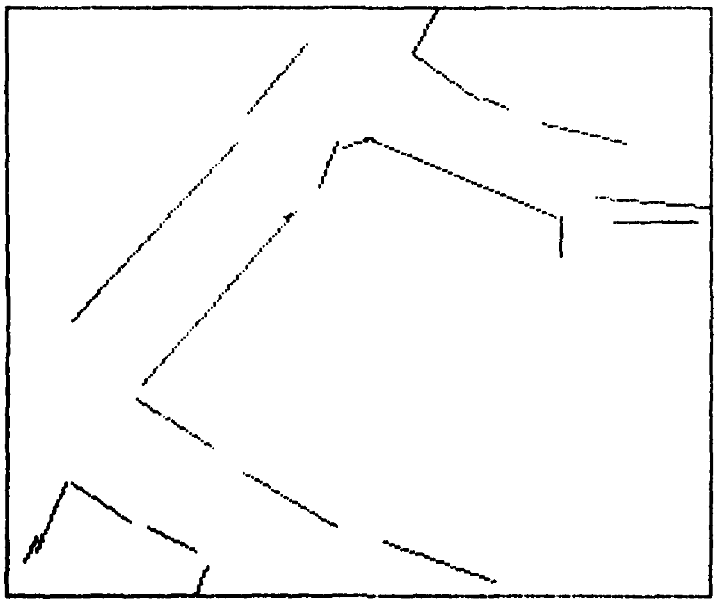

Figure 100. Roads with confidence 1 after dynamic-threshold length adjustment.

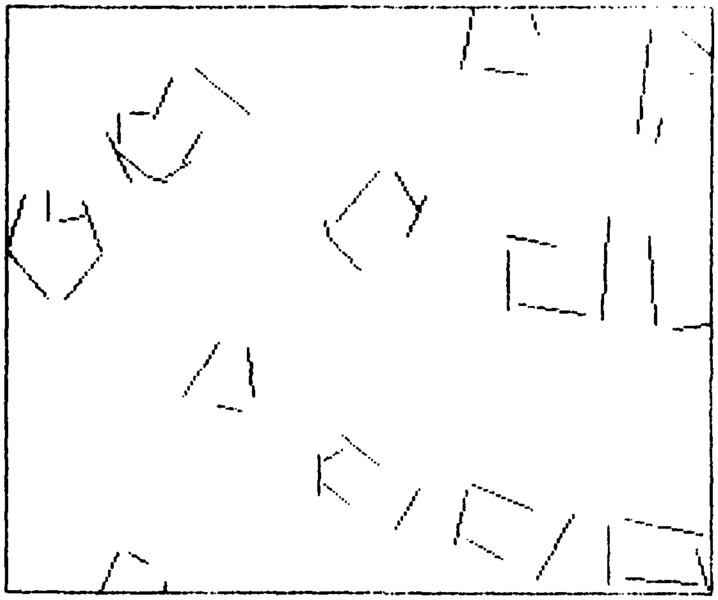

Figure 101. Buildings with confidence .75 after dynamic-threshold length adjustment.

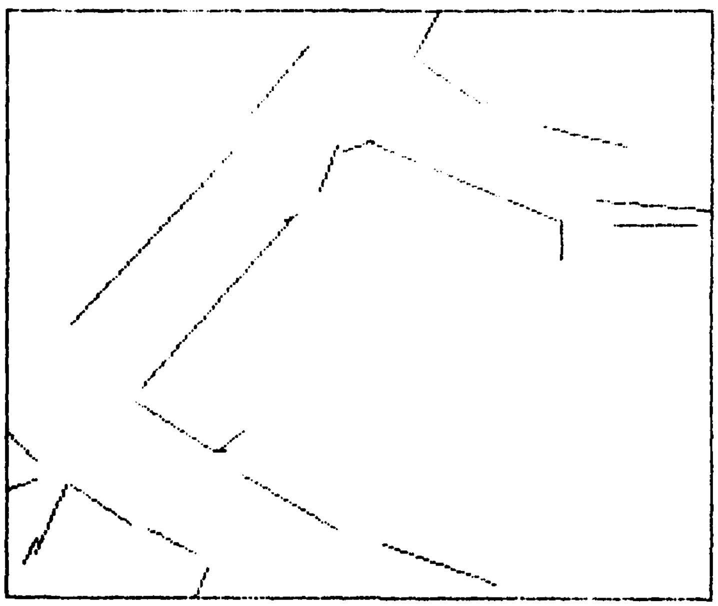

Figure 102. Roads with confidence .75 after dynamic-threshold length adjustment.

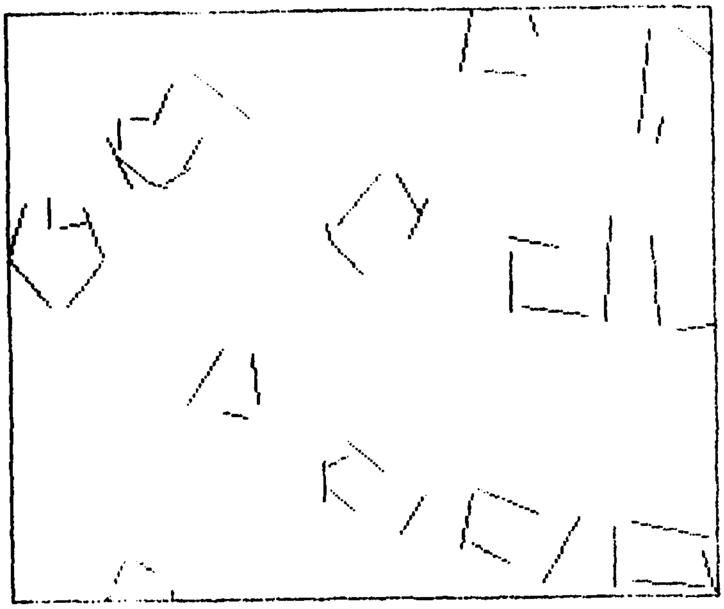

Figure 103. Buildings with confidence .5 after dynamic-threshold length adjustment.

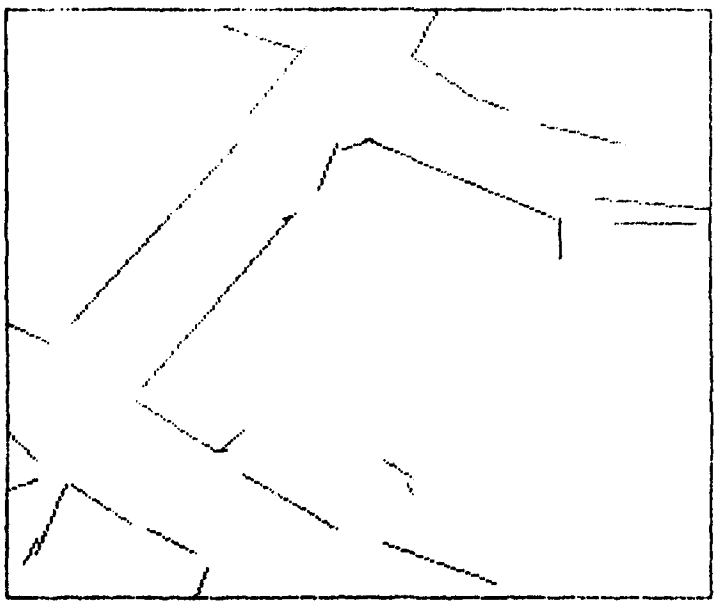

Figure 104. Roads with confidence .5 after dynamic-threshold length adjustment.

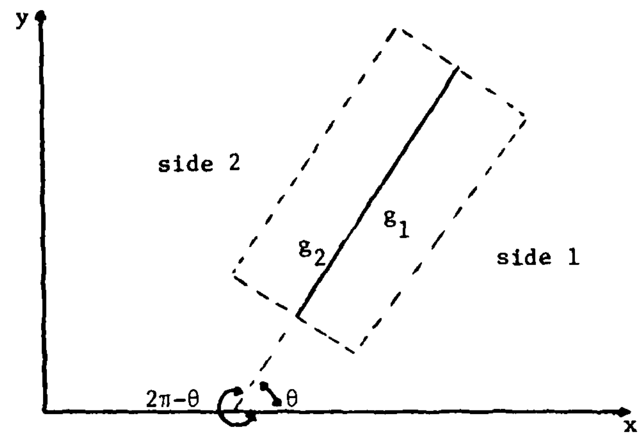

FIGURES 106-107
ON FOLLOWING PAGES

Figure 105. Angle convention for g_1 and g_2.

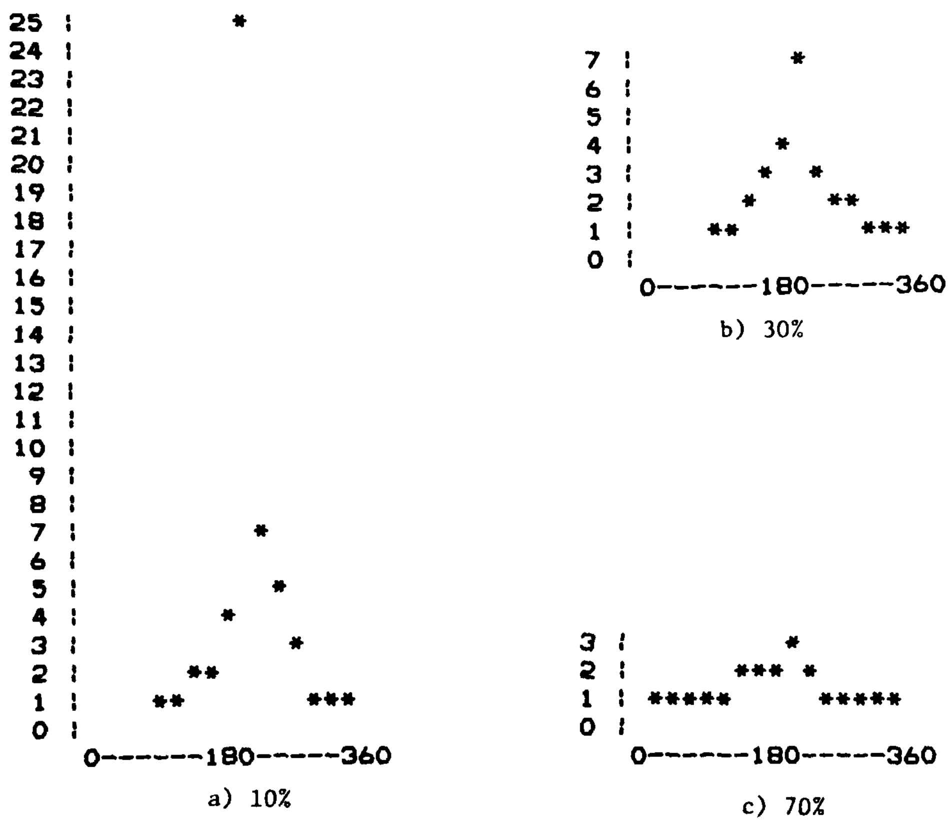

Figure 108. Plot of n_1/n_2 as a function of θ, after noise cleaning.

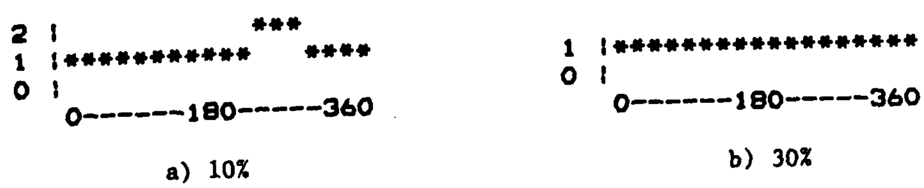

Figure 109. Plot of n_1/n_2 as a function of θ, before noise cleaning.

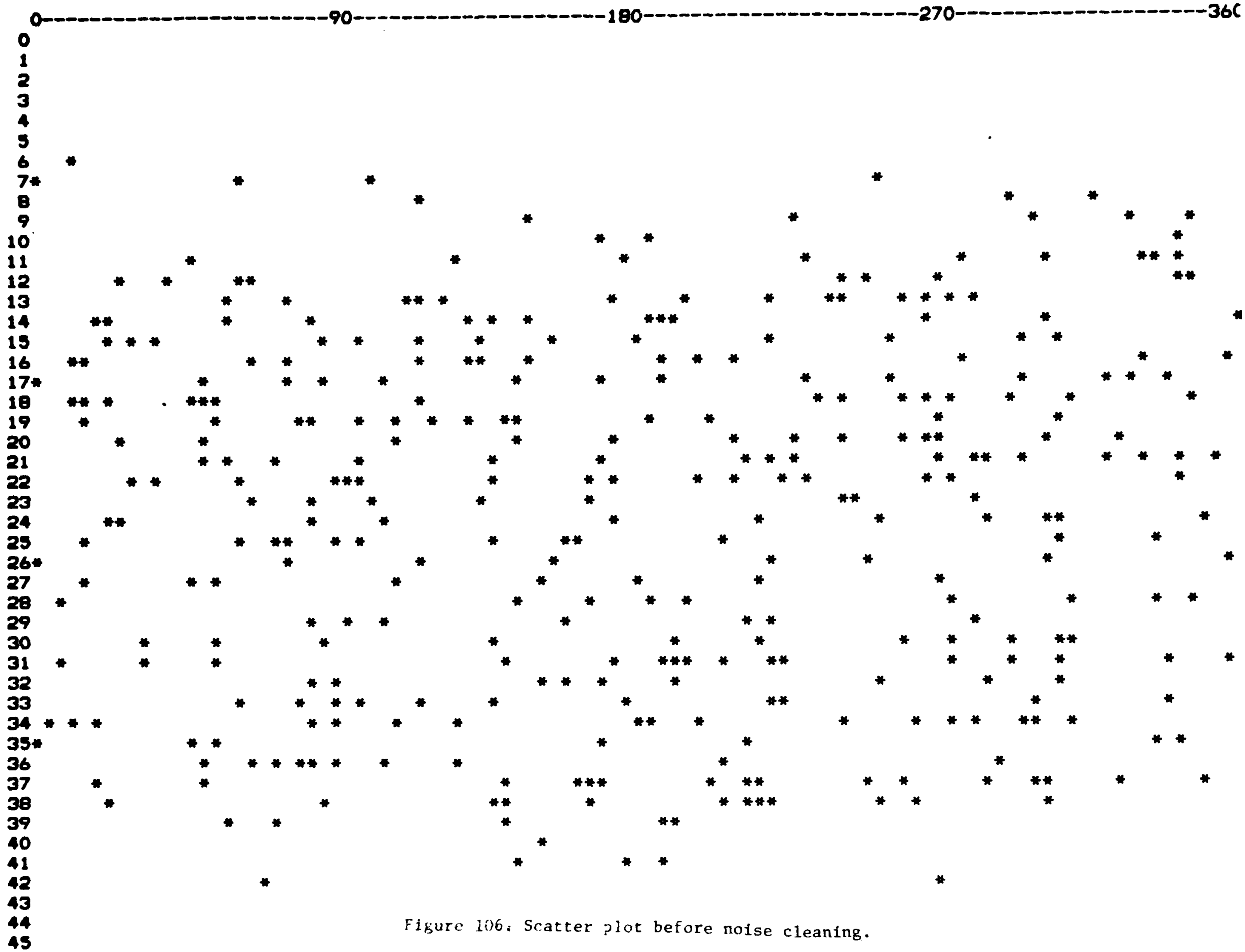

Figure 106. Scatter plot before noise cleaning.

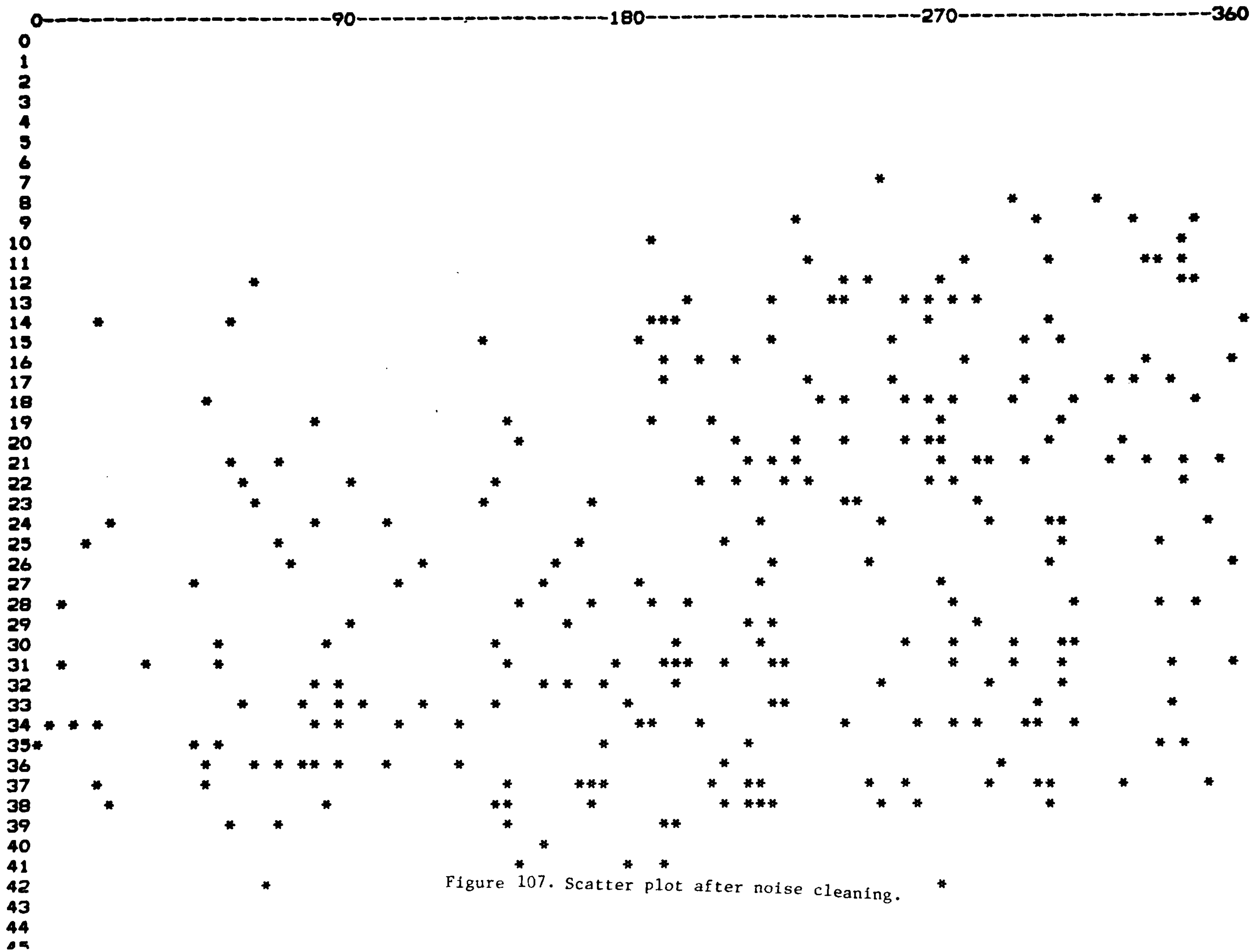

Figure 107. Scatter plot after noise cleaning.

UNCLASSIFIED

SECURITY CLASSIFICATION OF THIS PAGE (When Data Entered)

REPORT DOCUMENTATION PAGE

READ INSTRUCTIONS BEFORE COMPLETING FORM

1. REPORT NUMBER	2. GOVT ACCESSION NO. AD-A109 558
3. RECIPIENT'S CATALOG NUMBER	
4. TITLE (and Subtitle) TOWARD THE RECOGNITION OF BUILDINGS AND ROADS ON AERIAL PHOTOGRAPHS	5. TYPE OF REPORT & PERIOD COVERED Technical
	6. PERFORMING ORG. REPORT NUMBER TR-913
7. AUTHOR(s) Mohamad Tavakoli, Azriel Rosenfeld	8. CONTRACT OR GRANT NUMBER(s) DAAG-53-76C-0138
9. PERFORMING ORGANIZATION NAME AND ADDRESS Computer Vision Laboratory, Computer Science Center, University of Maryland, College Park, MD 20742	10. PROGRAM ELEMENT, PROJECT, TASK AREA & WORK UNIT NUMBERS
11. CONTROLLING OFFICE NAME AND ADDRESS U.S. Army Night Vision Laboratory Ft. Belvoir, VA 22060	12. REPORT DATE July 1980
	13. NUMBER OF PAGES 130
14. MONITORING AGENCY NAME & ADDRESS(if different from Controlling Office)	15. SECURITY CLASS. (of this report) Unclassified
	15a. DECLASSIFICATION/DOWNGRADING SCHEDULE

16. DISTRIBUTION STATEMENT (of this Report)

Approved for public release; distribution unlimited.

17. DISTRIBUTION STATEMENT (of the abstract entered in Block 20, if different from Report)

18. SUPPLEMENTARY NOTES

19. KEY WORDS (Continue on reverse side if necessary and identify by block number)

Image processing
Pattern recognition
Cultural features
Buildings
Roads

20. ABSTRACT (Continue on reverse side if necessary and identify by block number)

This paper describes steps toward the recognition of cultural features such as buildings and roads on aerial photographs. The approach involves several successive stages of grouping of edge segments. Straight line segments are fitted to sets of edge pixels; compatibilities between pairs of these segments, based on gray level and geometric information, are computed; and the segments are then grouped into building-like and road-like groupings based on these compatibilities. Examples of the results obtained using this

DD FORM 1 JAN 73 1473 EDITION OF 1 NOV 65 IS OBSOLETE

UNCLASSIFIED

SECURITY CLASSIFICATION OF THIS PAGE (When Data Entered) approach are given, and some variations on the initial stages of the process are also investigated.